The development of microfluidic paper-based analytical devices for point-of-care diagnosis of sheep scab

Valentina Busin

Submitted for the degree of Doctor of Philosophy

Heriot-Watt University

Institute of Biological Chemistry, Biophysics and Bioengineering. School of Engineering and Physical Sciences

September 2017

ABSTRACT

The recent growing interest and development of microfluidic paper-based analytical devices (μPADs) for point-of-care (POC) testing in human health in low-resource settings has great potential for the exploitation of these technologies in animal disease diagnosis. Sheep scab is a highly infectious, widespread and notifiable disease of sheep, which poses major economic and welfare concerns for the UK farming industry. The possibility of diagnosing sheep scab at the POC is, consequently, very important to controlling this disease. The overall aim of this project was, therefore, to develop μPADs based on a novel method of fabrication, in order to translate the existing lab-based sheep scab ELISA (Pso o 2) and a biomarker test for haptoglobin (Hp) into paper-based ELISA (P-ELISA), to enable POC diagnosis of this animal disease. In Chapter 3, the novel fabrication method is described, in Chapters 4 and 5, the translation of the lab-based ELISAs (Hp and Pso o 2 respectively) are explained and in Chapter 6 the development of a μPAD for incorporation of the POC tests into a multiplexed, rapid assay is covered. Experiments showed that both ELISAs were successfully transferred onto paper and that the devices developed were suitable for POC testing. This study has resulted in a novel fabrication method for μPADs, in successfully translated existing ELISAs to P-ELISA and in novel solutions for the POC diagnosis of an important veterinary disease.

DEDICATION

To Emma and Lore. Thanks for your constant and amazing support and for putting up with all the late night coming home.

ACKNOWLEDGMENTS

A special thank you to my supervisors, Stew and Will. For always pointing out the positive outcomes of my experiments, for giving me confidence in my work and most importantly for showing me how to be a good researcher. It has been truly a pleasure working with you.

Thanks to all the people in Will's group; you've been so welcoming and supportive, taking the time to introduce me to the basic skills of engineering. In particular, thanks to Alan for coming up with little brilliant ideas that saved me so many hours of work.

Thanks to everyone in lab 2.026 at Moredun; Fran, Mairi and Dave you've truly helped me so much. If my ELISAs got to work is undoubtedly for the patience you took to explain me every single detail of it.

Thanks to Pr. David Eckersall and his team for the essential assistance with the Hp assay and for sharing your interest in making this POC test to work.

Thanks to all the fellow PhD students I've met in these years; for the support and the fun we had, with a specific mention for Amy and Nisha. And finally, a big thank you to Isabelle for giving me a place to stay every time I couldn't face driving through the M8 once again.

HERIOT WATT UNIVERSITY

ACADEMIC REGISTRY
Research Thesis Submission

Name:	Valentina Busin		
School:	Engineering and Physical Science		
Version: *(i.e. First, Resubmission, Final)*	Final	Degree Sought:	PhD Mechanical Engineering

Declaration

In accordance with the appropriate regulations I hereby submit my thesis and I declare that:

1) the thesis embodies the results of my own work and has been composed by myself
2) where appropriate, I have made acknowledgement of the work of others and have made reference to work carried out in collaboration with other persons
3) the thesis is the correct version of the thesis for submission and is the same version as any electronic versions submitted*.
4) my thesis for the award referred to, deposited in the Heriot-Watt University Library, should be made available for loan or photocopying and be available via the Institutional Repository, subject to such conditions as the Librarian may require
5) I understand that as a student of the University I am required to abide by the Regulations of the University and to conform to its discipline.
6) I confirm that the thesis has been verified against plagiarism via an approved plagiarism detection application e.g. Turnitin.

* *Please note that it is the responsibility of the candidate to ensure that the correct version of the thesis is submitted.*

Signature of Candidate:	Valentina Busin	Date:	04.09.2017

Submission

Submitted By *(name in capitals)*:	
Signature of Individual Submitting:	
Date Submitted:	

For Completion in the Student Service Centre (SSC)

Received in the SSC by *(name in capitals)*:			
Method of Submission *(Handed in to SSC; posted through internal/external mail)*:			
E-thesis Submitted ***(mandatory for final theses)***			
Signature:		Date:	

Please note this form should be bound into the submitted thesis.
Academic Registry/Version (1) August 2016

TABLE OF CONTENTS

LIST OF TABLES

LIST OF FIGURES

ABBREVIATIONS

2D	Two-dimensional
3D	Three-dimensional
APP	Acute Phase Protein
ALP	Alkaline Phosphatase
BB	Blocking Buffer
BM	Biomarker
BSA	Bovine Serum Albumin
CAD	Computer-Aided Design
CO_2	Carbon Dioxide
ELISA	Enzyme-Linked Immunosorbent Assay
Hp	Haptoglobin
HRP	Horse Radish Peroxidase
IgG	Immunoglobulin G
LFIAs	Lateral flow immunoassays
µPAD	Microfluidic paper-based analytical devices
µg	Microgram
µl	Microliter
µm	Micrometre
mg	Milligram
min	Minute
ml	Millilitre
MP^3	Multi-pad paper plate
OD	Optical Density
PBS	Phosphate Buffered Saline
PDMS	Polydimethylsiloxane
P-ELISA	Paper-Enzyme-Linked Immunosorbent Assay
PMMA	Polymethylmethacrylate
POC	Point-of-care
RT	Room Temperature
s	Second

SAA	Serum Amyloid A
UK	United Kingdom
WB	Wash Buffer
£	British pounds
$	US dollars

LIST OF PUBLICATIONS BY THE CANDIDATE

Busin V., Shu W., and Burgess S. (2017). POC testing for sheep scab. (In preparation).

Busin V., Burgess S., and Shu W. (2017). A hybrid paper-based device for animal P-ELISA. *Sensors and actuators B: Chemical* (Submitted for publication).

Busin V., Burgess S., and Shu W. (2016). A novel multi-pad paper plate (MP^3) based assays for rapid animal disease diagnostics. *Procedia Engineering* **168**: 1418-1421.

Busin V., Wells B., Kersaudy-Kerhoas M., Shu W. and Burgess S. (2016). Opportunities and challenges for the application of microfluidic technologies in point-of-care veterinary diagnostics. *Molecular and Cellular Probes* **30**(5): 331-341.

Busin V., Burgess S., and Sargison N. (2015). Sheep scab, future perspective for disease diagnosis and control. *Livestock* **20**(3): 156-159.

Sargison N.D., Busin V. (2014). A model for the control of psoroptic mange in sheep. *Veterinary Record* **175**(19): 481-483.

Chapter 1 – Introduction

1.1 Introduction to the research

Sheep scab is the most important ectoparasitic disease of sheep in the UK and it represents a significant threat to both animal welfare and farm economics, making a rapid and accurate diagnosis of paramount importance. Recent improvements in the diagnosis of the disease have considerably broadened the tools available to combat sheep scab. At the same time, there has been a growing need for low-cost, rapid and reliable diagnostic tests in veterinary medicine. A considerable number of point-of-care tests are presently available, allowing cost-effective and decentralised diagnosis. Although, extremely useful, these tests come with some limitations. Recent advances in the field of microfluidics have brought about new and exciting opportunities for human health diagnostics, and there is now great potential for these new technologies to be applied in the field of veterinary diagnostics.

1.2 Sheep scab[1]

1.2.1 Sheep scab, the disease and its presence in the UK

Sheep scab is an allergic dermatitis caused by the non-burrowing ectoparasitic mite *Psoroptes ovis*. The disease is transmitted mainly by direct contact and is host specific, with the parasite spending its entire life-cycle on the sheep [1]. Mites, however, can survive off the sheep and remain infective for up to 16 days [2], making fences and handling facilities a possible alternative source of infestation, especially considering that a single ovigerous female is capable of producing an infestation [1]. The faecal deposition of *P. ovis* derived antigens/allergens on the skin of the host causes an intense inflammatory reaction, with marked pruritus resulting in self-trauma, extensive pyodermatitis, severe alopecia and considerable weight loss [3]. The sub-clinical phase can persist for 2 to 8 months in naturally occurring disease [4]. As lesions develop, they are distributed primarily along the trunk and if left untreated can quickly spread over the

[1] Much of this section is adapted from a recently published article: Busin V., Burgess S., and Sargison N. (2015). Sheep scab, future perspective for disease diagnosis and control. Livestock 20(3): 156-159.

entire body (Figure 1). As clinical signs resolve the mite population can die out completely, while in other cases mites can survive in cryptic sites, such as the ear canal, the inguinal and the infraorbital fossae [4]. In these cases, while animals may not exhibit clinical signs, none the less they still represent a potential source of infestation.

Figure 1 – An advanced case of sheep scab. It is evident that the lesion has spread across the entire body of the animal. (Valentina Busin).

Sheep scab represents a significant threat to animal welfare and has a tremendous impact on sheep farming economics, with an estimated annual cost of £8 million to the UK sheep industry [5]. In a recent training program organized by the Agriculture & Horticulture Development Board (AHDB Beef & Lamb), called "Stamp out Scab", the costs associated with an outbreak of scab reached £10.000, when diagnosis was delayed and treatment performed incorrectly [6]. Recent updates in legislation have made sheep scab a notifiable disease in Scotland. Based on the "Sheep Scab (Scotland) Order 2010" notification of sheep scab or suspected sheep scab to the Veterinary Authorities is

compulsory, with animal movement restrictions, notification to neighbouring farms, clearing of common lands and compulsory veterinary diagnosis to establish if the disease is present[2]. For England and Wales, under the "Sheep Scab Order 1997", it is a criminal offence to move infested animals (except to enable treatment or immediate slaughter) or fail to treat sheep visibly affected by scab[3].

Despite active legislation, however, sheep scab is currently endemic in the UK [7], with prevalence ranging from 8.6% to as high as 36% [8] and a total of 657 notifications to the Animal and Plant Health Agency (APHA) in Scotland between 2010 and 2016[4]. In particular, recent research has shown that 85% of flocks reporting a scab outbreak had a scab episode at least once in the past and 30% of these flocks had scab almost every year [9], with about 9% of UK farmers experiencing at least one outbreak of sheep scab a year [10]. These results highlight the reality that affected flocks are failing to eliminate the disease properly. Further research into the risk factors associated with disease outbreaks, has also shown that the risk of introducing sheep scab into a flock was increased up to 10-fold when confirmed cases of the disease where diagnosed in a neighbouring flock or in cases where common grazing was used [11].

Based on the severity of the disease and on the data shown by these recent studies, it is apparent that rapid and accurate diagnosis of sheep scab is of paramount importance, enabling the identification of cases prior to the advent of clinical signs (where possible) and therefore preventing further spread of disease and alleviating welfare concerns.

1.2.2 Diagnosis of sheep scab

The conventional diagnosis of *P. ovis* infestation is based on clinical observations and microscopic detection of mites in skin scrapings. Skin scrapings can be taken using a scalpel blade drawn at a right angle across the skin surface at the periphery of active lesions and observed microscopically under low magnification (x100) [12]. Although

[2] http://www.legislation.gov.uk/ssi/2010/419/pdfs/ssi_20100419_en.pdf
[3] http://www.legislation.gov.uk/uksi/1997/968/contents/made
[4] www.gov.scot/Topics/farmingrural/Agriculture/amimal-welfare/Diseases/disease/notifications

representing the conventional method for the diagnosis of ectoparasite infestation, it has been shown that this approach is often unable to detect sub-clinical infestation or sub-clinical carrier hosts [13], with sensitivity as low as 18% in animals not showing classical clinical signs of pruritus and alopecia [14]. Consequently, by the time *P. ovis* mites are detected, they have often already spread to the rest of the flock.

In the past few years, much work has been carried out to improve our knowledge of the causative agent [15] and of the host immune response to mite infestation [16]. Demonstration of specific antibodies against *P. ovis* in infested animals has allowed for several assays to be developed for antibody detection in sheep [14, 17, 18]. Some of the most promising antigens produced during sheep scab infestation are those homologous to house dust mite allergens, where a pronounced antibody response was detected [19, 20]. One has attracted particular attention, Pso o 2, a small (16kDa) polypeptide (protein) of the mite group II allergen (*Der f* 2 and *Lep d 2*) [20]. In this case, the use of immunodiagnostic tests such as the enzyme-linked immunosorbent assay (ELISA), could represent a valid alternative to the skin-scraping method, with far higher sensitivity being obtained [21]. Recently, the Moredun Research Institute (MRI) has developed a diagnostic ELISA for the detection of host antibodies specific to the mite allergen Pso o 2, which has proven highly effective in the diagnosis of sub-clinical infestation, since an antibody response can be detected as early as 2 weeks post-infestation [22]. A recombinant form of the mite protein Pso o 2 was synthesized [20] and used as a capture antigen in an indirect antibody ELISA for the detection of antigen-specific serum IgG. Testing performed on sheep serum samples of different origins and infestation status has demonstrated sensitivity of 93% and specificity of 90% [22]. This assay has recently been further optimized and now achieves sensitivity of 98.2% and specificity of 96.5% (S. Burgess, Personal Communication). The same diagnostic assay was also used in the face of a natural outbreak, showing its efficacy in the detection of sub-clinical disease in the field [23].

The main disadvantage of this assay, however, is that host antibodies may be present in previously-infested but successfully-treated animals for a prolonged period after treatment (3-6 months) potentially leading to false positives [24]. This is due to the considerable long half-life of Pso o 2 antibodies (56 days) following successful

treatment. Serum biomarkers (BMs) are generally host inflammatory proteins, which represent either specific, or non-specific indicators of disease, and/or current disease status. When combined with more specific immunodiagnostic elements (i.e. specific antibody tests), BMs have been shown to have the potential to discriminate between active infestation and disease resolution or successful treatment. A specific group of BMs are the acute phase proteins (APPs) which are serum proteins that increase rapidly following external or internal challenges, providing a quantification of the tissue damage in a diseased animal [25]. Two APPs have attracted attention in the veterinary field: haptoglobin (Hp) and serum amyloid A (SAA) [26-29]. Hp is an alpha-globulin constituent which is involved in reducing oxidative damage by binding free haemoglobin [25], usually present in two subunits, an α chain of 22kDa and a ß chain of 37kDa [29]. Increases in circulating Hp levels are caused by tissue damage, infection/infestation or inflammation and can be used to measure the course of infection as well as the response to therapy, while sex, age, pregnancy and lactation do not seem to influence circulating levels of Hp [30]. SAA is an apolipoprotein, the physiological role of which is still not fully understood [25], with a molecular weight of ~13kDa. Their application as diagnostic tools for sheep scab has also been recently investigated, showing a statistically significant increase in their serum levels with disease progression, but more importantly a rapid decline (half-life of less than 3 days) following successful treatment [31]. Specifically, serum Hp levels increased from a mean of 0.3mg/ml up to 3.53mg/ml at week 5 of infestation and down to 1.57mg/ml one week post-treatment and to pre-infestation levels between day 10 and 14 days post-treatment (half-life of Hp in serum post-treatment was 2.3 days). SAA is present at much lower quantities in the circulation (0.82µg/ml) prior to infestation, but peaked at 284.75µg/ml 5 weeks post-infestation. Following treatment, levels reached pre-infestation levels within 10 days (half-life for SAA was of 0.84 days) [31]. Currently, there are commercially available lab-based tests in the form of a colorimetric assay for HP analysis (Tridelta Development Ltd, Ireland) and as ELISA for SAA (Life Diagnostics Inc., UK). The first one is an indirect method of Hp measurement, based on the binding of Hp to haemoglobin. It is relatively quick but can be unreliable if the samples are haemolysed. The lab-based ELISA used for SAA measurement, is expensive and validated only for use in cow and goat serum. A diagnostic test combining the existing Pso o 2 antibody ELISA with an antigen ELISA for detection of

specific APPs, could represent a very powerful, improved diagnostic tool for sheep scab. Serum antibodies against Pso o 2 would inform on the contact between the host and the parasite, while the level of APPs would inform on the status of the disease (e.g. active vs resolved infestation).

1.3 Point-of-care diagnostics[5]

Point-of-care (POC) diagnostics is an area that has attracted considerable attention in the last decade. Testing at POC means that analytical procedures are carried out at the side of or near to the patient [32], for this reason, it is also sometimes referred to as "bed-side" testing [33]. The reasons for the considerable interest in the field of POC diagnostics are numerous: the potential to decrease costs of diagnosis [34], increasing the accessibility of these types of test to disadvantaged populations [35], and reducing the time between sampling and a treatment decision [36].

Following the global trend towards more affordable and accessible diagnostic testing, the Sexually Transmitted Diseases Diagnostics Initiative (SDI) within the World Health Organization (WHO) recently established a set of benchmark criteria for the ideal rapid test, under the acronym "ASSURED" [37]: Affordable, Sensitive, Specific, User-friendly (simple to perform in a few steps, with minimal technical training), Robust and Rapid (results available in less than 30 minutes), Equipment-free, Deliverable to those who need them. Ideally, POC tests should respect all or as many as possible of these characteristics [38].

1.3.1 Point-of-care testing in veterinary medicine

In the field of veterinary diagnostics, there is a similar need for low-cost, reliable and rapid diagnostic tests to be carried out at the POC [39]. So called on-site or animal-side tests will have considerable advantages over lab-based testing, which usually involves

[5] Much of this section is adapted from a recently published review article: Busin V., Wells B., Kesaudy-Kerhoas M., Shu W., and Burgess S. (2016). Opportunities and challenges for the application of microfluidic technologies in point-of-care veterinary diagnostics. Molecular and cellular probes, 30(5): 331-341.

laborious and expensive laboratory techniques and dedicated technical personnel. All of the analytical processes involved in testing, from collection of the sample to communication of the results, could potentially be performed in a single step, considerably reducing the time between testing and treatment [40]. This can translate into more affordable veterinary care, reduced handling of animals, targeted treatments and rapid testing in more remote geographic areas.

The need for more affordable, rapid and accessible tests is a recurrent theme in the literature, in particular as an invaluable tool in dealing with diseases that either represent a threat to public health [41], have substantial impact on animal welfare [42] and/or are of economic importance [43], with particular relevance to situations where laboratory facilities and funds are limited [44]. Furthermore, the general globalisation of trade of animals and animal products has greatly increased the risk of rapid and wide-ranging spread of emerging and exotic diseases, requiring timely and efficient ways of dealing with diseases that could have catastrophic repercussions for the individual farmer, as well as economic implications for the entire country and international trade [45]. In situations concerning disease outbreaks, where rapid propagation of infectious agents and/or high mortality are salient features, a rapid "animal-side" test would represent a critical tool for both collecting surveillance data and for assisting in the control of outbreaks [42, 46]. Currently available veterinary POC tests offer a good opportunity for a truly "animal-side" diagnosis, but the analytical performances of "on-site" testing are still considered limited compared with lab-based testing [47], whilst the possibility offered by the support of a central laboratory in the interpretation of the results is still perceived as critical [48].

1.3.2 Point-of-care devices currently available in veterinary diagnostics

At present, the most widely used technologies for POC testing in veterinary medicine are: dipstick tests and lateral flow immunoassays.

Dipstick and strip tests are based on the principle of immunoblotting and are made of paper strips with pads to analyse specific fluids. After the sample is introduced, the results are compared with a colour-coded chart to provide a semi-quantitative determination of the analyte(s). The most commonly used are test strips developed for human urine analysis, allowing the simultaneous detection or monitoring of leukocytes, nitrite, urobilinogen, protein, pH, haemoglobin, specific gravity, ketones, bilirubin and/or glucose [49]. While it has been developed for human patients, there is a high correlation between the dipstick results and other routinely used methods for urine analysis, which has resulted in this test being widely used in small animal private practice for first-line diagnosis of chronic kidney disease, mainly through an assessment of proteinuria [50, 51]. However, care should be taken when interpreting positive test results with low levels of proteins (traces) due to the high rate of false positive results [52].

A smaller version of the urine dipstick, restricted to detection of glucose and ketone bodies, is also largely applied for at-home management of pets with diabetes. This test is also widely used in farmed ruminants for the diagnosis of ketosis in cattle [53] and pregnancy toxaemia in sheep. Due to some variation in results, a further advance in the diagnosis of these diseases is the use of appropriate strips combined with electronic hand-held meters to accurately measure both glucose and one of the main ketone bodies, ß- bhydroxybutyrate (BHB) in blood, making diagnosis more reliable as well as sampling potentially more successful and less stressful [54]. This POC test has shown great potential for the quantitative detection of BHB, with improved sensitivity and specificity when compared with dipstick tests for detection of ketones in urine or milk [55, 56]. Its use for glucose measurement, however, does not seem to be reliable [54]. Dipstick tests have also been used for the detection of antibiotics in serum, milk and/or meat samples [57]. These rapid tests allow the detection of antibiotics within the µg/ml range, permitting on-site monitoring of non-authorised uses of antimicrobials, which could be especially useful in slaughterhouses and food processing plants.

The main advantage of these POC tests is that they can be readily carried out by the end-user, proving to be particularly useful for the long term management of chronic

diseases [58]. The major limitation, however, can be the subjective interpretation of results, based on a personal evaluation of a colorimetric reaction [50].

Lateral flow immunoassays (LFIAs) are based on the principle of capillary force: a liquid flowing on or through a strip of polymeric material, on or in which specific molecules (e.g., antigens, antibodies, DNA/RNA sequence) have been immobilized [59]. These strips usually consist of multiple pads: a sample application pad, a conjugate pad, a membrane for detection and an absorbent pad (Figure 2), usually made of different materials (e.g., nitrocellulose, glass fibre and fused silica) encased in a plastic cage for protection of a fragile paper membrane [60]. The best known example of a lateral flow test is the pregnancy test [61], which is probably the most used POC test worldwide. The main advantages of LFIAs over conventional lab-based tests are their simplicity, rapidity and low cost.

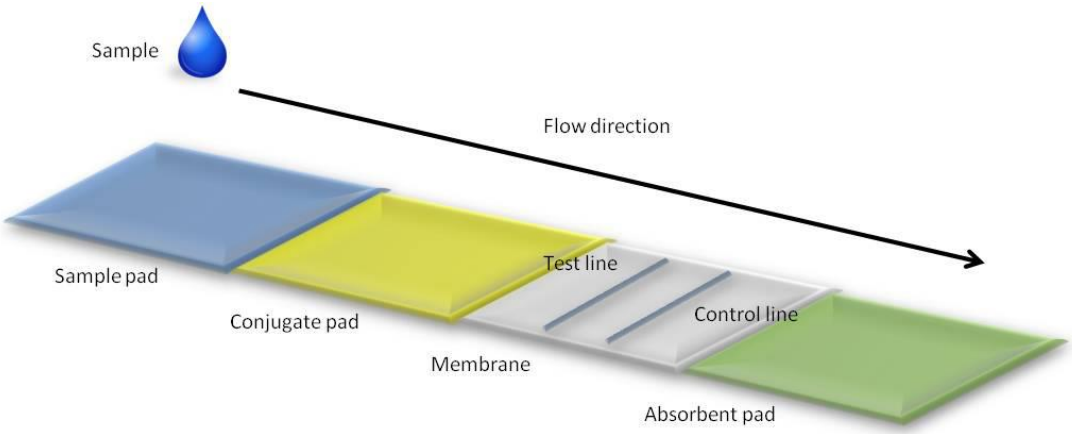

Figure 2 - Schematic representation of a lateral flow strip. A liquid sample is deposited on to the sample pad, migrating through a conjugate pad and a porous membrane for detection in a final absorbent pad. In most strip tests, the appearance of the control line indicates a valid test, while the appearance of a second test line indicates a positive result. (Valentina Busin).

There is a significant market for the use of LFIAs for a range of acute and chronic diseases or conditions in companion animals. Some diseases have received considerably greater attention, notably viral infection diseases, such as Feline Immunodeficiency Virus (FIV) and Feline Leukemia Virus (FeLV) in cats [62] and parvovirus in dogs [63], as well as arthropod-borne disease, especially anaplasmosis and dirofilariasis [64-66] with an extended range of assays being available. For livestock, LFIAs have been

focused mainly on illnesses that represent a substantial economic burden and/or serious zoonotic or epidemic diseases. Diagnosis of some of the OIE-listed diseases of the World Organization for Animal Health, such as Foot-and-Mouth Disease (FMD) [67-69], Rinderpest [70] and Peste des Petit Ruminants [71] have already been successfully translated into LFIAs, In these cases, endemic areas are frequently in developing countries, and often diagnosis is not reached due to the prolonged time between collection of samples, arrival at the reference laboratory and subsequent testing [72]. Finally, LFIAs have also been successfully applied for the detection of food-borne pathogens and of fraudulent substances in animal feed or in animal products. In the first case, much emphasis is placed on the prevention of serious zoonotic diseases, such as the highly pathogenic *Escherichia coli* O157:H7 [73] or salmonellosis [74], which represent a significant and widespread public health threat. In the second case, unauthorised drug residues [75, 76] and antimicrobial contamination [77-81] dominate the scene, both in terms of research and public attention. Here, an on-site test can be a powerful tool for rapid detection and subsequent action, especially when dealing with highly perishable products.

Compared with conventional lab-based tests, LFIAs are considerably less expensive, but, due to the different materials required, they are still relatively costly (~ £10 for a pregnancy test [60]) for application in low-resource settings [82], and, due to the multi-step processes involved, manufacturing time is extended, making them less suitable for high-throughput production. They usually provide a qualitative or semi-quantitative result, and analytical performance is generally poorer than lab-based tests, mainly due to reduced sensitivity [63, 83] and the possibility of errors due to testing by untrained personnel [33]. When compared with reference laboratory tests, specificity tends to be comparable, while sensitivity can be as low as 16%, suggesting that a positive result might be trusted, whereas, in the case of negative results, further confirmatory laboratory testing may be advisable. Several studies have assessed quantitation, but such devices still require instrumentation [84, 85] and trained personnel, and are still limited to single analyte testing.

1.4 Microfluidic technologies for disease diagnosis

One of the most promising technologies that has been applied recently in diagnostics is microfluidics, which involves the analysis of extremely small amounts (microlitres or nanolitres) of fluid using interconnected networks of channels measuring tens to hundreds of micrometres [86]. Since the introduction of microfluidics from the early 1990s [87], there has been a constant evolution of these methods, mainly following critical advances in microfabrication technologies [88]. Fluid transport in these devices is achieved by either passive (usually capillary forces) or active (generally pumping) mechanisms [89, 90], with the fluid flow being typically laminar [91].

Among the main advantages of microfluidics technologies for diagnostic applications are their portability and their low consumption of reagents; these attributes have made these devices inexpensive, rapid and generally easier to use compared with conventional (macroscale) testing [92]. The use of very small volumes, associated with shorter diffusional distances, results in significantly reduced time for analysis, making microfluidic assays significantly more rapid to perform than their macroscale equivalents [93]. Furthermore, being able to perform all necessary steps within one device and potentially in a single reaction represent a considerable advantage, allowing sample pre-treatment, analysis, signal detection and amplification in the same device [94]. Automated control of all steps can reduce inherent human error, which in turn increases the quality, reproducibility and reliability of assay results. The higher degree of control of fluid flow and the timing of binding reactions can also result in significantly improved analytical performance [95], while the opportunity for tests to be carried out simultaneously offers considerable potential for multiplexing [94]. Examples of the successful applications of these new technologies are in the clinical analysis of blood [96-98], pathogen identification [99, 100], genetic testing [101, 102], detection of environmental contaminants [103] and for drug screening [104].

Currently, two main types of microfluidic systems are used in the diagnostic field: micro total analysis systems (μTAS) and microfluidic paper-based analytical devices (μPADs). However, to date, there has been very limited application of this technology in the veterinary field [105].

1.4.1 Micro total analysis systems (µTAS)

These systems are also commonly known as "lab on a chip" (LOC) devices (Figure 3), which use fluid as a working medium and can integrate a number of different functionalities on a micro scale [88]. One of the main advantages of µTAS is that they allow for all steps (from sample pre-treatment to signal detection) to be carried out at once, on the same device, allowing complicated molecular techniques (i.e. polymerase chain reaction (PCR)) to be transferred on the chip for POC testing. These devices are fabricated using techniques from the microelectronics industry [106], mostly using materials, such as silicon, glass and/or polymers (e.g. PMMA or PDMS) [107]. At present, the most common materials used are thermoplastic polymers. These devices have reduced production costs, and have suitable mechanical, chemical and thermal properties [108].

Their diagnostic use is well established, with companies already commercialising POC devices on plastic platforms [109]. In the last decade, there has been a considerable focus on immunodiagnostic tests for the detection of disease markers, specifically for cardiac and cancer markers [110-113] and for the diagnosis of infectious diseases, including HIV/AIDS [114, 115], influenza [116] and hepatitis [117]. Some limitations of these devices are inherent in their physical effects, such as the need for pressure-driven liquid flow, with the possible consequence of heat generation and, therefore, detrimental effects on biomolecules, or low grade mass transfer and/or reduced mixing capacity [88].

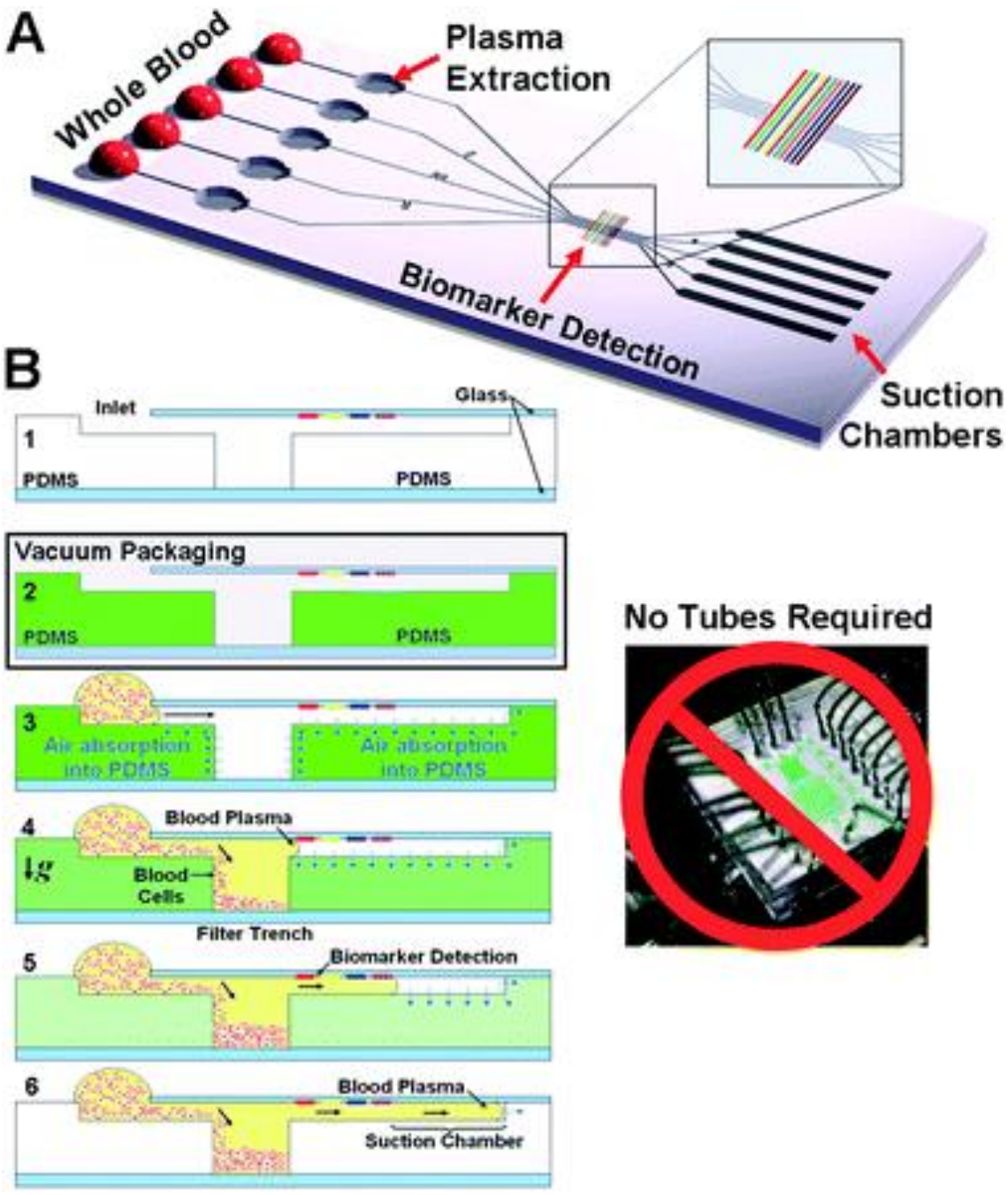

Figure 3 - Stand-alone, self-powered integrated microfluidic blood analysis system (SIMBAS). A) The microfluidic platform integrates plasma separation from whole-blood with multiple immunoassays. B) Cross section of the device: fabrication materials (1); storage of the device in a vacuum package (2); addition of 5ml of whole-blood sample on the inlet, degas-driven flow propels the sample into the device (3); blood cells sediment gravitationally and are filtered, while plasma flows into the channel (4); detection of multiple biomarkers (5); the flow is stopped by the suction chamber (6). Reprinted with permission from [98]. Copyright (2010) Royal Society of Chemistry.

1.4.2 Microfluidic paper-based analytical devices (µPADs)

These devices are commonly referred to as paper-based microfluidics (Figure 4), a concept that has been extensively explored by the Whiteside group at Harvard University and the Yager group at University of Washington, following on from initial research performed on paper strips for the determination of pH [118].

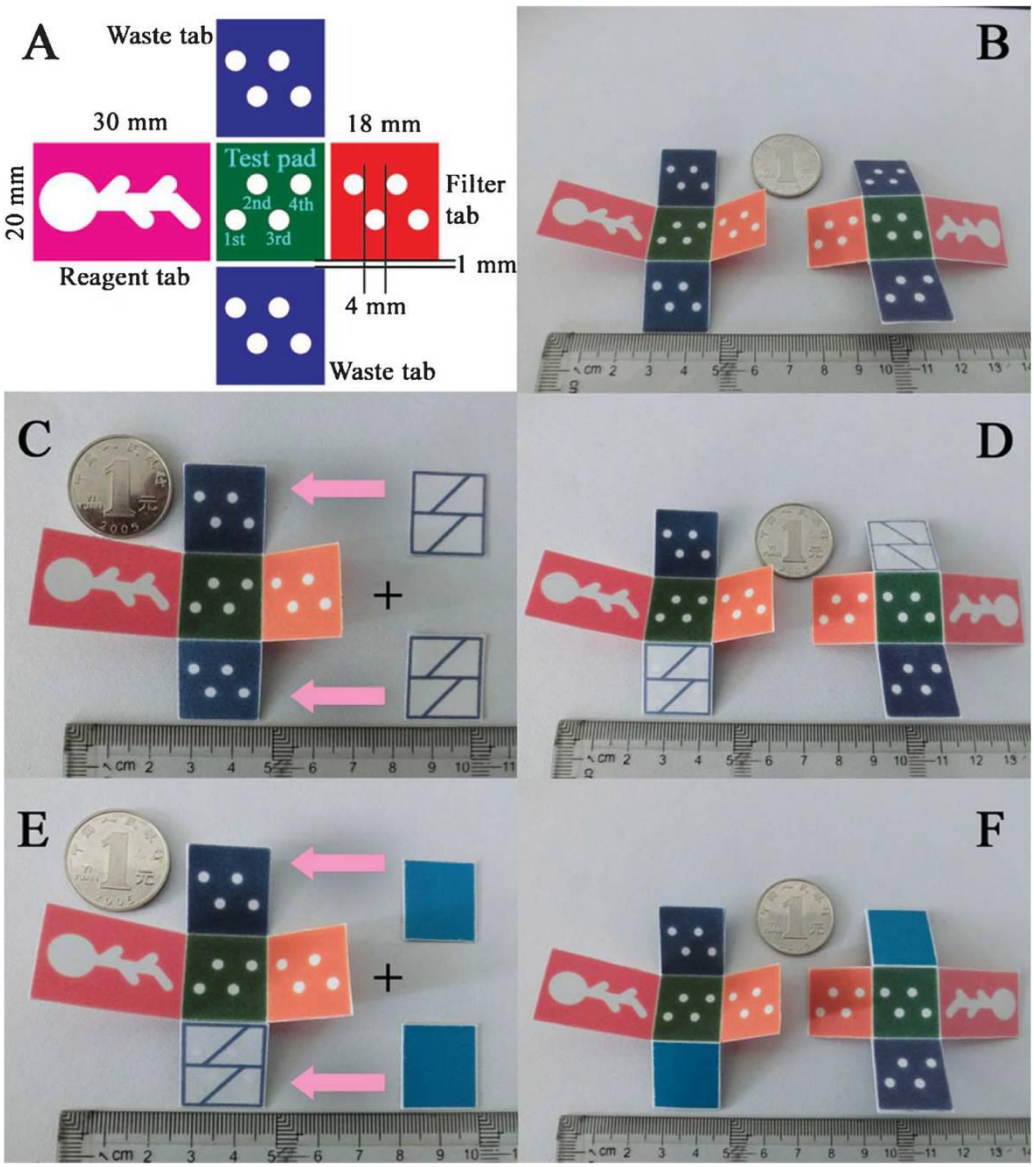

Figure 4 - 3D origami-based microfluidic paper based analytical device. A) Schematic representation, size and shape of the 3D origami-based device. B) The front and back surface of the device. C-D) Binding of a baked thin wax-patterned blotting paper on each waste tab, front (C) and back (D). E-F) Binding of an unbaked thick wax-patterned blotting paper on each waste tab. The assay procedure is carried out by folding the different tabs above the test pad and adding the reagents sequentially, with the aid of a customised device folder. Reprinted with permission from [119]. Copyright (2012) Royal Society of Chemistry.

Paper has considerable advantages over other materials in that it is cheap, easy to source, biodegradable and naturally abundant, but also simple to modify chemically [120]. POC devices made from paper also have the advantage of not requiring external power sources, whilst fabrication techniques and machinery for production are usually less expensive than those for other materials, with minimal technical expertise required [121]. Paper represents an excellent medium for diagnostic testing, due to its high surface to volume ratio, which allows reagents to be concentrated, enabling more rapid reaction times [122]. Surface-chemical properties characteristic of paper mean it does not swell with water and has high surface energy, with increased absorption properties [123].

Although μTAS are renowned for being less expensive than conventional lab-based testing, materials such as glass and silicon can still be considered expensive, either in terms of their environmental footprint or in their production costs [94]. Therefore, one of the main advantages of choosing μPADs over μTAS as a diagnostic platform is their further reduction in cost. μPADs are also considered to be "easier" to produce, with no requirement for valves or pumps, as they use capillary force to move fluids within the device [121]. However, there can be issues with sample retention and evaporation, making them less suited to the analysis of small volumes [124]. These devices allow inexpensive multiplexed analyses to be carried out [125], while maintaining the advantages of conventional microfluidic technology, such as size, speed and reduced sample volumes [38].

The most widely used types of paper to fabricate these devices are chromatography [126-128] and filter paper [129, 130]. These types of paper are made 100% from cotton, where fibre molecules are closely packed and parallel to one other, which result in high degree of reproducibility and uniformity [131], as well as being highly hydrophilic. They also have a white colour, which represent an important factor in image analysis.

Fabrication of μPADs is based on the construction of hydrophobic barriers/walls to physically separate hydrophilic zones, preventing cross contamination. At present, ten different techniques have been described in the literature for the fabrication of paper-based microfluidic devices: photolithography [132, 133], PDMS printing [134], ink jet

etching [60, 130], plasma treatment [135], wax printing [136-139], modified ink jet printing [140-142], flexography printing [143], screen printing [139], laser treatment [144] and paper cutting [127, 145, 146]. Among these, the wax printing method has become the most frequently used process for fabrication of μPADs. Using a wax-based ink printer, the wax is deposited onto a paper surface, then heated on a hot plate to melt the wax, generating hydrophobic areas. Although it represents a low-cost technique and it is a reasonably user-friendly method [137], it can be unstable at high temperatures [147], making it less suitable for long-term storage, especially in developing countries and it can also suffer from poor channel resolution [82]. Methods based on two-dimensional cutting, have been proposed has a valid alternative to the physical deposition of hydrophobic materials, as they are suitable for mass production and require less instrumentation. In this case, a computer-controlled knife plotter [146] or a CO_2 laser [148] is employed to physically remove paper and create microchannels and reaction zones. The main challenge in this case, is represented by the necessity to provide a robust support for the shaped paper, which can result in high-cost of the device [147].

1.4.2.1 P-ELISA

Within the field of µPADs, a very interesting application has recently been demonstrated in the translation of ELISA onto paper or P-ELISA [122]. P-ELISA combines the sensitivity and specificity of ELISA with the intrinsic low cost and ease-of-use of paper-based platforms [149]. There are increasing numbers of studies reporting the use of P-ELISA as a valid alternative to the conventional format [150-154].

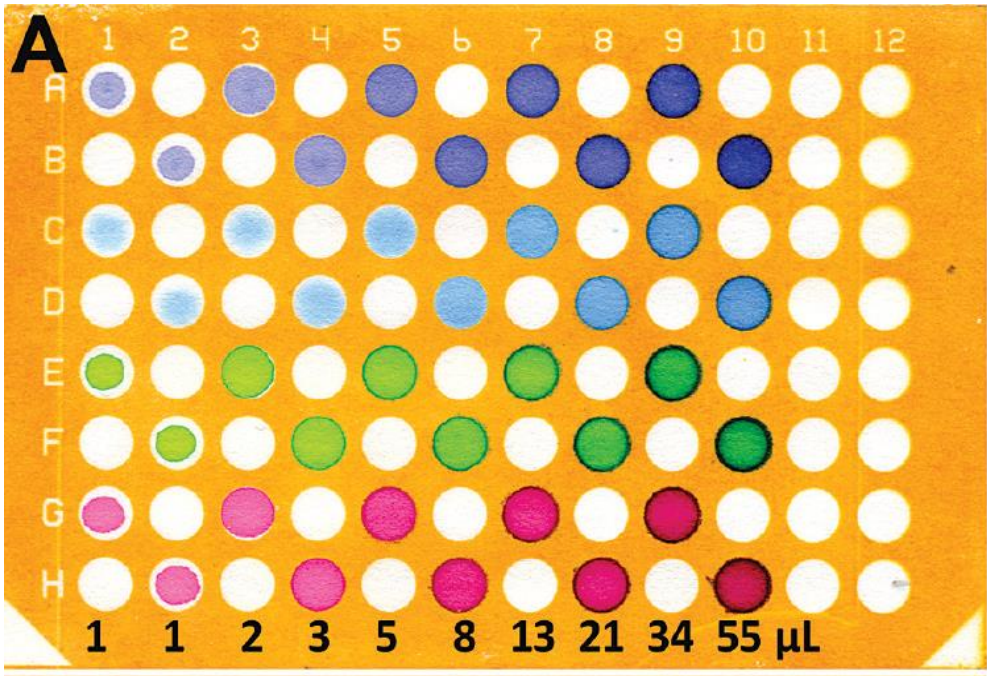

Figure 5 - 96-zone paper plate produced using photolithography after application of a range of volumes (1 to 55 µL) of coloured dye solutions. Reprinted with permission from [122]. Copyright (2009) American Chemical Society.

The conventional lab-based ELISA has substantial drawbacks in terms of cost and time. It needs dedicated instrumentation (a plate reader and a plate washer), it requires large volumes of reagents (usually 200-300µl) and it necessitates extending incubation time between steps (typically around 1hour). In the case of P-ELISA, 96-zone plates are created using the same techniques described for µPADS, with the additional possibility of custom-made format to widen the range of tests that can be performed and maximise the output [122]. Stages are comparable to those in the lab-based ELISA, where a capture molecule is immobilised within the paper substrate, a sample is incubated onto the platform and a detection reagent is used to visually assess the presence of the

analyte of interest. The most common detection method for P-ELISA is colorimetric [131, 151, 152, 155, 156], which allows for either visual detection by eye for qualitative measurement [157] or image analysis for quantitative measurement, with the option of using either a desktop scanner [151] or, even more appealing for POC application, a digital or a smartphone camera [150]. Other options include the use of chemiluminescence [154] and electrochemical methods [158], although they would require special instrumentation. Overall, the main advantages of P-ELISA are the significant reduction in cost, which can be around £6 [159] and time, which is usually below one hour.

While sensitivity is still about a magnitude below that normally expected from lab-based ELISA [152], nonetheless its potential for future application in the field at high-throughput and low cost is significant.

1.4.2.2 3D microfluidic paper-based analytical device (3D µPAD)

A further development in the concept of µPADs, has recently been introduced with the creation of 3D paper-based microfluidic devices. The main advantages are the possibility of multiplexing [119], the reduction in steps done by the operator [160] and the more rapid distribution of the sample [161], by having fluid moving in a vertical direction. At the moment, two main fabrication methods for these devices are reported in literature. One is to bond each patterned paper layer to the next, by using double-sided adhesive tape [160, 162, 163], adhesive spray [161] or thermal adhesive [164]. They allow for multiple layers (up to 8) to be contained in one device, but some might need cellulose powder [162] or hydrophilic material [165] to reduce the gaps between layers or require very high temperature for bonding [164], which could destroy heat sensitive reagents. The other one is based on the origami technique, where layers are folded together and hold in place with custom-made holders [119, 166, 167]. This method allows for direct contact between layers, but requires the fabrication of additional material. These devices have been used mainly for simple assays, like detection of glucose and protein [131, 161, 162, 164, 168], but recently some devices have been successfully employed for more complicated immunoassay, such as multiplex detection of cancer markers in whole blood [119], a sandwich ELISA for pregnancy diagnosis [163] and an indirect ELISA for IgG detection [165].

There is great scope in this research field to integrate these new platforms with more complex laboratory techniques, such as nucleic acid amplification [169, 170], DNA extraction [171] or whole blood analysis [172]. Focus should also be placed on enabling these devices to become truly POC, by taking advantage of the technologies already in place for remote and cost efficient diagnosis [173, 174] as well as on increasing commercialisation [175], in order to reach those at the end point and make a real contribution in advancing healthcare for both human and veterinary medicine.

1.4.3 Challenges for the application of microfluidic technologies in point-of-care veterinary diagnostics

One of the biggest challenges in the field of microfluidics is the translation from academic research to end-user products [176]. While the field of microfluidics has seen an exponential development in recent years, the launch of a commercialised platform that would revolutionise the concept of microfluidic technologies is still lacking [177]. Unfortunately, the fact that the diagnostic field is already quite mature, makes it harder to find companies willing to invest in new areas [147], and the difficulties in changing people's attitudes toward testing can represent an additional hurdle, especially when methods have been in place for many years. In this respect, the perception that analytical performances are still inferior to conventional lab-based tests remains a considerable constraint to the uptake of these technologies [33]. However, there is evidence that when a rapid result can achieve a better treatment rate, the sensitivity of a test can play a less important role [178]. This situation is extremely applicable in the veterinary field, where owners may struggle to find time for follow up visits after a test has been performed, or it may be problematic for farmers to re-gather animals days after testing [179]. Furthermore, as already in place for instrumental veterinary POC testing [180], specific guidelines should be put in place for the quality assurance of newly developed POC tests, in order to provide a consistent and practical approach to evaluating their performance and increasing veterinarians' confidence in test results [181].

While some of the challenges faced in human healthcare have been addressed by the use of microfluidic technologies, this is not the case for animal health-related areas. For

example, although the use of microfluidic technologies is suited for telemedicine, the handling or recording of data needs to be carefully organised. Data management systems are available for POC [182], which allow for valuable information to be stored and made available in real time. However, in the case of notifiable diseases, like the case of sheep scab, specific rules and strict controls will be required to ensure that legislation is followed.

1.5 Aim and objectives of the research

The overall aim of this highly interdisciplinary project, based on the close collaboration between the Moredun Research Institute and Heriot Watt University, is to develop a low-cost, multiplexed, pen-side diagnostic test for sheep scab, combining detection of serum antibody (IgG) specific to the mite antigen, Pso o 2, with the detection of a previously characterised serum biomarker (Hp), using microfluidic paper-based analytical devices. Once developed, this diagnostic platform could potentially be applied to other veterinary disease models where diagnostic assays are available (e.g. Maedi-Visna/Caprine Arthritis Encephalitis, Enzootic Abortion of Ewes etc.), representing a very interesting option for the end-user (both veterinarians in practice and farmers) as it could overcome some of the major constraints surrounding farm animal diagnostics (mainly cost and time).

The specific project objectives are as follows:

- To develop a simple and effective fabrication technique for high-throughput production of microfluidic paper-based analytical devices, based on paper cutting and lamination methods.
- To translate and validate the individual immunoassays for diagnosis of sheep scab (Pso o 2 and Hp) from the conventional lab-based format onto a paper-based microfluidic test platform (P-ELISA).
- To develop and fabricate a working 3D microfluidic paper-based analytical device (3D µPAD), based on the previously developed fabrication technique.
- To incorporate the individual assays into a single multiplexed platform on the developed 3D µPAD.

1.6 References

[1] van den Broek, A.H. and Huntley, J.F. Sheep Scab: the disease, pathogenesis and control. *Journal of Comparative Pathology*, 2003. **128**(2–3): p. 79-91.

[2] O'Brien, D.J., Gray, J.S., and Oreilly, P.F. Survival and retention of infectivity of the mite *Psoroptes ovis* off the host. *Veterinary Research Communications*, 1994. **18**(1): p. 27-36.

[3] Kirkwood, A.C. History, biology and control of sheep scab. *Parasitology Today*, 1986. **2**(11): p. 302-307.

[4] Bates, P. The pathogenesis and ageing of sheep scab lesions - part 1. *State Veterinary Journal*, 1997. **7**(3): p. 11-15.

[5] Nieuwhof, G.J. and Bishop, S.C. Costs of the major endemic diseases of sheep in Great Britain and the potential benefits of reduction in disease impact. *Animal Science*, 2005. **81**: p. 23-29.

[6] Phillips, K.A. Stamp out scab - Training and awarness campaign. *Proceedings of the Sheep Veterinary Society*, 2013. **37**: p. 21-23.

[7] Losson, B.J. Sheep psoroptic mange: An update. *Veterinary Parasitology*, 2012. **189**(1): p. 39-43.

[8] Cross, P., Edwards-Jones, G., Omed, H., and Williams, A.P. Use of a Randomized Response Technique to obtain sensitive information on animal disease prevalence. *Preventive Veterinary Medicine*, 2010. **96**(3-4): p. 252-262.

[9] Rose, H., Learmount, J., Taylor, M., and Wall, R. Mapping risk foci for endemic sheep scab. *Veterinary Parasitology*, 2009. **165**(1-2): p. 112-118.

[10] Bisdorff, B., Milnes, A., and Wall, R. Prevalence and regional distribution of scab, lice and blowfly strike in Great Britain. *Veterinary Record*, 2006. **158**(22): p. 749-752.

[11] Rose, H. and Wall, R. Endemic sheep scab: Risk factors and the behaviour of upland sheep flocks. *Preventive Veterinary Medicine*, 2012. **104**(1-2): p. 101-106.

[12] Taylor, M.A. Parasitological examinations in sheep health management. *Small Ruminant Research*, 2010. **92**(1-3): p. 120-125.

[13] Wells, B., Burgess, S.T.G., McNeilly, T.N., Huntley, J.F., and Nisbet, A.J. Recent developments in the diagnosis of ectoparasite infections and disease

through a better understanding of parasite biology and host responses. *Molecular and Cellular Probes*, 2012. **26**(1): p. 47-53.

[14] Ochs, H., Lonneux, J.F., Losson, B.J., and Deplazes, P. Diagnosis of psoroptic sheep scab with an improved enzyme-linked immunosorbent assay. *Veterinary Parasitology*, 2001. **96**(3): p. 233-242.

[15] He, M.L., Xu, J., He, R., Shen, N.X., Gu, X.B., Peng, X.R., and Yang, G.Y. Preliminary analysis of *Psoroptes ovis* transcriptome in different developmental stages. *Parasites & Vectors*, 2016. **9**: p. 570-582.

[16] van den Broek, A.H.M., Huntley, J.F., Machell, J., Taylor, M.A., and Miller, H.R.P. Temporal pattern of isotype-specific antibody responses in primary and challenge infestations of sheep with *Psoroptes ovis*—the sheep scab mite. *Veterinary Parasitology*, 2003. **111**(2–3): p. 217-230.

[17] Wassall, D.A., Kirkwood, A.C., Bates, P.G., and Sinclair, I.J. Enzyme-linked-immunosorbent-assay for the detection of antibodies to the sheep scab mite *Psoroptes ovis*. *Research in Veterinary Science*, 1987. **43**(1): p. 34-35.

[18] Boyce, W.M., Jessup, D.A., and Clark, R.K. Serodiagnostic antibody-resposnes to *Psoroptes sp.* infestations in bighorn sheep. *Journal of Wildlife Diseases*, 1991. **27**(1): p. 10-15.

[19] Lee, A.J., Machell, J., Van Den Broek, A.H., Nisbet, A.J., Miller, H.R., Isaac, R.E., and Huntley, J.F. Identification of an antigen from the sheep scab mite, *Psoroptes ovis*, homologous with house dust mite group I allergens. *Parasite Immunology*, 2002. **24**(8): p. 413-22.

[20] Temeyer, K.B., Soileau, L.C., and Pruett, J.H. Cloning and sequence analysis of a cDNA encoding Pso o II, a mite group II allergen of the sheep scab mite (Acari : Psoroptidae). *Journal of Medical Entomology*, 2002. **39**(2): p. 384-391.

[21] Rodríguez-Cadenas, F., Carbajal-González, M.T., Fregeneda-Grandes, J.M., Aller-Gancedo, J.M., Huntley, J.F., and Rojo-Vázquez, F.A. Development and evaluation of an antibody ELISA for sarcoptic mange in sheep and a comparison with the skin-scraping method. *Preventive Veterinary Medicine*, 2010. **96**(1–2): p. 82-92.

[22] Nunn, F.G., Burgess, S.T., Innocent, G., Nisbet, A.J., Bates, P., and Huntley, J.F. Development of a serodiagnostic test for sheep scab using recombinant protein Pso o 2. *Molecular and Cellular Probes*, 2011. **25**(5-6): p. 212-8.

[23] Burgess, S.T., Innocent, G., Nunn, F., Frew, D., Kenyon, F., Nisbet, A.J., and Huntley, J.F. The use of a *Psoroptes ovis* serodiagnostic test for the analysis of a natural outbreak of sheep scab. *Parasite & Vectors*, 2012. **5**: p. 7-17.

[24] Wells, B., Burgess, S.T., and Nisbet, A.J. Characterization of the ovine complement 4 binding protein-beta (C4BPB) chain as a serum biomarker for enhanced diagnosis of sheep scab. *Molecular and Cellular Probes*, 2013. **27**(3-4): p. 158-63.

[25] Murata, H., Shimada, N., and Yoshioka, M. Current research on acute phase proteins in veterinary diagnosis: an overview. *The Veterinary Journal*, 2004. **168**(1): p. 28-40.

[26] Eckersall, P.D., Lawson, F.P., Bence, L., Waterston, M.M., Lang, T.L., Donachie, W., and Fontaine, M.C. Acute phase protein response in an experimental model of ovine caseous lymphadenitis. *BMC veterinary research*, 2007. **3**: p. 35-41.

[27] Heegaard, P.M.H., Godson, D.L., Toussaint, M.J.M., Tjornehoj, K., Larsen, L.E., Viuff, B., and Ronsholt, L. The acute phase response of haptoglobin and serum amyloid A (SAA) in cattle undergoing experimental infection with bovine respiratory syncytial virus. *Veterinary Immunology and Immunopathology*, 2000. **77**(1-2): p. 151-159.

[28] Holland, B.P., Step, D.L., Burciaga-Robles, L.O., Fulton, R.W., Confer, A.W., Rose, T.K., Laidig, L.E., Richards, C.J., and Krehbiel, C.R. Effectiveness of sorting calves with high risk of developing bovine respiratory disease on the basis of serum haptoglobin concentration at the time of arrival at a feedlot. *American Journal of Veterinary Research*, 2011. **72**(10): p. 1349-1360.

[29] Godson, D.L., Campos, M., AttahPoku, S.K., Redmond, M.J., Cordeiro, D.M., Sethi, M.S., Harland, R.J., and Babiuk, L.A. Serum haptoglobin as an indicator of the acute phase response in bovine respiratory disease. *Veterinary Immunology and Immunopathology*, 1996. **51**(3-4): p. 277-292.

[30] Young, C.R., Eckersall, P.D., Saini, P.K., and Stanker, L.H. Validation of immunoassays for bovine haptoglobin. *Veterinary Immunology and Immunopathology*, 1995. **49**(1-2): p. 1-13.

[31] Wells, B., Innocent, G.T., Eckersall, P.D., McCulloch, E., Nisbet, A.J., and Burgess, S.T.G. Two major ruminant acute phase proteins, haptoglobin and

serum amyloid A, as serum biomarkers during active sheep scab infestation. *Veterinary Research*, 2013. **44**(103): p. 103-114.

[32] St-Louis, P. Status of point-of-care testing: Promise, realities, and possibilities. *Clinical Biochemistry*, 2000. **33**(6): p. 427-440.

[33] von Lode, P. Point-of-care immunotesting: Approaching the analytical performance of central laboratory methods. *Clinical Biochemistry*, 2005. **38**(7): p. 591-606.

[34] Foster, K., Despotis, G., and Scott, M.G. Point-of-care testing - Cost issues and impact on hospital operations. *Clinics in Laboratory Medicine*, 2001. **21**(2): p. 269-84.

[35] Mabey, D., Peeling, R.W., Ustianowski, A., and Perkins, M.D. Diagnostics for the developing world. *Nature Reviews Microbiology*, 2004. **2**(3): p. 231-240.

[36] Drenck, N.-E. Point of care testing in Critical Care Medicine: the clinician's view. *Clinica Chimica Acta*, 2001. **307**(1–2): p. 3-7.

[37] Peeling, R.W., Holmes, K.K., Mabey, D., and Ronald, A. Rapid tests for sexually transmitted infections (STIs): the way forward. *Sexually Transmitted Infections*, 2006. **82**: p. V1-V6.

[38] Rozand, C. Paper-based analytical devices for point-of-care infectious disease testing. *European Journal of Clinical Microbioliogy & Infectious Diseases*, 2013. **33**(2): p. 147-56.

[39] Bollo, E. Nanotechnologies applied to veterinary diagnostics. *Veterinary Research Communications*, 2007. **31**: p. 145-147.

[40] Kost, G.J. Guidelines for point-of-care testing. Improving patient outcomes. *American Journal of Clinical Pathology*, 1995. **104**(4): p. S111-S127.

[41] Adak, G.K., Long, S.M., and O'Brien, S.J. Trends in indigenous foodborne disease and deaths, England and Wales: 1992 to 2000. *Gut*, 2002. **51**(6): p. 832-841.

[42] Chen, K., He, W., Lu, H., Song, D., Gao, W., Lan, Y., Zhao, K., and Gao, F. Development of an Immunochromatographic Strip for Serological Diagnosis of Porcine Hemagglutinating Encephalomyelitis Virus. *Journal of Veterinary Diagnostic Investigation*, 2011. **23**(2): p. 288-296.

[43] Cui, S.J., Zhou, S.H., Chen, C.M., Qi, T., Zhang, C.F., and Oh, J. A simple and rapid immunochromatographic strip test for detecting antibody to porcine

reproductive and respiratory syndrome virus. *Journal of Virological Methods*, 2008. **152**(1-2): p. 38-42.

[44] Banyard, A.C., Horton, D.L., Freuling, C., Muller, T., and Fooks, A.R. Control and prevention of canine rabies: The need for building laboratory-based surveillance capacity. *Antiviral Research*, 2013. **98**(3): p. 357-364.

[45] Howe, K.S., Hasler, B., and Stark, K.D.C. Economic principles for resource allocation decisions at national level to mitigate the effects of disease in farm animal populations. *Epidemiology and Infection*, 2013. **141**(1): p. 91-101.

[46] Abd El Wahed, A., El-Deeb, A., El-Tholoth, M., Abd El Kader, H., Ahmed, A., Hassan, S., Hoffmann, B., Haas, B., Shalaby, M.A., Hufert, F.T., and Weidmann, M. A portable reverse transcription recombinase polymerase amplification assay for rapid detection of Foot-and-Mouth Disease Virus. *PLoS One*, 2013. **8**(8): p. e71642.

[47] Fraser, C.G. Optimal analytical performance for point of care testing. *Clinica Chimica Acta*, 2001. **307**(1–2): p. 37-43.

[48] Robinson, P.A. and Epperson, W.B. Farm animal practitioners' views on their use and expectations of veterinary diagnostic laboratories. *Veterinary Record*, 2013. **172**(19): p. 503-508.

[49] Smith, B.C., Peake, M.J., and Fraser, C.G. Urinalysis by use of multi-test reagent strips: 2 dipsticks compared. *Clinical Chemistry*, 1977. **23**(12): p. 2337-2340.

[50] Garner, B.C. and Wiedmeyer, C.E. Comparison of a semiquantitative point-of-care assay for the detection of canine microalbuminuria with routine semiquantitative methods for proteinuria. *Veterinary Clinical Pathology*, 2007. **36**(3): p. 240-244.

[51] Zatelli, A., Paltrinieri, S., Nizi, F., Roura, X., and Zini, E. Evaluation of a urine dipstick test for confirmation or exclusion of proteinuria in dogs. *American Journal of Veterinary Research*, 2010. **71**(2): p. 235-240.

[52] Lyon, S.D., Sanderson, M.W., Vaden, S.L., Lappin, M.R., Jensen, W.A., and Grauer, G.F. Comparison of urine dipstick, sulfosalicylic acid, urine protein-to-creatinine ratio, and species-specific ELISA methods for detection of albumin in urine samples of cats and dogs. *Journal of the American Veterinary Medical Association*, 2010. **236**(8): p. 874-879.

[53] Oetzel, G.R. Monitoring and testing dairy herds for metabolic disease. *Veterinary Clinics of North America - Food Animal Practice*, 2004. **20**(3): p. 651-674.

[54] Hornig, K.J., Byers, S.R., Callan, R.J., Holt, T., Field, M., and Han, H. Evaluation of a point-of-care glucose and beta-hydroxybutyrate meter operated in various environmental conditions in prepartum and postpartum sheep. *American Journal of Veterinary Research*, 2013. **74**(8): p. 1059-1065.

[55] Iwersen, M., Falkenberg, U., Voigtsberger, R., Forderung, D., and Heuwieser, W. Evaluation of an electronic cowside test to detect subclinical ketosis in dairy cows. *Journal of Dairy Science*, 2009. **92**(6): p. 2618-2624.

[56] Panousis, N., Brozos, C., Karagiannis, I., Giadinis, N.D., Lafi, S., and Kritsepi-Konstantinou, M. Evaluation of Precision Xceed (R) meter for on-site monitoring of blood beta-hydroxybutyric acid and glucose concentrations in dairy sheep. *Research in Veterinary Science*, 2012. **93**(1): p. 435-439.

[57] Link, N., Weber, W., and Fussenegger, M. A novel generic dipstick-based technology for rapid and precise detection of tetracycline, streptogramin and macrolide antibiotics in food samples. *Journal of Biotechnology*, 2007. **128**(3): p. 668-680.

[58] Plotnick, A.N. and Greco, D.S. Home management of cats and dogs with diabetes mellitus. Common questions asked by veterinarians and clients. *Veterinary Clinics of North America - Small Animal Practice*, 1995. **25**(3): p. 753-759.

[59] Posthuma-Trumpie, G.A., Korf, J., and van Amerongen, A. Lateral flow (immuno) assay: its strengths, weaknesses, opportunities and threats. A literature survey. *Analytical and Bioanalytical Chemistry*, 2009. **393**(2): p. 569-582.

[60] Abe, K., Kotera, K., Suzuki, K., and Citterio, D. Inkjet-printed paperfluidic immuno-chemical sensing device. *Analytical and Bioanalytical Chemistry*, 2010. **398**(2): p. 885-893.

[61] May, K. Home tests to monitor fertility. *American Journal of Obstetrics and Gynecology*, 1991. **165**(6): p. 2000-2002.

[62] Hartmann, K., Werner, R.M., Egberink, H., and Jarrett, O. Comparison of six in-house tests for the rapid diagnosis of feline immunodeficiency and feline leukaemia virus infections. *Veterinary Record*, 2001. **149**(11): p. 317-320.

[63] Schmitz, S., Coenen, C., Matthias, K., Heinz-Jürgen, T., and Neiger, R. Comparison of three rapid commercial canine parvovirus antigen detection tests with electron microscopy and polymerase chain reaction. *Journal of Veterinary Diagnostic Investigation*, 2009. **21**(3): p. 344-345.

[64] Wong, S.S.Y., Teng, J.L.L., Poon, R.W.S., Choi, G.K.Y., Chan, K.H., Yeung, M.L., Hui, J.J.Y., and Yuen, K.Y. Comparative evaluation of a point-of-care immunochromatographic test SNAP 4Dx with molecular detection tests for vector-borne canine pathogens in Hong Kong. *Vector-Borne and Zoonotic Diseases*, 2011. **11**(9): p. 1269-1277.

[65] Couto, C.G., Lorentzen, L., Beall, M.J., Shields, J., Bertolone, N., Couto, J.I., Couto, K.M., Nash, S., Slack, J., Kvitko, H., Westendorf, N., Marin, L., Iazbik, M.C., Vicario, F.C., Sanz, P., and Ruano, R. Serological study of selected vector-borne diseases in shelter dogs in central Spain using point-of-care assays. *Vector-Borne and Zoonotic Diseases*, 2010. **10**(9): p. 885-888.

[66] Berdoulay, P., Levy, J.K., Snyder, P.S., Pegelow, M.J., Hooks, J.L., Tavares, L.M., Gibson, N.M., and Salute, M.E. Comparison of serological tests for the detection of natural heartworm infection in cats. *Journal of the American Animal Hospital Association*, 2004. **40**(5): p. 376-384.

[67] Lin, T., Shao, J.J., Du, J.Z., Cong, G.Z., Gao, S.D., and Chang, H.Y. Development of a serotype colloidal gold strip using monoclonal antibody for rapid detection type Asia1 foot-and-mouth disease. *Virology Journal*, 2011. **8**: p. 418.

[68] Reid, S.M., Ferris, N.P., Bruning, A., Hutchings, G.H., Kowalska, Z., and Akerblom, L. Development of a rapid chromatographic strip test for the pen-side detection of foot-and-mouth disease virus antigen. *Journal of Virological Methods*, 2001. **96**(2): p. 189-202.

[69] Yang, S.Z., Yang, J.F., Zhang, G.P., Qiao, S.L., Wang, X.N., Zhao, D., Li, X.W., Deng, R.G., Zhi, A.M., You, L.M., Chai, S.J., and Teng, M. Development of a peptide-based immunochromatographic strip for differentiation of serotype O Foot-and-mouth disease virus-infected pigs from vaccinated pigs. *Journal of Veterinary Diagnostic Investigation*, 2010. **22**(3): p. 412-415.

[70] Bruning, A., Bellamy, K., Talbot, D., and Anderson, J. A rapid chromatographic strip test for the pen-side diagnosis of rinderpest virus. *Journal of Virological Methods*, 1999. **81**(1-2): p. 143-154.

[71] Bruening-Richardson, A., Akerblom, L., Klingeborn, B., and Anderson, J. Improvement and development of rapid chromatographic strip-tests for the diagnosis of rinderpest and peste des petits ruminants viruses. *Journal of Virological Methods*, 2011. **174**(1-2): p. 42-46.

[72] Ferris, N.P., Nordengrahn, A., Hutchings, G.H., Reid, S.M., King, D.P., Ebert, K., Paton, D.J., Kristersson, T., Brocchi, E., Grazioli, S., and Merza, M. Development and laboratory validation of a lateral flow device for the detection of foot-and-mouth disease virus in clinical samples. *Journal of Virological Methods*, 2009. **155**(1): p. 10-17.

[73] Aldus, C.F., van Amerongen, A., Ariens, R.M.C., Peck, M.W., Wichers, J.H., and Wyatt, G.M. Principles of some novel rapid dipstick methods for detection and characterization of verotoxigenic *Escherichia coli*. *Journal of Applied Microbiology*, 2003. **95**(2): p. 380-389.

[74] Moongkarndi, P., Rodpai, E., and Kanarat, S. Evaluation of an immunochromatographic assay for rapid detection of *Salmonella enterica* serovars *typhimurium* and *enteritidis*. *Journal of Veterinary Diagnostic Investigation*, 2011. **23**(4): p. 797-801.

[75] Huo, T.M., Peng, C.F., Xu, C.L., and Liu, L.Q. Development of colloidal gold-based immunochromatographic assay for the rapid detection of medroxyprogesterone acetate residues. *Food and Agricultural Immunology*, 2006. **17**(3-4): p. 183-190.

[76] Zhang, G.P., Wang, X.N., Yang, J.F., Yang, Y.Y., Xing, G.X., Li, Q.M., Zhao, D., Chai, S.J., and Guo, J.Q. Development of an immunochromatographic lateral flow test strip for detection of beta-adrenergic agonist Clenbuterol residues. *Journal of Immunological Methods*, 2006. **312**(1-2): p. 27-33.

[77] Pazzola, M., Piras, G., Noce, A., Dettori, M.L., and Vacca, G.M. Evaluation of the rapid assay Betastar Combo 3.0 for the detection of Penicillin, Amoxicillin, Cefazolin and Oxytetracycline in individual sheep milk. *Small Ruminant Research*, 2015. **124**: p. 127-131.

[78] Reybroeck, W., Ooghe, S., De Brabander, H.F., and Daeseleire, E. Validation of the ßeta-s.t.a.r. 1+1 for rapid screening of residues of ß-lactam antibiotics in milk. *Food Additives and Contaminants Part a-Chemistry Analysis Control Exposure & Risk Assessment*, 2010. **27**(8): p. 1084-1095.

[79] O'Keeffe, M., Crabbe, P., Salden, M., Wichers, J., Van Peteghem, C., Kohen, F., Pieraccini, G., and Moneti, G. Preliminary evaluation of a lateral flow immunoassay device for screening urine samples for the presence of sulphamethazine. *Journal of Immunological Methods*, 2003. **278**(1-2): p. 117-126.

[80] Verheijen, R., Osswald, I.K., Dietrich, R., and Haasnoot, W. Development of a one step strip test for the detection of (dihydro)streptomycin residues in raw milk. *Food and Agricultural Immunology*, 2000. **12**(1): p. 31-40.

[81] Wang, X.L., Li, K., Shi, D.S., Xiong, N., Jin, X., Yi, J.D., and Bi, D.R. Development of an immunochromatographic lateral-flow test strip for rapid detection of sulfonamides in eggs and chicken muscles. *Journal of Agricultural and Food Chemistry*, 2007. **55**(6): p. 2072-2078.

[82] Ballerini, D.R., Li, X., and Shen, W. Patterned paper and alternative materials as substrates for low-cost microfluidic diagnostics. *Microfluidics and Nanofluidics*, 2012. **13**(5): p. 769-787.

[83] Al-Yousif, Y., Anderson, J., Chard-Bergstrom, C., and Kapil, S. Development, evaluation, and application of lateral-flow immunoassay (immunochromatography) for detection of rotavirus in bovine fecal samples. *Clinical and Diagnostic Laboratory Immunology*, 2002. **9**(3): p. 723-724.

[84] Lin, Y.Y., Wang, J., Liu, G.D., Wu, H., Wai, C.M., and Lin, Y.H. A nanoparticle label/immunochromatographic electrochemical biosensor for rapid and sensitive detection of prostate-specific antigen. *Biosensors & Bioelectronics*, 2008. **23**(11): p. 1659-1665.

[85] Mao, X., Baloda, M., Gurung, A.S., Lin, Y.H., and Liu, G.D. Multiplex electrochemical immunoassay using gold nanoparticle probes and immunochromatographic strips. *Electrochemistry Communications*, 2008. **10**(10): p. 1636-1640.

[86] Whitesides, G.M. The origins and the future of microfluidics. *Nature*, 2006. **442**(7101): p. 368-373.

[87] Manz, A., Graber, N., and Widmer, H.M. Miniaturized total chemical-analysis systems. A novel concept for chemical sensing. *Sensors and Actuators B-Chemical*, 1990. **1**(1-6): p. 244-248.

[88] Hardt, S. and Schönfeld, F. Chapter 1. Microfluidics: fundamentals and engineering concepts. *Microfluidic Technologies for Miniaturized Analysis Systems*, ed. Hardt, S. and Schonfeld, F. 2007, New York: Springer. 1-58.

[89] Juncker, D., Schmid, H., Drechsler, U., Wolf, H., Wolf, M., Michel, B., de Rooij, N., and Delamarche, E. Autonomous microfluidic capillary system. *Analytical Chemistry*, 2002. **74**(24): p. 6139-6144.

[90] Laser, D.J. and Santiago, J.G. A review of micropumps. *Journal of Micromechanics and Microengineering*, 2004. **14**(6): p. R35-R64.

[91] Stone, H.A., Stroock, A.D., and Ajdari, A. Engineering flows in small devices: Microfluidics toward a lab-on-a-chip. *Annual Review of Fluid Mechanics*, 2004. **36**: p. 381-411.

[92] de Mello, A. Plastic fantastic? *Lab on a Chip*, 2002. **2**(2): p. 31N-36N.

[93] Rattle, S., Hofmann, O., Price, C.P., Kricka, L.J., and Wild, D. Lab-on-a-Chip, Micro- and Nanoscale Immunoassay Systems, and Microarrays, in *The Immunoassay Handbook*, Wild, D., Editor. 2013, Elsevier: Oxford. p. 175-202.

[94] Chin, C.D., Linder, V., and Sia, S.K. Lab-on-a-chip devices for global health: Past studies and future opportunities. *Lab on a Chip*, 2007. **7**(1): p. 41-57.

[95] Gervais, L., de Rooij, N., and Delamarche, E. Microfluidic Chips for Point-of-Care Immunodiagnostics. *Advanced Materials*, 2011. **23**(24): p. H151-H176.

[96] Khan, M.S., Thouas, G., Shen, W., Whyte, G., and Garnier, G. Paper diagnostic for instantaneous blood typing. *Analytical Chemistry*, 2010. **82**(10): p. 4158-4164.

[97] Floris, A., Staal, S., Lenk, S., Staijen, E., Kohlheyer, D., Eijkel, J., and van den Berg, A. A prefilled, ready-to-use electrophoresis based lab-on-a-chip device for monitoring lithium in blood. *Lab on a Chip*, 2010. **10**(14): p. 1799-1806.

[98] Dimov, I.K., Basabe-Desmonts, L., Garcia-Cordero, J.L., Ross, B.M., Ricco, A.J., and Lee, L.P. Stand-alone self-powered integrated microfluidic blood analysis system (SIMBAS). *Lab on a Chip*, 2011. **11**(5): p. 845-850.

[99] Bunyakul, N., Edwards, K.A., Promptmas, C., and Baeumner, A.J. Cholera toxin subunit B detection in microfluidic devices. *Analytical and Bioanalytical Chemistry*, 2009. **393**(1): p. 177-186.

[100] Diercks, A.H., Ozinsky, A., Hansen, C.L., Spotts, J.M., Rodriguez, D.J., and Aderem, A. A microfluidic device for multiplexed protein detection in nano-liter volumes. *Analytical Biochemistry*, 2009. **386**(1): p. 30-35.

[101] Hopwood, A.J., Hurth, C., Yang, J.N., Cai, Z., Moran, N., Lee-Edghill, J.G., Nordquist, A., Lenigk, R., Estes, M.D., Haley, J.P., McAlister, C.R., Chen, X., Brooks, C., Smith, S., Elliott, K., Koumi, P., Zenhausern, F., and Tully, G. Integrated microfluidic system for rapid forensic DNA analysis: sample collection to DNA profile. *Analytical Chemistry*, 2010. **82**(16): p. 6991-6999.

[102] Shui, L.L., Bomer, J.G., Jin, M.L., Carlen, E.T., and van den Berg, A. Microfluidic DNA fragmentation for on-chip genomic analysis. *Nanotechnology*, 2011. **22**(49).

[103] Lafleur, J.P., Senkbeil, S., Jensen, T.G., and Kutter, J.P. Gold nanoparticle-based optical microfluidic sensors for analysis of environmental pollutants. *Lab on a Chip*, 2012. **12**(22): p. 4651-4656.

[104] Liu, C., Wang, L., Xu, Z., Li, J.M., Ding, X.P., Wang, Q., and Li, C.Y. A multilayer microdevice for cell-based high-throughput drug screening. *Journal of Micromechanics and Microengineering*, 2012. **22**(6).

[105] Garcia-Cordero, J.L., Barrett, L.M., O'Kennedy, R., and Ricco, A.J. Microfluidic sedimentation cytometer for milk quality and bovine mastitis monitoring. *Biomedical Microdevices*, 2010. **12**(6): p. 1051-1059.

[106] Kricka, L.J. Microchips, microarrays, biochips and nanochips: personal laboratories for the 21st century. *Clinica Chimica Acta*, 2001. **307**(1–2): p. 219-223.

[107] Lisowski, P. and Zarzycki, P. Microfluidic paper-based analytical devices (μPADs) and micro total analysis systems (μTAS): development, applications and future trends. *Chromatographia*, 2013. **76**(19/20): p. 1201-1214.

[108] Zhou, P., Young, L., and Chen, Z.Y. Weak solvent based chip lamination and characterization of on-chip valve and pump. *Biomedical Microdevices*, 2010. **12**(5): p. 821-832.

[109] Tomazelli Coltro, W.K., Cheng, C.-M., Carrilho, E., and de Jesus, D.P. Recent advances in low-cost microfluidic platforms for diagnostic applications. *Electrophoresis*, 2014. **35**(16): p. 2309-2324.

[110] Kallempudi, S.S., Altintas, Z., Niazi, J.H., and Gurbuz, Y. A new microfluidics system with a hand-operated, on-chip actuator for immunosensor applications. *Sensors and Actuators B: Chemical*, 2012. **163**(1): p. 194-201.

[111] Caulum, M.M., Murphy, B.M., Ramsay, L.M., and Henry, C.S. Detection of cardiac biomarkers using micellar electrokinetic chromatography and a cleavable tag immunoassay. *Analytical Chemistry*, 2007. **79**(14): p. 5249-5256.

[112] Darain, F., Yager, P., Gan, K.L., and Tjin, S.C. On-chip detection of myoglobin based on fluorescence. *Biosensors & Bioelectronics*, 2009. **24**(6): p. 1744-1750.

[113] Wang, S.Q., Zhao, X.H., Khimji, I., Akbas, R., Qiu, W.L., Edwards, D., Cramer, D.W., Ye, B., and Demirci, U. Integration of cell phone imaging with microchip ELISA to detect ovarian cancer HE4 biomarker in urine at the point-of-care. *Lab on a Chip*, 2011. **11**(20): p. 3411-3418.

[114] Cheng, X.H., Irimia, D., Dixon, M., Sekine, K., Demirci, U., Zamir, L., Tompkins, R.G., Rodriguez, W., and Toner, M. A microfluidic device for practical label-free CD4+T cell counting of HIV-infected subjects. *Lab on a Chip*, 2007. **7**(2): p. 170-178.

[115] Kim, Y.-G., Moon, S., Kuritzkes, D.R., and Demirci, U. Quantum dot-based HIV capture and imaging in a microfluidic channel. *Biosensors & Bioelectronics*, 2009. **25**(1): p. 253-258.

[116] Ferguson, B.S., Buchsbaum, S.F., Wu, T.-T., Hsieh, K., Xiao, Y., Sun, R., and Soh, H.T. Genetic analysis of H1N1 influenza virus from throat swab samples in a microfluidic system for point-of-care diagnostics. *Journal of the American Chemical Society*, 2011. **133**(23): p. 9129-9135.

[117] Lee, B.S., Lee, J.-N., Park, J.-M., Lee, J.-G., Kim, S., Cho, Y.-K., and Ko, C. A fully automated immunoassay from whole blood on a disc. *Lab on a Chip*, 2009. **9**(11): p. 1548-1555.

[118] Muller, R.H. and Clegg, D.L. Automatic paper chromatography. *Analytical Chemistry*, 1949. **21**(9): p. 1123-1125.

[119] Ge, L., Wang, S., Song, X., Ge, S., and Yu, J. 3D Origami-based multifunction-integrated immunodevice: low-cost and multiplexed sandwich

chemiluminescence immunoassay on microfluidic paper-based analytical device. *Lab on a Chip*, 2012. **12**(17): p. 3150-3158.

[120] Zhao, W.A. and van den Berg, A. Lab on paper. *Lab on a Chip*, 2008. **8**(12): p. 1988-1991.

[121] Martinez, A.W. Microfluidic paper-based analytical devices: from POCKET to paper-based ELISA. *Bioanalysis*, 2011. **3**(23): p. 2589-2592.

[122] Carrilho, E., Phillips, S.T., Vella, S.J., Martinez, A.W., and Whitesides, G.M. Paper microzone plates. *Analytical Chemistry*, 2009. **81**(15): p. 5990-5998.

[123] Pelton, R. Bioactive paper provides a low-cost platform for diagnostics. *Trends in Analytical Chemistry*, 2009. **28**(8): p. 925-942.

[124] Tian, J., Kannangara, D., Li, X., and Shen, W. Capillary driven low-cost V-groove microfluidic device with high sample transport efficiency. *Lab on a Chip*, 2010. **10**(17): p. 2258-2264.

[125] Li, X., Ballerini, D.R., and Shen, W. A perspective on paper-based microfluidics: Current status and future trends. *Biomicrofluidics*, 2012. **6**(1): p. 011301 1-13.

[126] Vella, S.J., Beattie, P., Cademartiri, R., Laromaine, A., Martinez, A.W., Phillips, S.T., Mirica, K.A., and Whitesides, G.M. Measuring markers of liver function using a micropatterned paper device designed for blood from a fingerstick. *Analytical Chemistry*, 2012. **84**(6): p. 2883-2891.

[127] Wang, W., Wu, W.Y., and Zhu, J.J. Tree-shaped paper strip for semiquantitative colorimetric detection of protein with self-calibration. *Journal of Chromatography A*, 2010. **1217**(24): p. 3896-3899.

[128] Zhao, C. and Liu, X. A portable paper-based microfluidic platform for multiplexed electrochemical detection of human immunodeficiency virus and hepatitis C virus antibodies in serum. *Biomicrofluidics*, 2016. **10**(2): p. 024119 1-10.

[129] Li, X., Tian, J.F., and Shen, W. Quantitative biomarker assay with microfluidic paper-based analytical devices. *Analytical and Bioanalytical Chemistry*, 2010. **396**(1): p. 495-501.

[130] Abe, K., Suzuki, K., and Citterio, D. Inkjet-printed microfluidic multianalyte chemical sensing paper. *Analytical Chemistry*, 2008. **80**(18): p. 6928-6934.

[131] Costa, M.N., Veigas, B., Jacob, J.M., Santos, D.S., Gomes, J., Baptista, P.V., Martins, R., Inacio, J., and Fortunato, E. A low cost, safe, disposable, rapid and self-sustainable paper-based platform for diagnostic testing: lab-on-paper. *Nanotechnology*, 2014. **25**(9): p. 094006.

[132] Martinez, A.W., Phillips, S.T., Carrilho, E., Thomas, S.W., Sindi, H., and Whitesides, G.M. Simple telemedicine for developing regions: Camera phones and paper-based microfluidic devices for real-time, off-site diagnosis. *Analytical Chemistry*, 2008. **80**(10): p. 3699-3707.

[133] Klasner, S.A., Price, A.K., Hoeman, K.W., Wilson, R.S., Bell, K.J., and Culbertson, C.T. Paper-based microfluidic devices for analysis of clinically relevant analytes present in urine and saliva. *Analytical and Bioanalytical Chemistry*, 2010. **397**(5): p. 1821-1829.

[134] Bruzewicz, D.A., Reches, M., and Whitesides, G.M. Low-cost printing of poly(dimethylsiloxane) barriers to define microchannels in paper. *Analytical Chemistry*, 2008. **80**(9): p. 3387-3392.

[135] Li, X., Tian, J.F., Nguyen, T., and Shen, W. Paper-based microfluidic devices by plasma treatment. *Analytical Chemistry*, 2008. **80**(23): p. 9131-9134.

[136] Lu, Y., Shi, W.W., Jiang, L., Qin, J.H., and Lin, B.C. Rapid prototyping of paper-based microfluidics with wax for low-cost, portable bioassay. *Electrophoresis*, 2009. **30**(9): p. 1497-1500.

[137] Carrilho, E., Martinez, A.W., and Whitesides, G.M. Understanding wax printing: a simple micropatterning process for paper-based microfluidics. *Analytical Chemistry*, 2009. **81**(16): p. 7091-7095.

[138] Leung, V., Shehata, A.A.M., Filipe, C.D.M., and Pelton, R. Streaming potential sensing in paper-based microfluidic channels. *Colloids and Surfaces a-Physicochemical and Engineering Aspects*, 2010. **364**(1-3): p. 16-18.

[139] Dungchai, W., Chailapakul, O., and Henry, C.S. A low-cost, simple, and rapid fabrication method for paper-based microfluidics using wax screen-printing. *Analyst*, 2011. **136**(1): p. 77-82.

[140] Li, X., Tian, J.F., Garnier, G., and Shen, W. Fabrication of paper-based microfluidic sensors by printing. *Colloids and Surfaces B-Biointerfaces*, 2010. **76**(2): p. 564-570.

[141] Delaney, J.L., Hogan, C.F., Tian, J.F., and Shen, W. Electrogenerated chemiluminescence detection in paper-based microfluidic sensors. *Analytical Chemistry*, 2011. **83**(4): p. 1300-1306.

[142] Li, X., Tian, J.F., and Shen, W. Progress in patterned paper sizing for fabrication of paper-based microfluidic sensors. *Cellulose*, 2010. **17**(3): p. 649-659.

[143] Olkkonen, J., Lehtinen, K., and Erho, T. Flexographically printed fluidic structures in paper. *Analytical Chemistry*, 2010. **82**(24): p. 10246-10250.

[144] Chitnis, G., Ding, Z.W., Chang, C.L., Savran, C.A., and Ziaie, B. Laser-treated hydrophobic paper: an inexpensive microfluidic platform. *Lab on a Chip*, 2011. **11**(6): p. 1161-1165.

[145] Cassano, C.L. and Fan, Z.H. Laminated paper-based analytical devices (LPAD): fabrication, characterization, and assays. *Microfluidics and Nanofluidics*, 2013. **15**(2): p. 173-181.

[146] Fenton, E.M., Mascarenas, M.R., Lopez, G.P., and Sibbett, S.S. Multiplex lateral-flow test strips fabricated by two-dimensional shaping. *Acs Applied Materials & Interfaces*, 2009. **1**(1): p. 124-129.

[147] Yetisen, A.K., Akram, M.S., and Lowe, C.R. Paper-based microfluidic point-of-care diagnostic devices. *Lab on a Chip*, 2013. **13**(12): p. 2210-2251.

[148] Fu, E., Kauffman, P., Lutz, B., and Yager, P. Chemical signal amplification in two-dimensional paper networks. *Sensors and Actuators B: Chemical*, 2010. **149**(1): p. 325-328.

[149] Apilux, A., Ukita, Y., Chikae, M., Chailapakul, O., and Takamura, Y. Development of automated paper-based devices for sequential multistep sandwich enzyme-linked immunosorbent assays using inkjet printing. *Lab on a Chip*, 2013. **13**(1): p. 126-135.

[150] Murdock, R.C., Shen, L., Griffin, D.K., Kelley-Loughnane, N., Papautsky, I., and Hagen, J.A. Optimization of a paper-based ELISA for a human performance biomarker. *Analytical Chemistry*, 2013. **85**(23): p. 11634-11642.

[151] Hsu, C.-K., Huang, H.-Y., Chen, W.-R., Nishie, W., Ujiie, H., Natsuga, K., Fan, S.-T., Wang, H.-K., Lee, J.Y.-Y., Tsai, W.-L., Shimizu, H., and Cheng, C.-M. Paper-based ELISA for the detection of autoimmune antibodies in body fluid—The case of bullous pemphigoid. *Analytical Chemistry*, 2014. **86**(9): p. 4605-4610.

[152] Cheng, C.M., Martinez, A.W., Gong, J., Mace, C.R., Phillips, S.T., Carrilho, E., Mirica, K.A., and Whitesides, G.M. Paper-based ELISA. *Angewandte Chemie (International ed. in English)*, 2010. **49**(28): p. 4771-4774.

[153] Glavan, A.C., Christodouleas, D.C., Mosadegh, B., Yu, H.D., Smith, B.S., Lessing, J., Fernández-Abedul, M.T., and Whitesides, G.M. Folding analytical devices for electrochemical ELISA in hydrophobic R^H paper. *Analytical Chemistry*, 2014. **86**(24): p. 11999-12007.

[154] Wang, S., Ge, L., Song, X., Yu, J., Ge, S., Huang, J., and Zeng, F. Paper-based chemiluminescence ELISA: Lab-on-paper based on chitosan modified paper device and wax-screen-printing. *Biosensors and Bioelectronics*, 2012. **31**(1): p. 212-218.

[155] Hsu, M.-Y., Yang, C.-Y., Hsu, W.-H., Lin, K.-H., Wang, C.-Y., Shen, Y.-C., Chen, Y.-C., Chau, S.-F., Tsai, H.-Y., and Cheng, C.-M. Monitoring the VEGF level in aqueous humor of patients with ophthalmologically relevant diseases via ultrahigh sensitive paper-based ELISA. *Biomaterials*, 2014. **35**(12): p. 3729-3735.

[156] Lathwal, S. and Sikes, H.D. Assessment of colorimetric amplification methods in a paper-based immunoassay for diagnosis of malaria. *Lab on a Chip*, 2016: p. 1374-1382.

[157] Badu-Tawiah, A.K., Lathwal, S., Kaastrup, K., Al-Sayah, M., Christodouleas, D.C., Smith, B.S., Whitesides, G.M., and Sikes, H.D. Polymerization-based signal amplification for paper-based immunoassays. *Lab on a Chip*, 2015. **15**(3): p. 655-659.

[158] Wang, P., Ge, L., Yan, M., Song, X., Ge, S., and Yu, J. Paper-based three-dimensional electrochemical immunodevice based on multi-walled carbon nanotubes functionalized paper for sensitive point-of-care testing. *Biosensors and Bioelectronics*, 2012. **32**(1): p. 238-243.

[159] Busin, V., Burgess, S., and Shu, W. A novel multi-pad paper plate (MP^3) based assays for rapid animal disease diagnostics. *Procedia Engineering*, 2016. **168**: p. 1418-1421.

[160] Liu, X.Y., Cheng, C.M., Martinez, A.W., Mirica, K.A., Li, X.J., Phillips, S.T., Mascarenas, M., Whitesides, G.M., and Ieee. A portable microfluidic paper-

based device for ELISA. *2011 Ieee 24th International Conference on Micro Electro Mechanical Systems*, 2011: p. 75-78.

[161] Lewis, G.G., DiTucci, M.J., Baker, M.S., and Phillips, S.T. High throughput method for prototyping three-dimensional, paper-based microfluidic devices. *Lab on a Chip*, 2012. **12**(15): p. 2630-2633.

[162] Martinez, A.W., Phillips, S.T., and Whitesides, G.M. Three-dimensional microfluidic devices fabricated in layered paper and tape. *Proceedings of the National Academy of Sciences of the United States of America*, 2008. **105**(50): p. 19606-19611.

[163] Schonhorn, J.E., Fernandes, S.C., Rajaratnam, A., Deraney, R.N., Rolland, J.P., and Mace, C.R. A device architecture for three-dimensional, patterned paper immunoassays. *Lab on a Chip*, 2014. **14**(24): p. 4653-4658.

[164] Schilling, K.M., Jauregui, D., and Martinez, A.W. Paper and toner three-dimensional fluidic devices: programming fluid flow to improve point-of-care diagnostics. *Lab on a Chip*, 2013. **13**(4): p. 628-631.

[165] Gerbers, R., Foellscher, W., Chen, H., Anagnostopoulos, C., and Faghri, M. A new paper-based platform technology for point-of-care diagnostics. *Lab on a Chip*, 2014. **14**(20): p. 4042-4049.

[166] Liu, H. and Crooks, R.M. Three-dimensional paper microfluidic devices assembled using the principles of origami. *Journal of the American Chemical Society*, 2011. **133**(44): p. 17564-17566.

[167] Lu, J., Ge, S., Ge, L., Yan, M., and Yu, J. Electrochemical DNA sensor based on three-dimensional folding paper device for specific and sensitive point-of-care testing. *Electrochimica Acta*, 2012. **80**(0): p. 334-341.

[168] Sechi, D., Greer, B., Johnson, J., and Hashemi, N. Three-dimensional paper-based microfluidic device for assays of protein and glucose in urine. *Analytical Chemistry*, 2013. **85**(22): p. 10733-10737.

[169] Bridle, H., Kersaudy-Kerhoas, M., Miller, B., Gavriilidou, D., Katzer, F., Innes, E.A., and Desmulliez, M.P.Y. Detection of *Cryptosporidium* in miniaturised fluidic devices. *Water Research*, 2012. **46**(6): p. 1641-1661.

[170] Fang, X.E., Liu, Y.Y., Kong, J.L., and Jiang, X.Y. Loop-mediated isothermal amplification integrated on microfluidic chips for point-of-care quantitative detection of pathogens. *Analytical Chemistry*, 2010. **82**(7): p. 3002-3006.

[171] Govindarajan, A.V., Ramachandran, S., Vigil, G.D., Yager, P., and Boehringer, K.F. A low cost point-of-care viscous sample preparation device for molecular diagnosis in the developing world; an example of microfluidic origami. *Lab on a Chip*, 2012. **12**(1): p. 174-181.

[172] Kersaudy-Kerhoas, M., Kavanagh, D.M., Dhariwal, R.S., Campbell, C.J., and Desmulliez, M.P.Y. Validation of a blood plasma separation system by biomarker detection. *Lab on a Chip*, 2010. **10**(12): p. 1587-1595.

[173] Coskun, A.F., Nagi, R., Sadeghi, K., Phillips, S., and Ozcan, A. Albumin testing in urine using a smart-phone. *Lab on a Chip*, 2013. **13**(21): p. 4231-4238.

[174] Funes-Huacca, M., Wu, A., Szepesvari, E., Rajendran, P., Kwan-Wong, N., Razgulin, A., Shen, Y., Kagira, J., Campbell, R., and Derda, R. Portable self-contained cultures for phage and bacteria made of paper and tape. *Lab on a Chip*, 2012. **12**(21): p. 4269-4278.

[175] Yetisen, A.K. and Volpatti, L.R. Patent protection and licensing in microfluidics. *Lab on a Chip*, 2014. **14**(13): p. 2217-2225.

[176] Mark, D., Haeberle, S., Roth, G., von Stetten, F., and Zengerle, R. Microfluidic lab-on-a-chip platforms: requirements, characteristics and applications. *Chemical Society Reviews*, 2010. **39**(3): p. 1153-1182.

[177] Becker, H. Chips, money, industry, education and the "killer application". *Lab on a Chip*, 2009. **9**(12): p. 1659-1660.

[178] Gift, T.L., Pate, M.S., Hook, E.W., and Kassler, W.J. The rapid test paradox: When fewer cases defected lead to more cases treated - A decision analysis of tests for *Chlamydia trachomatis. Sexually Transmitted Diseases*, 1999. **26**(4): p. 232-240.

[179] Morgan-Davies, C., Waterhouse, A., Milne, C.E., and Stott, A.W. Farmers' opinions on welfare, health and production practices in extensive hill sheep flocks in Great Britain. *Livestock Science*, 2006. **104**(3): p. 268-277.

[180] Flatland, B., Freeman, K.P., Vap, L.M., and Harr, K.E. ASVCP guidelines: quality assurance for point-of-care testing in veterinary medicine. *Veterinary Clinical Pathology*, 2013. **42**(4): p. 405-423.

[181] Mitzner, B.T. It's time for in-house quality assurance. *Journal of the American Animal Hospital Association*, 2002. **38**(1): p. 12-13.

[182] Blick, K.E. The essential role of information management in point-of-care/critical care testing. *Clinica Chimica Acta*, 2001. **307**(1-2): p. 159-168.

Chapter 2 – Experimental techniques

2.1 Introduction

In this chapter, the experimental techniques used throughout the thesis are explained. Experiments were performed at the Institute of Biological Chemistry, Biophysics and Bioengineering of Heriot-Watt University for the fabrication of the microfluidics paper-based analytical devices (μPADs) and at the Moredun Research Institute (MRI) for the analysis of samples. If materials or techniques different from the ones reported here have been used at any point in the experiments, they will be reported in the corresponding chapters.

2.2 Ovine serum samples

2.2.1 Clinical samples

To validate the paper-based diagnostic tests, serum from naïve sheep and from sheep with known degrees of sheep scab pathology were used. Serum samples were sourced from sheep kept at the MRI for the maintenance of a *P. ovis* mite colony (Figure 6). A total of 8 animals were sourced from a non-infected flock. Following experimental infestation with a bolus of approximately 20-50 *P. ovis* mites placed directly on the withers, animals were euthanized at 6 weeks post-infestation. Whole blood samples were collected by jugular veni-puncture before infestation and at weekly intervals for 6 weeks. A total of 52 data points was analysed by ELISA (8 animals from which serum samples were obtained over 7 time points).

After collection, samples were left at room temperature for 30 minutes for blood clotting. Samples were then centrifuged at 2000rpm for 10 minutes and serum was collected using Pasteur pipettes. It was then aliquoted in 200μl and stored at -20°C in 1.5ml plastic micro centrifuge tubes. Serum was thawed at room temperature prior to analysis and unused samples were discarded.

Figure 6 - Sheep kept within the MRI premises to maintain a mite colony. Serum samples from these animals were used for this project.

2.2.2 Positive and negative control serum samples

Serum samples used as positive and negative controls for the commercial Pso o 2 ELISA were also available. These samples had been sourced from non-infested sheep (n=6 MRI) and from terminal bleeds from experimentally infested sheep (n=6 MRI). They were used for the optimisation of the Pso o 2 indirect P-ELISA and in the form of pooled blood samples, as positive and negative controls for the analysis of clinical samples for both the lab-based ELISA and the P-ELISA.

2.3 Lab-based ELISAs technique and reagents

The lab-based ELISA protocol for detection of Hp in bovine and sheep serum samples is reported in Appendix A (Chapter 8).

The lab-based ELISAs for detection of Pso o 2 antibodies was carried out by Dr. Francesca Nunn, at MRI for all the animal samples used in this project. The protocol used is reported in Appendix B (Chapter 9).

Reagents used for both P-ELISAs were sourced and prepared as reported in the Appendixes. Further reagents used for the indirect Pso o 2 P-ELISA and not reported in the Appendixes were as follow. Bovine serum albumin (BSA) (Sigma Aldrich, USA; Catalogue No A9647) and gelatin from cold water fish skin (fish gelatin) (Sigma Aldrich, USA; Catalogue No G7765) were used to prepare blocking buffers.

2.4 Fabrication and performance testing of the microfluidic paper-based analytical devices

A new fabrication technique for μPADs was developed within this project and implemented for all paper-based devices reported in this thesis. Devices were fabricated using a paper cutting and lamination technique. Paper and lamination sheets were cut in the desired format and then laminated to produce the final device. The basis for this technique had been inspired by work from the Yager group [1, 2], where sophisticated paper networks where fabricated using a CO_2 laser, which represented a user-friendly procedure, requiring minimal training and easily available machinery. The major drawback of these devices was the requirement for external support for the wet paper (double-sided tape on a glass substrate). A possible alternative to maintain the low-cost and ease of production is the use of lamination [3, 4]. The combination of these two procedures formed the foundation of the new technique developed herein.

2.4.1 Design of the microfluidic paper-based analytical devices

A 3D mechanical computer-aided design (SolidWorks 2012x64 edition, USA) was used to design both the paper devices and the plastic lamination used for device packaging. The designs where based on 2D engineering drawings and for creation of the 3D μPADs (Chapter 6), a 3D arrangement of parts was used. The designs were then exported as .DXF files into CorelDraw for processing by the laser system (Figure 7).

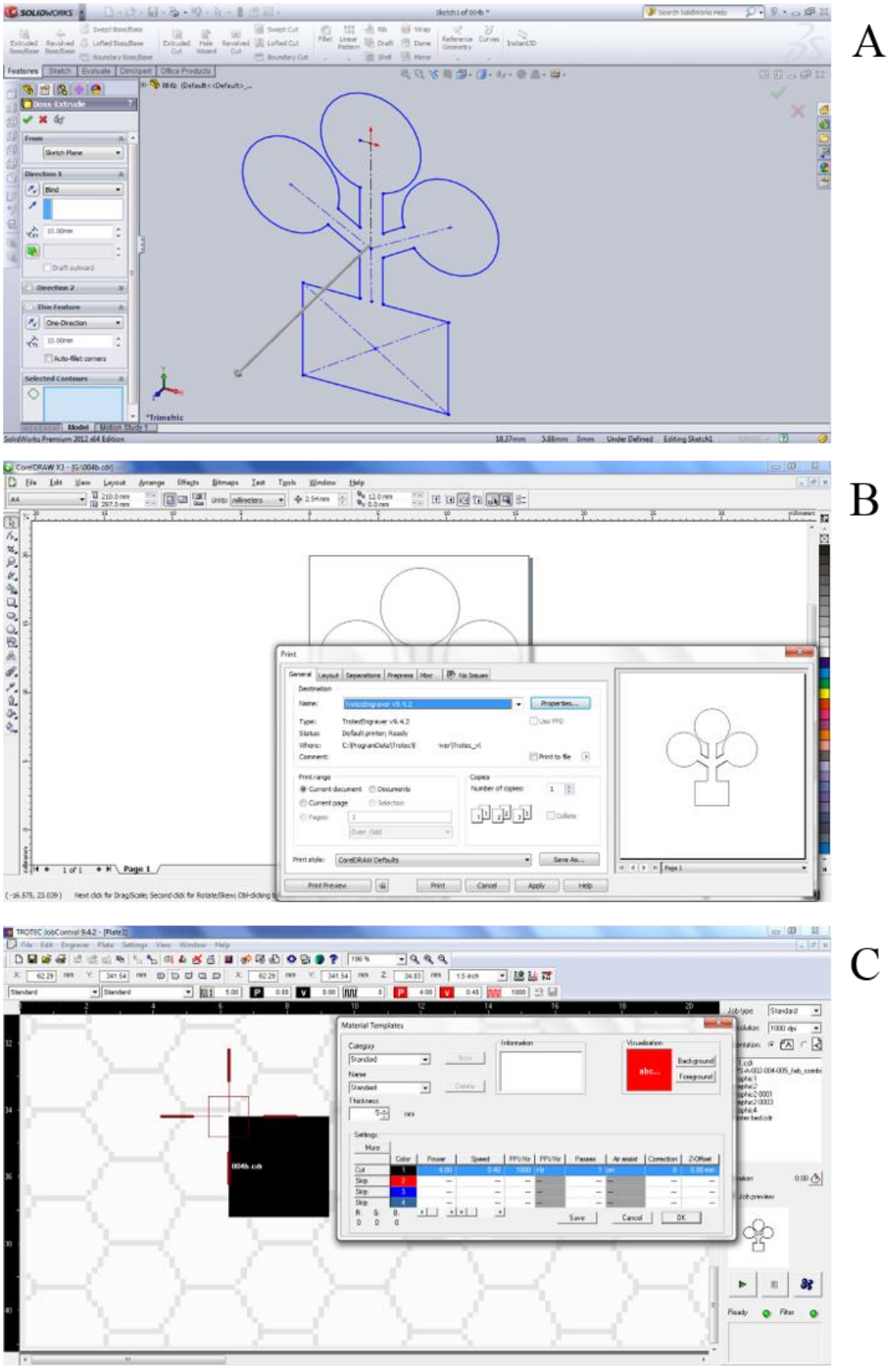

Figure 7 - Design process for production of µPADs. A) Drawing using a CAD program. B) After saving as a .DXF file, CorelDraw was used for final adjustments and the print panel was used to process the design by the laser system. C) The laser system software with the panel for cutting settings.

Using CorelDraw, selected areas of the design can be assigned different colours, which can be processed by the laser at different settings or at different times (Figure 7C). This facility was utilised to make a single design incorporating both the paper and the lamination cutting, which were fabricated at different times. It also allowed for settings to be optimised and compared at the same time.

2.4.2 Paper and lamination sheets

Cellulose chromatography paper (Whatman grade 1, Sigma-Aldrich, UK) was used throughout experiments. The main characteristics of this paper are an 88 g/m² basis weight, 180 µm thickness and 11µm pore size (medium fluid retention), with a linear flow rate (water) of 130 mm/30 min (medium flow). Lamination sheets (Staples, UK) were 75µ gloss lamination pouches (commercially available lamination sheets with the lowest thickness where chosen, to minimise the space between layers for the creation of the 3D µPADs). A considerable number of paper-based devices have used the same type of paper [5-9] and interesting recent work has also been carried out comparing the characteristics of different types of paper [10], showing that chromatography paper Whatman no. 1 is an ideal matrix for paper-based microfluidic devices.

2.4.3 CO_2 laser cutter

A class 2 carbon dioxide (CO_2) laser cutter (Trotec Speedy 300 Laser Engraver) was used to cut both the paper and the lamination sheets (Figure 8). The optimised settings for cutting both materials were: power 4%, speed 0.4, PPI/Hz 1000, passes 1, air assist on. These settings were chosen as the best combination for fast and precise production, while avoiding material burning.

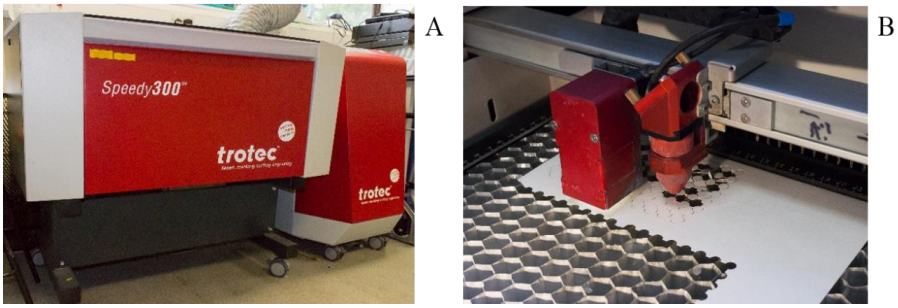

Figure 8 - Class 2 CO_2 laser cutter. A) Trotec Speedy 300 Laser Engraver. B) The inside of the laser.

2.4.4 Lamination

Paper devices were assembled within the pre-cut lamination sheets and lamination was performed using a roll laminator (GBC Catena 35 Roll Laminator) (Figure 9). Settings for lamination were: 110°C, at the lowest speed (1) and with rollers set at 1mm gauge distance.

Figure 9 - GBC Catena 35 Roll Laminator.

2.4.5 Performance testing

To assess the performance of the fabricated devices (complete wet out, flow rate and mixing), food colours were used through the experiments. Morrisons Ltd. Natural Food Colouring Blue, Green, Yellow and Red were used, all diluted 1:10 with tap water. The prepared colour solutions were applied to the devices with a pipette.

2.5 Image and statistical analysis

Images of the paper devices were taken using a desktop scanner (Epson Perfection V350 photo) set to "colour photo scanning" and 1200 dpi resolution. Images were transformed in 8-bit greyscale with PixBuilder Studio 2.2 (WnSoft Ltd., UK) and mean grey value (mean pixel intensity) was measured with Image J (1.48v, National Institute of Health, USA), after image inversion and after selection of the area to be measured (Figure 10).

Data were saved as Microsoft Excel 2007 files and data analysis was carried out with the statistical package GraphPad Prism 7 (GraphPad Software, Inc., USA).

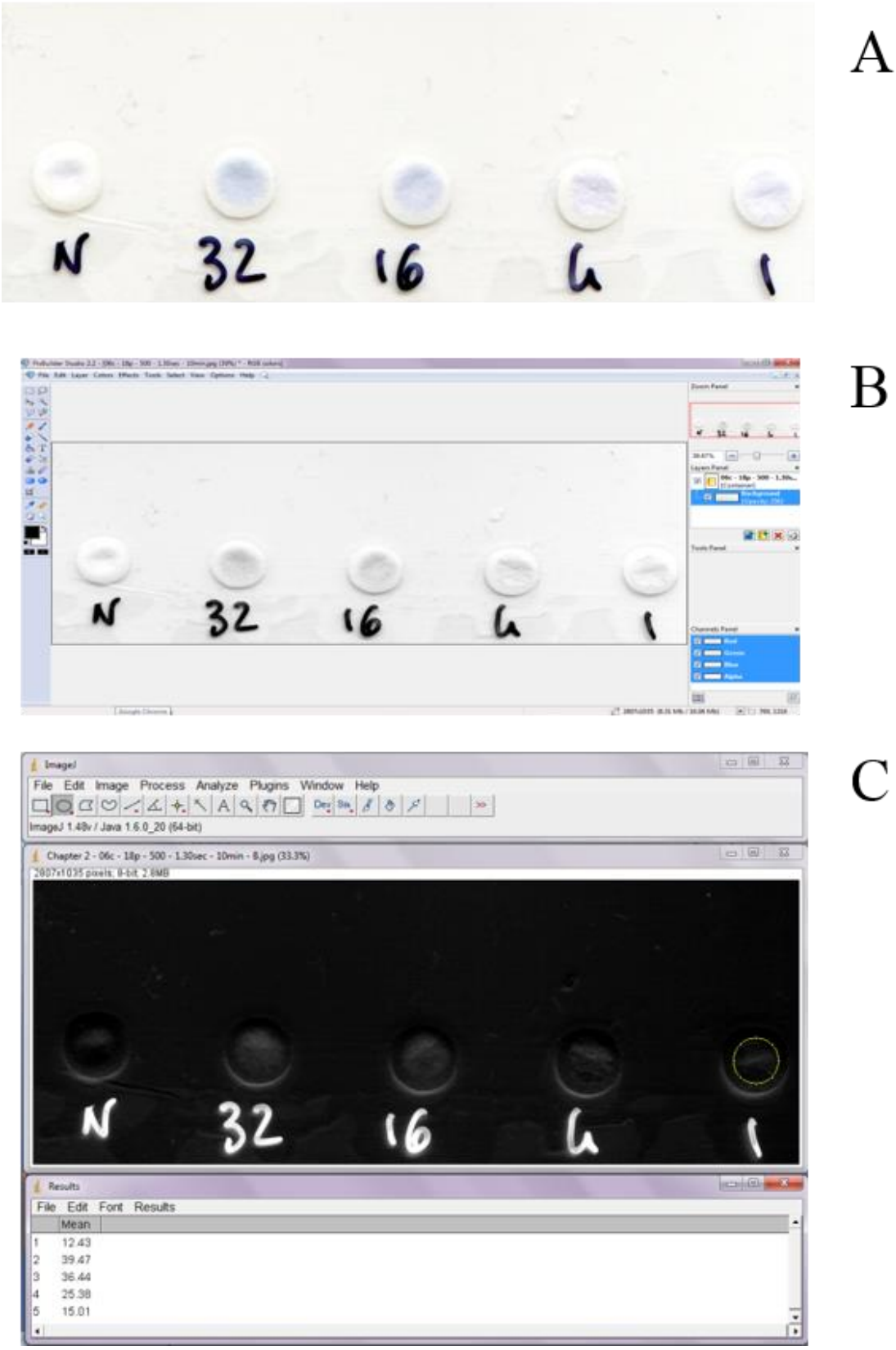

Figure 10 - Image analysis. A) Image of a paper-based device taken using a desktop scanner. B) Image transformed into grayscale. C) Image analysed with Image J, after image invert and after oval selection of the area to be measured. Results show measurement in mean grey value.

2.6 References

[1] Fu, E., Lutz, B., Kauffman, P., and Yager, P. Controlled reagent transport in disposable 2D paper networks. *Lab on a Chip*, 2010. **10**(7): p. 918-920.

[2] Fu, E., Liang, T., Spicar-Mihalic, P., Houghtaling, J., Ramachandran, S., and Yager, P. Two-dimensional paper network format that enables simple multistep assays for use in low-resource settings in the context of malaria antigen detection. *Analytical Chemistry*, 2012. **84**(10): p. 4574-4579.

[3] Cassano, C.L. and Fan, Z.H. Laminated paper-based analytical devices (LPAD): fabrication, characterization, and assays. *Microfluidics and Nanofluidics*, 2013. **15**(2): p. 173-181.

[4] Liu, W., Cassano, C.L., Xu, X., and Fan, Z.H. Laminated paper-based analytical devices (LPAD) with origami-enabled chemiluminescence immunoassay for cotinine detection in mouse serum. *Analytical Chemistry*, 2013. **85**(21): p. 10270-10276.

[5] Martinez, A.W., Phillips, S.T., Wiley, B.J., Gupta, M., and Whitesides, G.M. FLASH: A rapid method for prototyping paper-based microfluidic devices. *Lab on a Chip*, 2008. **8**(12): p. 2146-2150.

[6] Nie, Z.H., Deiss, F., Liu, X.Y., Akbulut, O., and Whitesides, G.M. Integration of paper-based microfluidic devices with commercial electrochemical readers. *Lab on a Chip*, 2010. **10**(22): p. 3163-3169.

[7] Wang, W., Wu, W.Y., and Zhu, J.J. Tree-shaped paper strip for semiquantitative colorimetric detection of protein with self-calibration. *Journal of Chromatography A*, 2010. **1217**(24): p. 3896-3899.

[8] Pollock, N.R., Rolland, J.P., Kumar, S., Beattie, P.D., Jain, S., Noubary, F., Wong, V.L., Pohlmann, R.A., Ryan, U.S., and Whitesides, G.M. A paper-based multiplexed transaminase test for low-cost, point-of-care liver function testing. *Science Translational Medicine*, 2012. **4**(152): p. 129-139.

[9] Wang, S., Ge, L., Song, X., Yu, J., Ge, S., Huang, J., and Zeng, F. Paper-based chemiluminescence ELISA: Lab-on-paper based on chitosan modified paper device and wax-screen-printing. *Biosensors and Bioelectronics*, 2012. **31**(1): p. 212-218.

[10] Costa, M.N., Veigas, B., Jacob, J.M., Santos, D.S., Gomes, J., Baptista, P.V., Martins, R., Inacio, J., and Fortunato, E. A low cost, safe, disposable, rapid and

self-sustainable paper-based platform for diagnostic testing: lab-on-paper. *Nanotechnology*, 2014. **25**(9): p. 094006.

Chapter 3 – Development of a multi-pad paper plate (MP^3) for P-ELISA

3.1 Introduction

The conventional methods used for fabrication of P-ELISA platforms involve photolithography [1] and wax printing techniques [2-7]. The first is based on the physical blocking of pores with photoresistant chemical substances (SU-8 photoresist) and requires a UV light, a hot plate and a transparency mask with the desired patterning design. The main drawbacks are the numerous steps involved for production of the final device, including impregnation of the paper with the photoresist, baking, cooling, exposure to UV light using the designed mask, a second baking and cooling step, bathing and rinsing in acetone and isopropyl alcohol and a drying time of at least one hour [8] and the cost of the photoresist [9]. The second is based on the physical deposition of reagents (wax) onto the paper surface and requires a solid-ink printer and a hot plate or oven. It involves deposition of wax on paper, following a pre-design patterning template, and a heating step for the wax to melt into the paper. Although much cheaper than photolithography, it suffers from poor channel resolution [9]. To overcome some of the drawbacks of these methods, specifically to maintain low-cost and simplicity of production, while offering precise microchannels fabrication, an alternative method of production could be based on combining paper cutting techniques to create the desired patterns [10, 11] with lamination [12] to provide the required robustness to the final device. Although these techniques have been exploited in the fabrication of paper-based devices, none has been specifically applied to P-ELISA platforms.

The aim of this chapter was therefore to develop a new and suitable alternative technique to produce a paper-based platform for P-ELISA, based on a combination of paper cutting and lamination. The experiments were focused on the reproduction of a conventional plastic 96-well microplate, commonly used for ELISA, but with paper as a substrate material. The research question was aimed at demonstrating that the new technique could solve some of the intrinsic limitations of the other two techniques reported (e.g. cumbersome production and low-resolution technique), while maintaining

low cost of fabrication and rapid production. The development of this platform, termed herein multi-pad paper plate (MP^3), including the main challenge in assuring complete independency of the paper pads and further possible applications, are described and discussed in this chapter. The techniques developed in this chapter also form the foundation for the development of the devices reported in Chapter 6.

3.2 MP^3 design and fabrication

3.2.1 Initial design

Different prototypes (a total of 10) were designed and tested before the final MP^3 device was finished, all based on the final aim of enclosing 96 circular paper pads. Initially a simple single row of 5 circular paper pads (5mm diameter) was used (Figure 11). The main function of this prototype was to test the production system for robustness and deposition of samples (e.g. serum) on the circular paper pad. Furthermore, the first prototype allowed for paper cutting and lamination settings to be optimised (optimised settings described in Chapter 2), by reducing the material and time required before committing to a more complicated structure. The main learning point of these initial prototypes, was the need for laminated sheets to be cut on both sides, to allow for washing steps to be carried out effectively. Therefore, all following prototypes and the final device, used lamination sheets cut on both sides.

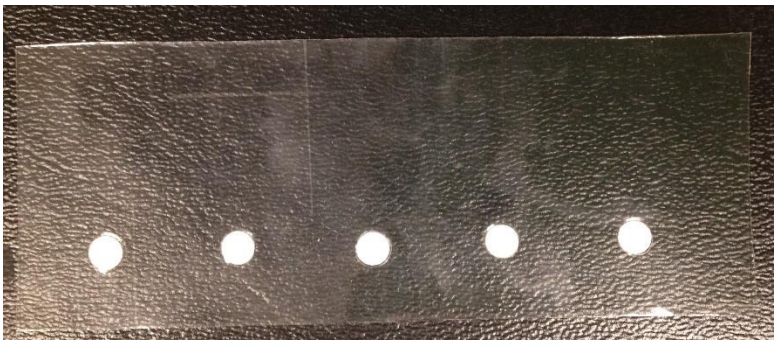

Figure 11 - First prototype of the paper-based device. The prototype consisted of 5 circular paper pads enclosed in a lamination pouch and laminated. Lamination pouches were cut on both sides.

The prototypes also used different lamination dimensions, in order to determine the minimum lamination surface needed to cover the paper for uniform lamination (circle centred within the lamination sheets) and to provide sufficient robustness, while

maximising the analytical surface available. A difference of 2 mm diameter between paper and lamination was deemed to provide the desired results (Figure 12).

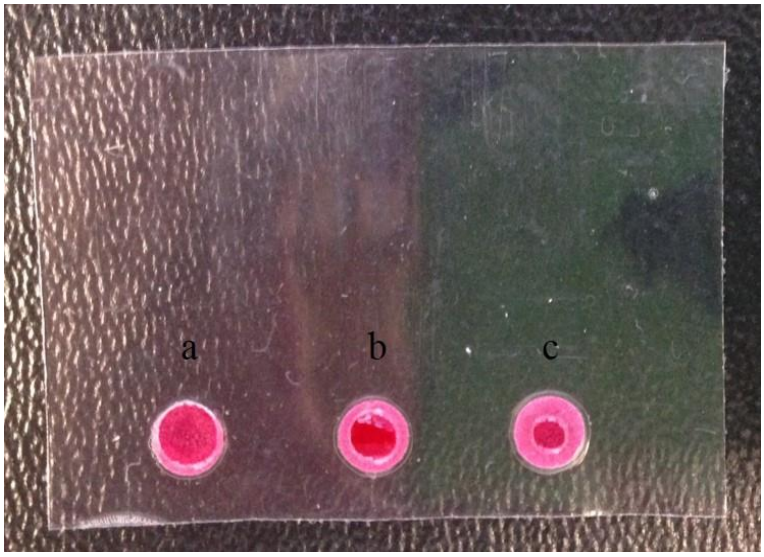

Figure 12 - Different lamination sizes. Difference between paper and lamination diameters: 1mm (a), 2mm (b) and 3mm (c).

3.2.2 Design to replicate a 96-well microplate

Further experiments were designed to replicate a 96-well microplate. These plates are generally used to perform ELISA and common instruments used in the lab (e.g. multichannel pipettes and washing manifolds) are designed to fit these measurements. The bottom of a 96-well microplate is 8mm diameter, with an intra-well spacing of 9mm. Based on these measurements, a first design was produced to recreate the same measurements as a standard 96-well microplate (Figure 13) with a 2 mm diameter difference between paper and lamination.

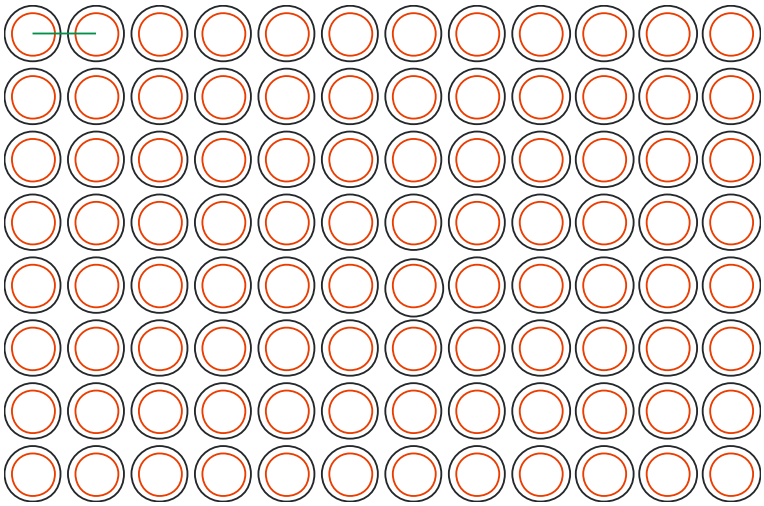

Figure 13 - Design to reproduce the measurement of a standard 96-well microplate. Black drawings represent the paper cutting (8mm diameter), red drawings are the lamination cutting (6mm diameter) and the green line represents the in-between wells space (9mm).

3.2.3 Assembly of the device

The major obstacle encountered with this new technique of paper cutting and lamination, was device assembly. The initial prototypes based on 5 circular paper pads, allowed for paper pads to be fitted manually with the help of tweezers (Figure 14).

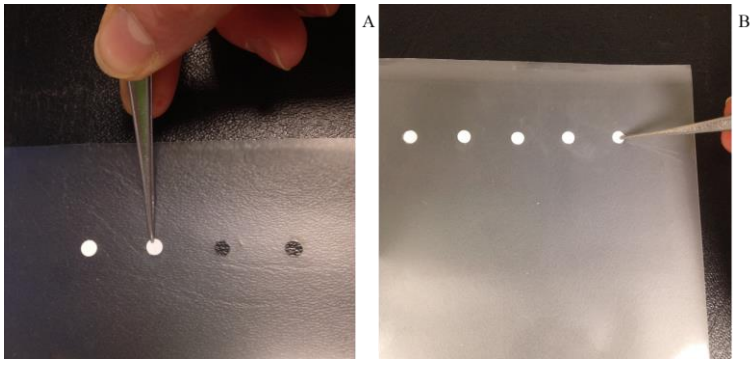

Figure 14 - Manual positioning of paper pads within the device. A) Paper pads were positioned within the lamination circles with the aid of tweezers. B) After all the circles were enclosed within the two lamination sheets, paper pads were centred with tweezers.

This technique was not possible for the final design, as manually fitting 96 pads would be extremely time consuming and highly likely to result in human error with inter-batch variability (Figure 15).

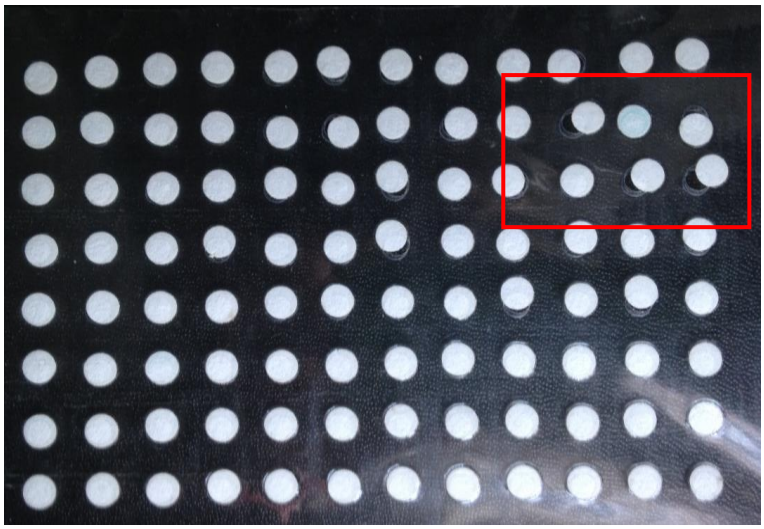

Figure 15 - Device created by manual assemble of 96 paper pads. Red square highlighting misaligned pads within the lamination.

Consequently, different solutions were considered. A smaller version of the 96 circular pads was designed and used to test different options, as well as to reduce material consumption and time. The design was therefore reduced to 4 circular pads with the same measurements for both paper and lamination. Three different options were tested. Initially laser settings were changed to obtain incomplete cutting of the paper. Power was reduced from 4% to 2.5% (all other parameters were kept the same) to change from cutting to etching of the paper. This resulted in the circular pad being still physically attached to the original paper sheet (Figure 16A). Although this prototype was very easy and quick to assemble, it resulted in fluid leakage between pads when tested with food colouring (Figure 16B).

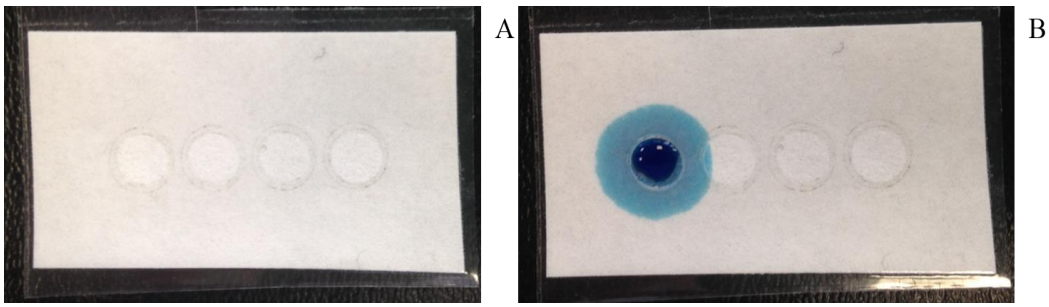

Figure 16 - Testing of different assembly options using modified laser settings. A) The power of the laser was reduced to 2.5% to obtain an incomplete cut of the paper. B) When tested with food colouring (10µl), leakage of fluid from the pad into the paper sheet and the next pad was observed.

A different approach, with complete cutting of the paper except for 4 contact points maintained between the pad and the original paper sheet showed the same problem (Figure 17). Although still unsuccessful, this approach suggested that maintaining a connection between the paper pads was necessary for easy assembly with this connection then being severed to produce the final device.

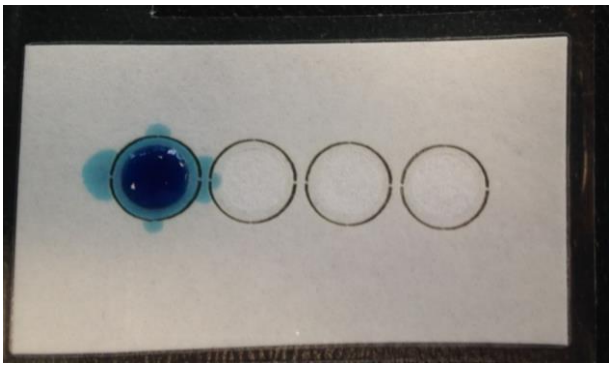

Figure 17 - Testing of different assembly options using a modified paper design. The paper was cut using the optimised settings, but the design was changed to leave 4 limited areas (0.2mm each) where the paper was not cut. When tested with food colour (10µl), leakage of fluid from the pad into the paper sheet through the 4 connecting areas was observed.

An alternative and novel approach was to create a matrix with interconnecting microchannels between pads and after assembly (which is fast, easy and repeatable) channels were severed using a laser cutter. The resulting device demonstrated that the approach was capable of producing independent pads and required minimal time for assembly (Figure 18A), however the proximity of the pads made the precise severing of the microchannels inconsistent, which could result in some pads within the device not being completely separated (Figure 18B).

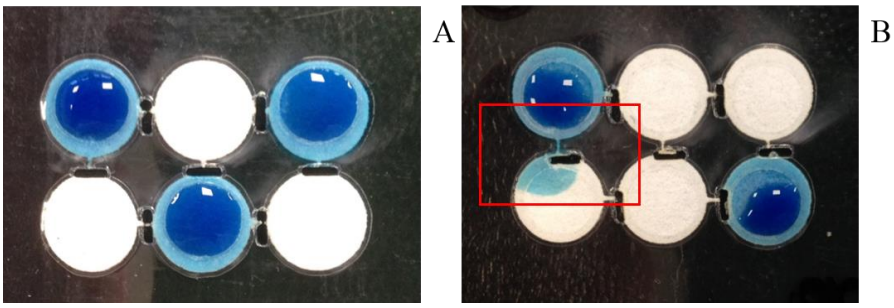

Figure 18 - Testing of different assembly options using microchannels. The design was changed to create interconnecting microchannels which allowed manual fitting of the device within the lamination sheet. After lamination, the device was placed in the laser once more and the microchannels severed. A) When food colouring (10µl) was applied, there was no evidence of leakage. B) Evidence of fluid leakage when severing of the microchannels between pads was not complete.

Therefore, a new design, with smaller pads (6mm diameter), but with the same inter-pad distance was created. The design also included small rectangular shapes for severing of the interconnecting microchannels (Figure 19).

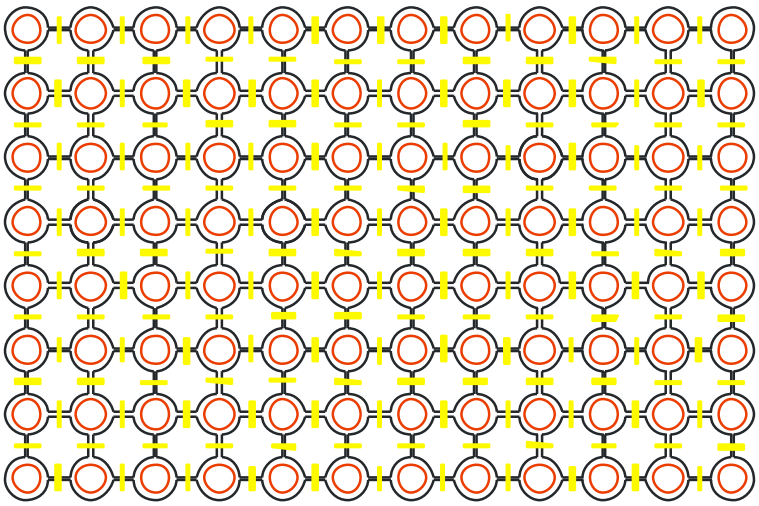

Figure 19 - Final design and measurements for the MP^3. Black drawings represent the paper cutting (6mm diameter), red drawings show the lamination cutting (4mm diameter) and yellow lines show the severing of the interconnecting microchannels (0.5x3mm).

One of the challenges related to this approach, was the difficulty in the precise re-alignment of the laser to cut in between the pads and within the connecting channel. Initially, re-alignment was done manually, which was time consuming and subject to human error (Figure 20).

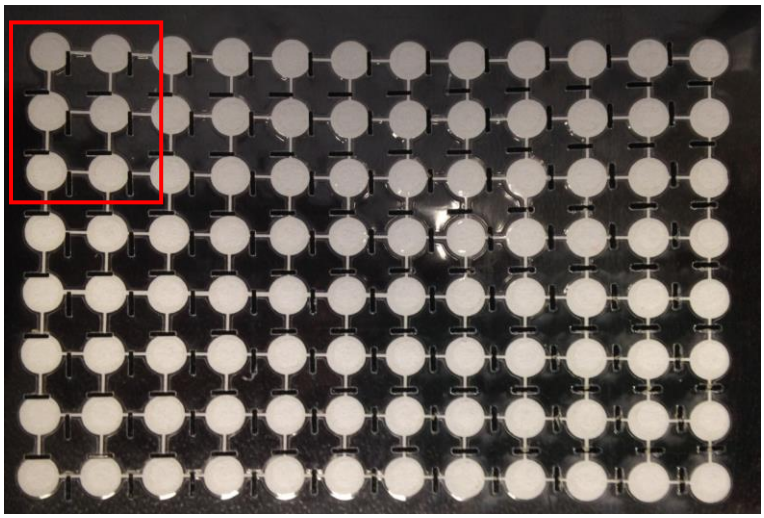

Figure 20 - Manual re-alignment of the MP³. After manual re-alignment of the device in the laser, as shown in the red square, some channels were not correctly severed.

A more efficient and precise approach was taken, by selecting a specific point within the design (the chosen point was the centre of the first paper pad) and, using the corresponding location within the file, the laser beam was directed at the same location. The x and y coordinates from CorelDraw were subtracted to the x and y coordinates on the laser position, the laser beam is therefore centred on the middle of the first paper pad (Figure 21), resulting in the microchannels being precisely severed in the middle, requiring minimal timing for alignment and high reproducibility.

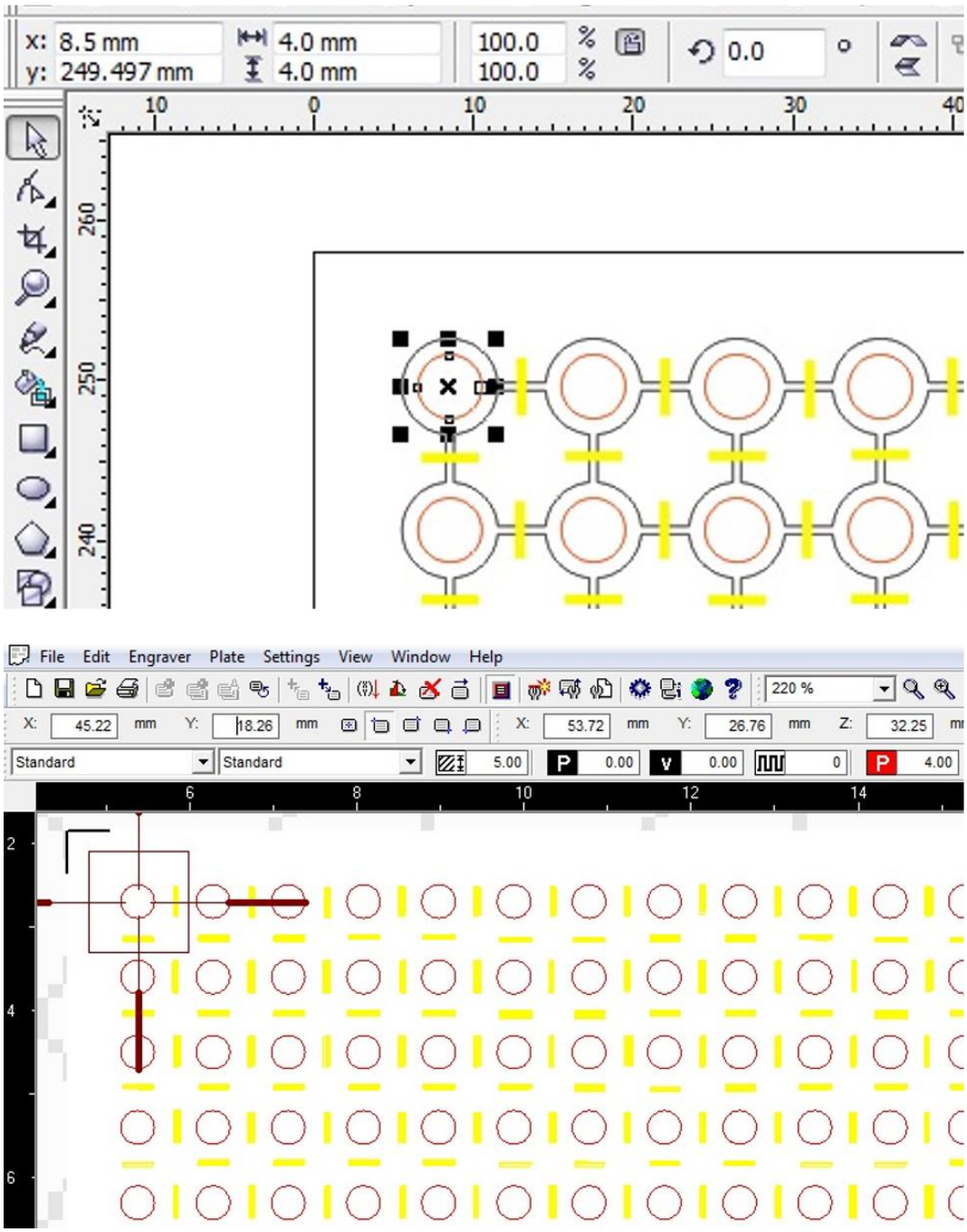

Figure 21 - Calculation process for the exact re-alignment of the laser to obtain precise severing of microchannels. A) The coordinates on the design file (CorelDraw) for the centre of the first paper pad were calculated: x=8.5mm, y was calculated as the difference between y of the file dimension (258mm) and y of the first paper pad (249.5mm), corresponding to y=8.5mm. B) The calculated coordinates (x=8.5 and y=8.5) were subtracted from the laser position (x=53.27 and y=26.76) and the value was entered into the job position (x=45.22, y=18.26). The result of calculating and subsequently re-directing the laser beam, was the exact alignment of the laser with the first paper pad.

3.2.4 High-throughput fabrication of the device

One of the most important features to allow future application in commercial settings of the designed platform, was to achieve large scale high-throughput fabrication. In this case, the production of one MP^3 took an average of 10 minutes. Although still within experimental settings, it was possible to reduce the production time to just over 3 minutes per MP^3 by modifying the CAD design to fit 3 devices in a single A4 sheet. This allowed 3 paper and lamination sheets for the MP^3 to be cut at the same time and once assembled and laminated as one, the A4 sheet containing the 3 devices was placed back into the laser for final severing of the interconnecting channels. During this final step, a simple modification of the CAD design allowed each device to be easily detachable from the A4 sheet. The final cut-out of the device was assigned a different colour and a different style (from continuous line to dotted line) and, due to the precision of the laser beam, a single point laser cut was achieved. The devices were therefore still attached to the laminated A4 sheet, but could be easily peeled off and ready to be used once all devices within the sheet were cut (Figure 22).

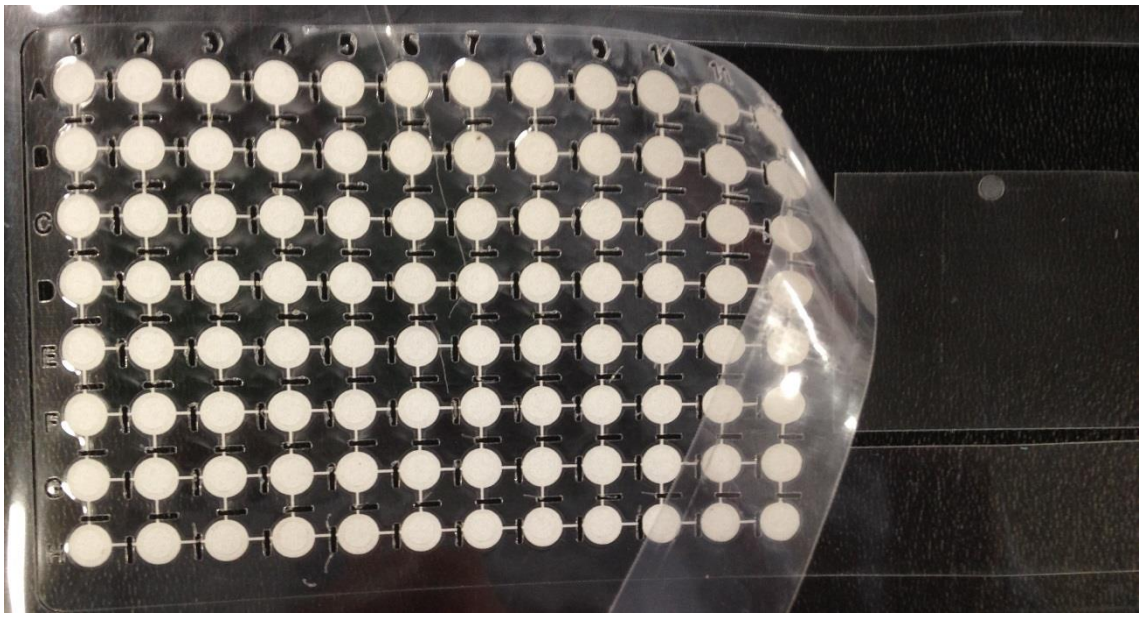

Figure 22 - The MP^3 can be peeled off from the lamination sheet ready for use.

3.2.5 Built-in information on the device

A further modification of the design, allowed for plate information including numbers, letters and other information to be cut or engraved on the final device (Figure 23). This

did not require changes to the original CAD file, but the desired information was added on the CorelDraw file and applied to the final process (laser cutting of interconnecting microchannels) as needed.

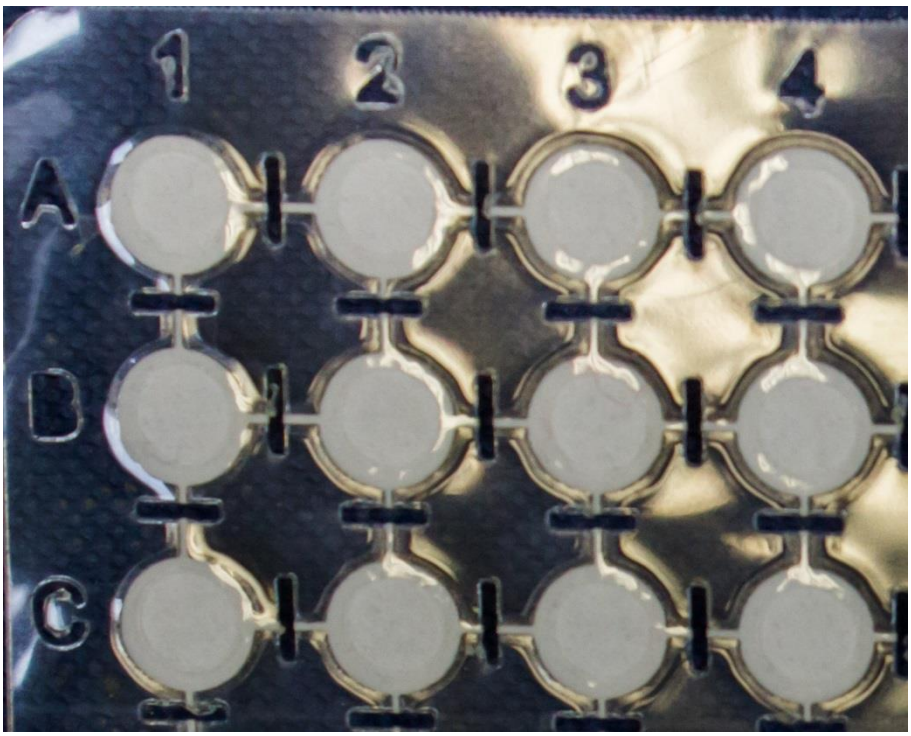

Figure 23 - Letters and numbers cut on the laminated device.

3.3 Final MP^3

The final MP^3 consisted of 96 circular paper pads of 6mm diameter connected by microchannels of 0.5mm width and 3mm in length (Figure 24A) and a complementary lamination sheet of 96 circular holes of 4mm diameter (Figure 24B), assembled in the pre-cut lamination sheet (Figure 24C) and laminated (Figure 24D). After lamination, the laminated MP^3 was placed back into the laser and the connecting microchannels between pads were severed (Figure 24E), making each pad completely independent from the others. Numbers (1 to 12) and letters (A to H), normally present on 96-well microplates for referencing, where also cut on the device. The final device was tested with food colouring for determination of the optimum volume of liquid to allow complete wetting of each paper pad. A range of 1 to 50µl were applied to the platform (Figure 24F), showing that the fluid volume was 2µl, which allowed complete wetting whilst minimising drying time.

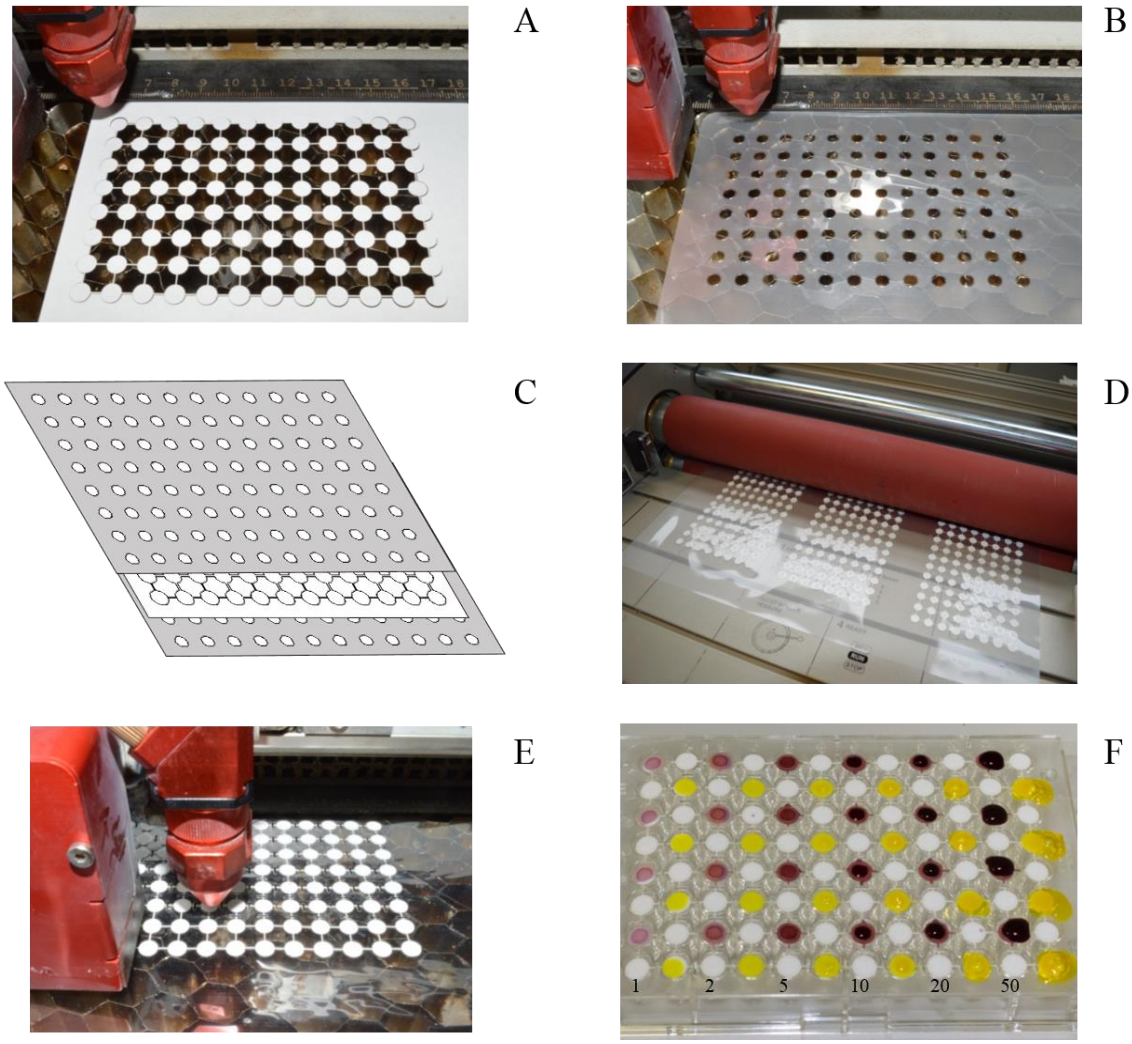

Figure 24 - Schematic of the fabrication of the MP^3. A) Paper cut with a laser cutter. B) Laminating pouches cut with a laser cutter. C) Assembly of device in the pre-cut lamination sheets. D) Lamination of device. E) Severing of interconnecting paper channels by laser cutter. F) Application of food colour to the device. Numbers represent volume of fluids applied (µl). For this procedure, the MP^3 was placed on top of a 96-well microplate for support.

The MP^3 was also tested with commonly used laboratory instruments (Figure 25).

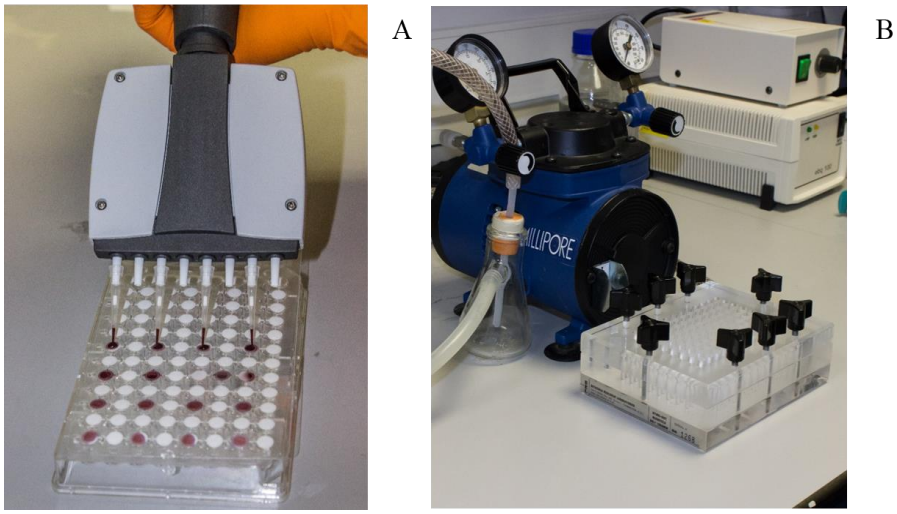

Figure 25 - MP^3 tested using common laboratory instruments. A) 8 Multichannel pipette. B) 96 well vacuum manifold for automated washing.

The cost of the materials for production of a single MP^3 was calculated to be £0.27 (cost of £40 for a pack of 100 chromatography paper sheets and £20 for a pack of 50 lamination sheets, which would both produce 3 devices/sheet).

3.4 MP^3 fabricated with different types of paper

Although different grades of filter and chromatography paper are available, comparison of their properties in relation to the immunological assay is not routinely performed. The new technique also allowed different types of paper with different pore sizes to be incorporated into one MP^3. The CAD design was modified to include 3 different types of paper in a single device, by removing the interconnecting microchannels at every 4^{th} column. In a set of experiments, WHT 4 (Whatman filter paper, Grade 4, pore size 20-25µm) and WHT 597 papers (Whatman filter paper, Grade 597, pore size 4-7µm) where directly compared to the standard paper used in the previous experiments (WHT 1, Whatman chromatography paper, Grade 1). To compare the light transmission through different types of paper, a transilluminator (Alpha Imager™ 2200), set at "transilluminator" mode, with 1 second exposure was used and images were analysed using Image J as described in 2.5.

By the naked eye, it was not possible to appreciate any visible differences between the 3 types of paper. However, when pixel intensities were compared, there were highly significant differences ($p<0.0001$) between the 3 paper types (Figure 26).

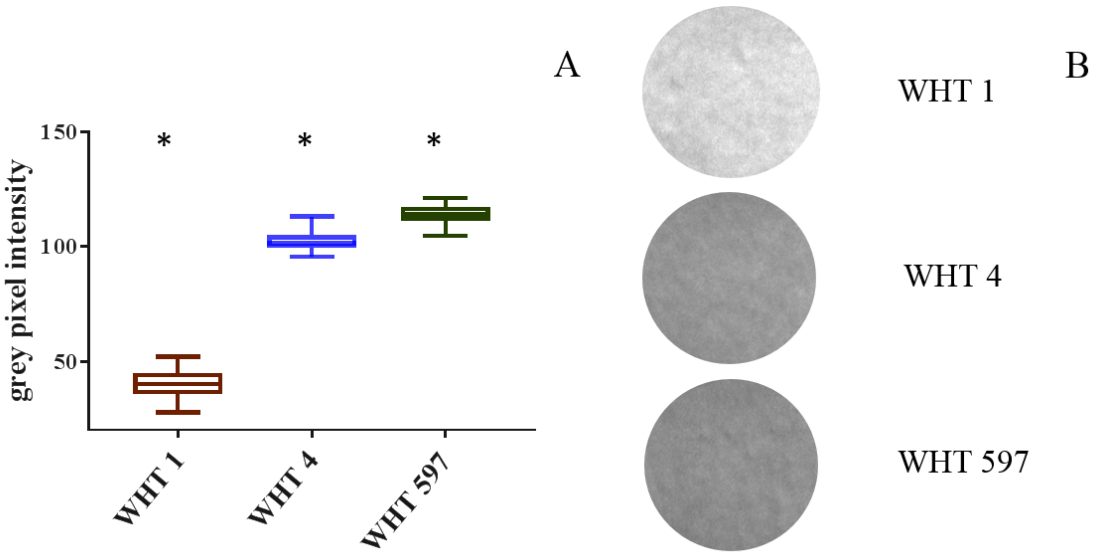

Figure 26 - Comparison of light transmission through different paper types. WHT1: Whatman chromatography paper grade 1, WHT4: Whatman filter paper grade 4, WHT 597: Whatman filter paper grade 597. A) Boxplot of grey intensity values (n=32), showing the mean, min and max values. *= p<0.0001 by One-way ANOVA and t-test to compare each set of papers. B) Images taken from the transluminator showing light transmission through the different types of paper.

3.5 Modified MP^3 to enable for multiplexed testing

To further reduce consumption of the reagents and/or sample material, as well as timings, a multiplex format of the conventional 96-well microplate could be produced, allowing for one sample to be simultaneously tested for multiple markers/diseases (up to 4 per sample). Using the methods described above, it was therefore possible to produce a different version of the MP^3 with 480 pads, by having each of the 96 central pads connected to 4 smaller pads (Figure 27). Again, a simple variation of the original CAD design was used to generate the modified MP^3. First, the in-between pad distance for each row was increased from 9mm to 14mm. Then each pad (diameter was kept the same) was converted into a central pad with 4 microchannels (1mm width x 0.72mm length), each connecting to a smaller lateral pad (2mm diameter). Lamination design was modified accordingly, with lamination for the smaller paper pads of 1mm diameter.

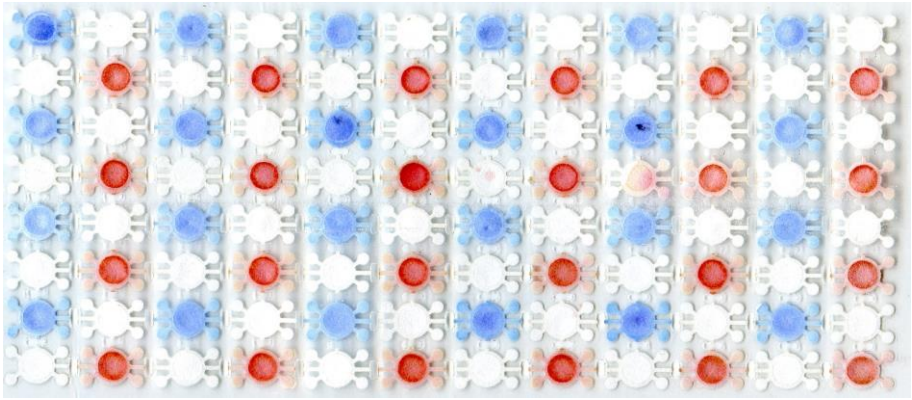

Figure 27 - Modified MP³ to enable for multiplexed testing. The device comprises 480 paper pads: 96 central paper pads each connecting to 4 smaller paper pads (2mm diameter) via paper microchannels (1mmx0.72mm).

3.6 Discussion

In this chapter, a novel fabrication method to create a paper-based platform for P-ELISA is described. This method was proven to be low-cost, rapid and simple to produce. A laser cutter and a laminator are required, but no other specialised machinery or clean room facilities are needed. Class 2 laser cutters are easily available within Universities and are often employed for other paper device fabrication methods, where masks or other devices are usually needed [8, 13, 14]. Computer-controlled knife plotters have also been used for production of paper-based devices by paper cutting, but three sequential overlapping cuts where needed in order to precisely cut the chromatography paper without tearing [10]. The use of a laser cutter provided precise cutting without tearing or burning of the paper substrate with only a single pass of the laser (Section 2.4.3). Although a professional laser machine was employed in this case, commercially available CO_2 laser cutting machines could potentially be used, which have a similar price to solid-ink printers, commonly used for wax printing of paper-based devices. Furthermore, the wax printing technique lacks the high resolution achieved by other methods (e.g. reduction of the hydrophilic circle diameter from approximately 5.56mm to 3.8mm before and after melting [7]), due to the wax spreading by capillary action [15]. In this case, dimensions are the same from design to production of the final device and a resolution of 200μm (Figure 17) could be achieved. Although precision may not be the priority for P-ELISA platforms, it is the case for more complicated designs, like 3D paper-based devices. Moreover, wax is soluble in

organic compounds, which would have made this platform unsuitable for reagents solubilised in urea, as is the case for the recombinant Pso o 2 antigen, used in the sheep scab diagnostic test [16]. This new fabrication method also eliminated the need for chemical treatments as required by another method of fabrication, photolithography, which can pose health and safety issues and increase the overall costs of fabrication (estimated cost of commercial SU-8 is $2.00/plate [8] vs an estimated cost of $0.4/MP^3). Additionally, lamination affords extra strength, which makes these devices more robust but still foldable and bendable.

Another considerable benefit of this technique is the high degree of flexibility when designing a new device. Different prototypes can be created from easily made changes to the original CAD file, without requiring purpose-built devices (e.g. masks), which allows for different conditions and/or parameters to be tested in a cost and time efficient manner. A practical example is the modification of the MP^3 from 96 to 480 paper pads, made possible because of the high degree of precision and the extreme flexibility of this technique. A possible application of this modified MP^3 would be to have multiple tests performed on a single serum sample at the same time (e.g. 4 tests per sample). Multiplexing has been shown to reduce cost, time and sample use [17], which makes it an attractive option for disease diagnostics. It could also be used to increase the information available, in order to obtain a more accurate diagnosis [18]. Applications in veterinary diagnostics would be of particular benefit in cases where multiple agents are involved, like for abortion outbreaks [19] or for respiratory disease complex [20]. In the case of sheep scab, it has been shown that diagnosis and management of the disease could be further enhanced by combining a specific antibody test with serum biomarker detection for current disease status [21].

This technique also offers the possibility of having built-in information, without the need for changes to the original design. A custom-made device could be built, where specific information (e.g. farm holding number or disease to be tested) are added, upon request, to the basic platform. This could minimize the end-user input (information the operator is manually adding) or the operator error (no need for hand writing of information).

Correct assembly techniques can sometimes be an issue with paper-based devices [22]. In this case, the concept of microfluidics, which is based on interconnecting microchannels [23], has been exploited for easy and rapid device assembly, minimising inter-batch differences and reducing wastage. Because of the precise assembly, the spatial distances between the circular pads were kept as per a standard 96-well microplate, which allowed for laboratory instruments, like multichannel pipettes and washing manifolds, to be used with this platform, minimising the operator hands-on time. The precision developed in severing the interconnecting microchannels, also allowed for the same principle to be applied to the modified device, where the spaces between paper pads was further reduced and a more complicated structure was introduced.

Although the technology is, at the moment, suitable specifically for laboratory prototyping, future high-throughput industrial manufacturing could be envisaged. A digital laser cutter and laminating machine, like those used in the label making industry, could be employed. Combining the two fabrication processes in a single machine would decrease the total time of production, as well as the manual operations to a minimum (i.e. starting of the machine and uploading of materials). More devices per sheets could also be produce by using bigger size sheets (i.e. from A4 to A0). Finally, the possibility of peeling off the devices, as demonstrated here, would also make them ready to be used by the final operator as they come out of the production line.

Something that would be interesting to pursue further, is the possibility of using different types of paper, or even material, on the same device. In this case, an MP^3 with three different pore size papers was fabricated, which could allow for optimisation of reagent deposition (e.g. the lowest possible concentration) and reaction/incubation time (e.g. the fastest reaction time), while maintaining analytical properties. Although no further testing of the other two grades of paper (WHT 4 and WHT 597) was carried out with immunological assays, there was a significant difference in the light transmission. This result is likely related to the intrinsic characteristic of the paper (specifically pore size and thickness) and has the potential to affect the specific requirements of an assay, like concentration of reagents and procedures for washing. Referring to the possibility of multiplexing, it would also be possible to integrate different immunoassays, which

might require specific substrates (i.e. nitrocellulose), on the same device. The type of paper used in paper-based devices has usually been chosen mainly based on fabrication techniques. For example, standard grade filter paper is compatible with most patterning techniques, while larger pore sizes (e.g. 20-25µm) are usually needed for techniques that requires full penetration of the cellulose fibres (e.g. ink jet printing) [24]. Using the technique described here, any pore size paper can be used, leaving the choice entirely based on the performance of the assay. Furthermore, the MP^3 could be used as a platform to directly compare assays run on different types of papers/materials, since they could be performed on one device, avoiding the use of multiple devices [25] and possibly inter-assay differences.

3.7 Conclusions

In conclusion, the MP^3 developed here is a valid alternative to other platforms used to perform P-ELISA previously described in literature. The new method of production is simple, rapid and of high-resolution and can produce robust, versatile and low-cost devices, providing 96 completely independent paper pads and compatible with standard laboratory microplates and instruments. It also has specific advantages in relation to this project and offers a platform for rapid optimisation of assay conditions. Therefore, it could potentially be used to transfer any type of existing ELISA into P-ELISA and become a diagnostic platform for detection of other disease. Although it cannot be considered a POC device, this fabrication technique can be applied toward the production of a 3D µPAD, in order to enable true POC testing at the "animal-side".

3.8 References

[1] Cheng, C.M., Martinez, A.W., Gong, J., Mace, C.R., Phillips, S.T., Carrilho, E., Mirica, K.A., and Whitesides, G.M. Paper-based ELISA. *Angewandte Chemie (International ed. in English)*, 2010. **49**(28): p. 4771-4774.

[2] Ge, L., Wang, S., Song, X., Ge, S., and Yu, J. 3D Origami-based multifunction-integrated immunodevice: low-cost and multiplexed sandwich chemiluminescence immunoassay on microfluidic paper-based analytical device. *Lab on a Chip*, 2012. **12**(17): p. 3150-3158.

[3] Hsu, C.-K., Huang, H.-Y., Chen, W.-R., Nishie, W., Ujiie, H., Natsuga, K., Fan, S.-T., Wang, H.-K., Lee, J.Y.-Y., Tsai, W.-L., Shimizu, H., and Cheng, C.-M. Paper-based ELISA for the detection of autoimmune antibodies in body fluid—The case of bullous pemphigoid. *Analytical Chemistry*, 2014. **86**(9): p. 4605-4610.

[4] Wang, S., Ge, L., Song, X., Yu, J., Ge, S., Huang, J., and Zeng, F. Paper-based chemiluminescence ELISA: Lab-on-paper based on chitosan modified paper device and wax-screen-printing. *Biosensors and Bioelectronics*, 2012. **31**(1): p. 212-218.

[5] Badu-Tawiah, A.K., Lathwal, S., Kaastrup, K., Al-Sayah, M., Christodouleas, D.C., Smith, B.S., Whitesides, G.M., and Sikes, H.D. Polymerization-based signal amplification for paper-based immunoassays. *Lab on a Chip*, 2015. **15**(3): p. 655-659.

[6] Hsu, M.-Y., Yang, C.-Y., Hsu, W.-H., Lin, K.-H., Wang, C.-Y., Shen, Y.-C., Chen, Y.-C., Chau, S.-F., Tsai, H.-Y., and Cheng, C.-M. Monitoring the VEGF level in aqueous humor of patients with ophthalmologically relevant diseases via ultrahigh sensitive paper-based ELISA. *Biomaterials*, 2014. **35**(12): p. 3729-3735.

[7] Murdock, R.C., Shen, L., Griffin, D.K., Kelley-Loughnane, N., Papautsky, I., and Hagen, J.A. Optimization of a paper-based ELISA for a human performance biomarker. *Analytical Chemistry*, 2013. **85**(23): p. 11634-11642.

[8] Carrilho, E., Phillips, S.T., Vella, S.J., Martinez, A.W., and Whitesides, G.M. Paper microzone plates. *Analytical Chemistry*, 2009. **81**(15): p. 5990-5998.

[9] Ballerini, D.R., Li, X., and Shen, W. Patterned paper and alternative materials as substrates for low-cost microfluidic diagnostics. *Microfluidics and Nanofluidics*, 2012. **13**(5): p. 769-787.

[10] Fenton, E.M., Mascarenas, M.R., Lopez, G.P., and Sibbett, S.S. Multiplex lateral-flow test strips fabricated by two-dimensional shaping. *Acs Applied Materials & Interfaces*, 2009. **1**(1): p. 124-129.

[11] Fu, E., Kauffman, P., Lutz, B., and Yager, P. Chemical signal amplification in two-dimensional paper networks. *Sensors and Actuators B: Chemical*, 2010. **149**(1): p. 325-328.

[12] Cassano, C.L. and Fan, Z.H. Laminated paper-based analytical devices (LPAD): fabrication, characterization, and assays. *Microfluidics and Nanofluidics*, 2013. **15**(2): p. 173-181.

[13] Abe, K., Kotera, K., Suzuki, K., and Citterio, D. Inkjet-printed paperfluidic immuno-chemical sensing device. *Analytical and Bioanalytical Chemistry*, 2010. **398**(2): p. 885-893.

[14] Dungchai, W., Chailapakul, O., and Henry, C.S. A low-cost, simple, and rapid fabrication method for paper-based microfluidics using wax screen-printing. *Analyst*, 2011. **136**(1): p. 77-82.

[15] Carrilho, E., Martinez, A.W., and Whitesides, G.M. Understanding wax printing: a simple micropatterning process for paper-based microfluidics. *Analytical Chemistry*, 2009. **81**(16): p. 7091-7095.

[16] Nunn, F.G., Burgess, S.T., Innocent, G., Nisbet, A.J., Bates, P., and Huntley, J.F. Development of a serodiagnostic test for sheep scab using recombinant protein Pso o 2. *Molecular and Cellular Probes*, 2011. **25**(5-6): p. 212-8.

[17] Christopher-Hennings, J., Araujo, K.P.C., Souza, C.J.H., Fang, Y., Lawson, S., Nelson, E.A., Clement, T., Dunn, M., and Lunney, J.K. Opportunities for bead-based multiplex assays in veterinary diagnostic laboratories. *Journal of Veterinary Diagnostic Investigation*, 2013. **25**(6): p. 671-691.

[18] McKenna, S.L.B. and Dohoo, I.R. Using and interpreting diagnostic tests. *Veterinary Clinics of North America-Food Animal Practice*, 2006. **22**(1): p. 195-205.

[19] Tramuta, C., Lacerenza, D., Zoppi, S., Goria, M., Dondo, A., Ferroglio, E., Nebbia, P., and Rosati, S. Development of a set of multiplex standard polymerase chain reaction assays for the identification of infectious agents from aborted bovine clinical samples. *Journal of Veterinary Diagnostic Investigation*, 2011. **23**(4): p. 657-664.

[20] Tarasov, A., Gray, D.W., Tsai, M.-Y., Shields, N., Montrose, A., Creedon, N., Lovera, P., O'Riordan, A., Mooney, M.H., and Vogel, E.M. A potentiometric biosensor for rapid on-site disease diagnostics. *Biosensors and Bioelectronics*, 2016. **79**: p. 669-678.

[21] Wells, B., Innocent, G.T., Eckersall, P.D., McCulloch, E., Nisbet, A.J., and Burgess, S.T.G. Two major ruminant acute phase proteins, haptoglobin and

serum amyloid A, as serum biomarkers during active sheep scab infestation. *Veterinary Research*, 2013. **44**(103): p. 103-114.

[22] Lewis, G.G., DiTucci, M.J., Baker, M.S., and Phillips, S.T. High throughput method for prototyping three-dimensional, paper-based microfluidic devices. *Lab on a Chip*, 2012. **12**(15): p. 2630-2633.

[23] Stone, H.A. and Kim, S. Microfluidics: Basic issues, applications, and challenges. *Aiche Journal*, 2001. **47**(6): p. 1250-1254.

[24] Tian, J., Li, X., and Shen, W. Printed two-dimensional micro-zone plates for chemical analysis and ELISA. *Lab on a Chip*, 2011. **11**(17): p. 2869-2875.

[25] Busa, L.S.A., Maeki, M., Ishida, A., Tani, H., and Tokeshi, M. Simple and sensitive colorimetric assay system for horseradish peroxidase using microfluidic paper-based devices. *Sensors and Actuators B: Chemical*, 2016. **236**: p. 433-441.

Chapter 4 – Translation and optimisation of a lab-based sandwich haptoglobin ELISA onto P-ELISA

4.1 Introduction

The use of biomarkers, such as acute phase proteins, has been shown to provide significant aid for disease diagnosis in veterinary medicine [1]. Specifically, in the case of sheep scab, there is evidence that two acute phase proteins, Hp and SAA, could provide valuable additional information in regards of the status of the disease (active vs resolved) [2]. In case of a sheep scab outbreak, veterinary surgeons in Scotland need to certify that animals are no longer infested and/or contagious for the animal movement restriction to be lifted[6]. Using these biomarkers, coupled with a specific diagnostic test for sheep scab, could ensure that the correct treatment of the flock is followed and also establish the absence of an active infestation [2]. At the moment, the lack of low-cost and rapid assays to determine the concentration of either Hp or SAA in serum has hindered the potential of this diagnostic tool.

Recently, a sandwich lab-based Hp ELISA protocol has been developed by Pr. David Eckersall (University of Glasgow). The protocol had previously been validated on sheep and cattle serum and used within the group for research purposes only.

The aim of this chapter was therefore to translate the lab-based ELISA for the determination of Hp in serum into a P-ELISA, using the previously developed MP^3 (Chapter 3). The research question to address was the possibility of performing the same assay on a paper substrate, looking specifically at a reduction in the time and cost involved, while providing a reliable assay with analytical performances comparable to the conventional lab-based technique. The main expected challenges where related to the optimisation of the assay, in order to obtain the best possible signal with the minimum volume and concentration of reagents, a suitable timing for the immunoreactions and a functional washing technique. If successful, this would establish

the proof of concept that this immunoassay could be applied onto a different solid phase (paper instead of plastic) and the optimisation process would be applicable for translation of other existing lab-based ELISA onto P-ELISA.

4.2 Optimisation of the sandwich Hp P-ELISA

The protocol of the lab-based sandwich Hp ELISA can be found in Appendix A (Chapter 8) and a diagram of the assay is explained in Figure 28. All reagents mentioned in here, unless otherwise stated, have been sourced and prepared as reported in the protocol. Due to the nature of the P-ELISA assay, a different substrate solution (suitable for membranes) was sourced. In this case, a ready-to-use buffered alkaline phosphatase substrate solution, BCIP®/NBT Blue Liquid Substrate System for Membranes (Sigma-Aldrich, UK: Catalogue No B3804) was used.

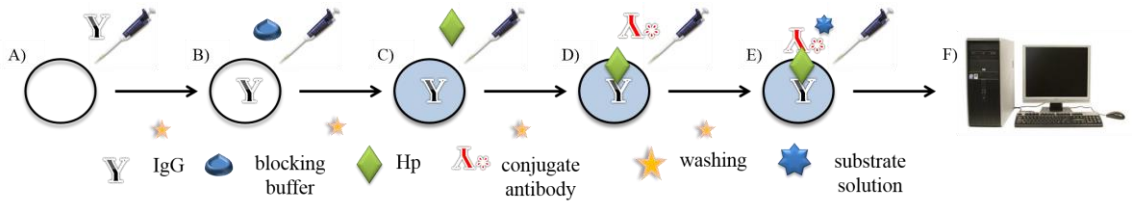

Figure 28- Diagram of the Hp ELISA. A) Deposition of capture antibody (rabbit anti-bovine IgG). B) Blocking to prevent unspecific binding. C) Deposition of samples containing Hp. D) Deposition of conjugate antibody (conjugated rabbit anti-bovine IgG). E) Deposition of substrate. F) Recording of the assay results.

To translate the lab-based protocol to a P-ELISA, a number of assay conditions had to be optimised. These included: optimisation of washing conditions, titration of reagents, selection of the optimal buffers and optimisation of reaction times.

4.2.1 Washing of the MP³

A significant challenge in the development of the P-ELISA, was the optimisation of the washing technique for the MP[3]. Conventionally in P-ELISA, washing is done by adding

[6] http://www.legislation.gov.uk/ssi/2010/419/pdfs/ssi_20100419_en.pdf

wash buffer to the top of the platform while pressing the bottom to a piece of absorbing paper [3-5]. Based on initial experiments, carried out on the simplified design (Section 3.2.1), this technique produced variable results (Figure 29), resulted in spillage of fluid on the bench top and proved difficult to control the exact time each pad within the device would be in contact with the wash buffer (variable time between paper pads for the wash buffer to fully cross the device into the absorbing paper).

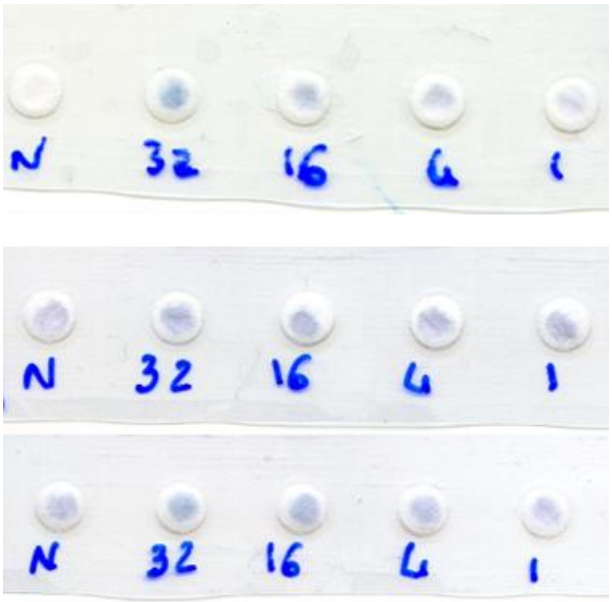

Figure 29 - Conventional washing technique for P-ELISA (3 replicates). Deposition of 2µl of WB (N=negative control), 32µg/ml Hp (32), 16µg/ml Hp (16), 4µg/ml Hp (4) and 1µg/ml Hp (1). After drying at RT for 10 min, 2µl of conjugate diluted 1:500 were deposited onto the device. After 60seconds, 20µl WB were dispensed onto each pad and the device was placed onto a sheet of absorbing paper. When all the WB had been absorbed from the device to the absorbing paper, 4µl of substrate solution were added onto each pad and the device was scanned after 10 min. Non-specific binding can be observed in the negative controls and was present in the second and third replicates.

It was also assumed that when moving from the initial design (5 paper pads) to the MP^3, proper alignment of a multichannel pipette on top of the paper pads would require careful positioning and therefore extended timing for washing. A more controlled and effective washing technique was therefore deemed necessary. A different approach, which had not been applied for P-ELISA before, was based on the use of an apparatus for automatic washing [6].

Since the MP^3 was designed to maintain the proportions of a standard 96-well microplate, a commonly used 96-well plate vacuum manifold (Bethesda Research

Laboratories, UK) connected to a vacuum pump (Millipore Chemical Duty Vacuum/pressure Pump, 115 V/60 Hz, UK) was used for plate washing (Figure 25). The MP^3 was placed within the manifold with paper pads aligned with the sample application plate and the manifold was sealed with the use of thumb screws. This resulted in improved control of assay conditions, i.e. application of the same amount of washing buffer for each paper pad and the uniform exposure of the solid phase to the buffer. It was also considered to be a more efficient technique (average of 1 minute for 20µl of WB to completely absorb from the MP^3 into a piece of absorbing paper vs 15s for the vacuum to clear 100µl of WB), with prevention of liquid spillage onto the bench top, as waste liquid was contained in the base of the manifold for later, safe disposal. A set of experiments, based on the analysis of the background signal after conjugate antibody was deposited and washing was applied, were performed to optimise the specific conditions of this technique. Based on the results, the technique with the lowest background signal was chosen: the MP^3 was placed in the vacuum manifold, with an absorbent pad made from Whatman Grade 1 cellulose chromatography paper placed underneath the MP^3. After filling all the wells of the manifold with 100µl WB, the vacuum (set at -10Pa) was activated and remained on until all WB was cleared from the wells (average 15s). This procedure was repeated three times.

4.2.2 Direct Hp P-ELISA

Initially, a direct ELISA (Figure 30) was performed to assess conjugate antibody titrations and incubation, as well as different formulations of blocking buffer. Based on the literature, the simplest and yet effective method of reagents immobilisation on P-ELISA is by physical absorption, by applying the solution onto the paper and allowing it to dry at room temperature [3, 5, 7-9]. Visual assessment of the MP^3 showed that within 10 minutes of reagent deposition, all the paper pads were dry, therefore this was chosen as the binding time for Hp to the MP^3.

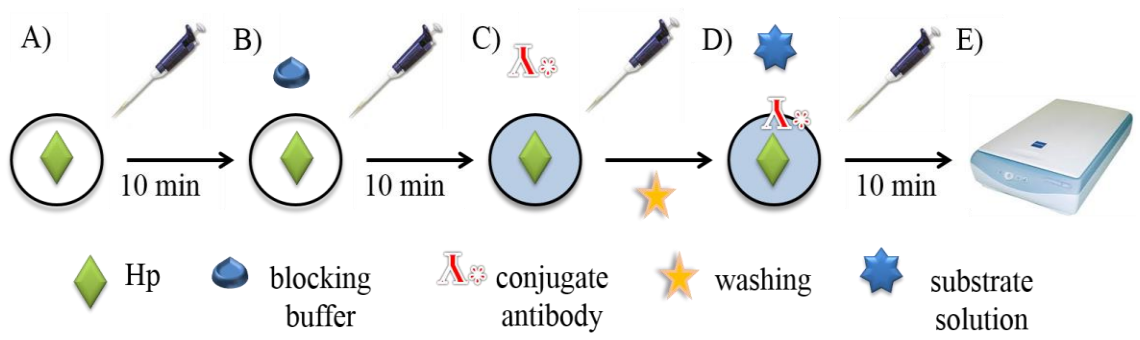

Figure 30 - Schematic of the direct Hp P-ELISA. A) Deposition of 2µl Hp onto each paper pad. B) After 10 min at RT, 2µl blocking buffer were deposited. C) After 10 min at RT, the MP³ was placed into the vacuum manifold and 4µl conjugate antibody were deposited. Washing was performed as reported in Section 4.2.1. After washing, the MP³ was removed from the manifold and 4µl substrate were added. E) After 10 min at RT, the MP³ was scanned. All reagents were deposited using a multichannel pipette.

Conjugate antibody titrations were evaluated against a range of Hp dilutions and, based on similar results obtained at concentration of 1:500 and 1:1000, an optimum dilution of 1:750 was selected (Figure 31).

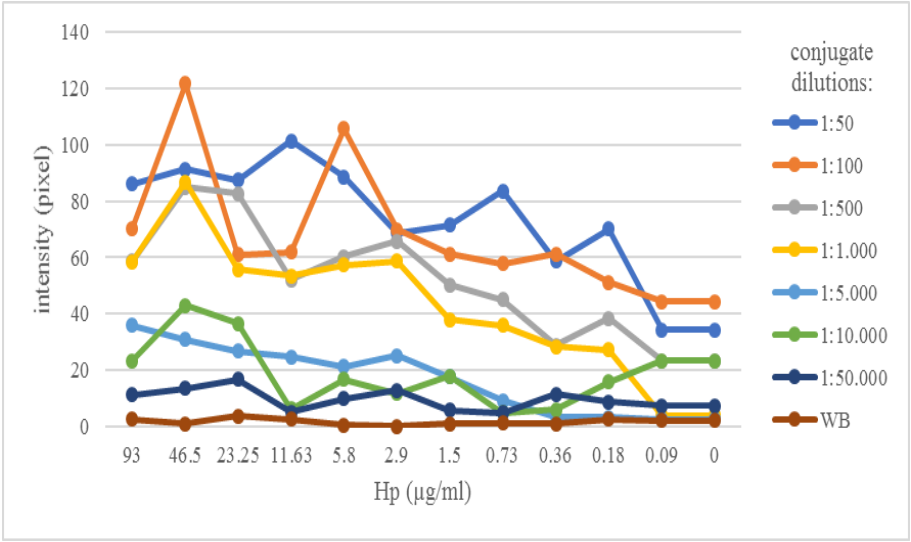

Figure 31 - Conjugate antibody titrations. Using the protocol described in Figure 2, Hp was diluted 1:10 (93µg/ml) in WB, then double diluted to 1:10240 (91ng/ml). A volume of 2µl of each dilution was applied to each column of the MP³ and the last column was left as negative control (0=WB). Conjugate antibody was diluted 1:50 in WB then double diluted to 1:50.000 and 4µl were applied to each row of the MP³ and the last row was left as negative control (WB). Washing was applied after a 60s incubation time. The graph shows the pixel intensity of each conjugate dilution against the Hp dilutions.

The incubation time of the conjugate antibody to the antigen was also evaluated. This stage is critical, as leaving the reagent for too long could increase the background noise, but not leaving it long enough would reduce the sensitivity and the limit of detection of

the assay. The experiments were based on the available literature and incubation time ranged from 60s [3, 10] to 150s [11]. For this assay, the optimal incubation time was determined as 90s (Figure 32).

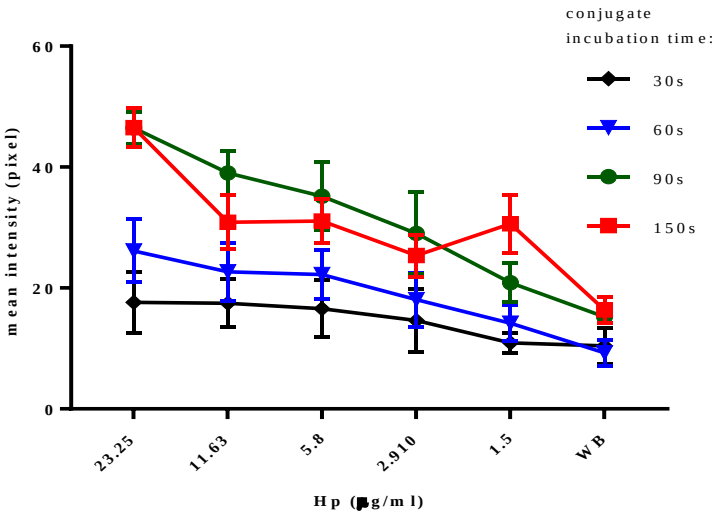

Figure 32 - Conjugate antibody incubation time. Using the protocol described in Figure 2, Hp was diluted 1:40 (23.25µg/ml) in WB, then double diluted to 1:640 (1.45µg/ml) and 2µl applied to each row of the MP^3 and the last row was left as negative control (WB). Conjugate antibody was diluted 1:750 in WB and 4µl were applied to each column of the MP^3. Washing was activated 30s, 60s, 90s and 150s after conjugate deposition. The graph shows the mean pixel intensity of 3 replicates and the error bars represent the SEM.

As with lab-based ELISA, blocking of the paper was necessary to avoid non-specific binding. The most commonly used blocking buffer for P-ELISA is bovine serum albumin (BSA) [3] and casein [12], while the sandwich Hp ELISA in the conventional format uses a 10% milk protein blocking buffer (Chapter 8). Different formulations of blocking buffers were assessed by comparing binding of conjugate antibody to the paper with or without blocking buffers. Based on the results it was confirmed that the blocking buffer used in the conventional format was the most suitable (Figure 33).

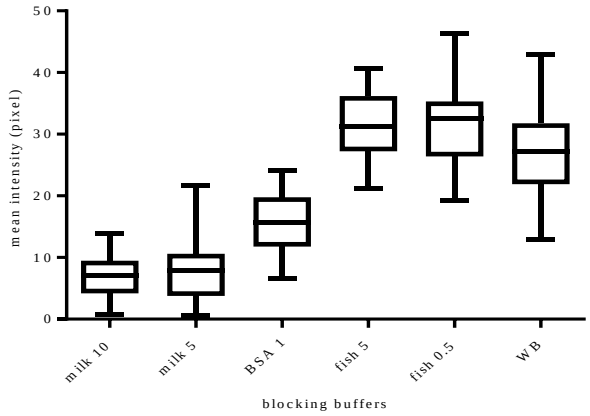

Figure 33 - Selection of the blocking buffer. Each column of the MP³ was blocked using different formulations of blocking buffers: milk 10 (10% Marvel milk protein in WB), milk 5 (5% Marvel milk protein in WB), BSA 1 (1% BSA in WB), fish 5 (5% fish gelatin in WB), fish 0.5 (0.5% fish gelatin in WB) and negative control (WB). After 10 min at RT, the MP³ was placed into the vacuum manifold and 4µl conjugate antibody diluted 1:750 were deposited. Washing was performed after 90s as reported in Section 4.2.1. After washing, 4µl substrate were added. After 10 min at RT, the MP³ was scanned. The graph shows the box plots of 16 replicates for each buffer.

4.2.3 Dilution and immobilisation of the capture antibody

Once the conditions for the direct ELISA were optimised, the final step of optimising the dilution and immobilization of the capture antibody was evaluated. Initially, the same coating buffer used in the conventional assay was used for dilution (3 replicates), showing no visible difference in the colorimetric reaction when serial dilutions of antibody titrations were evaluated against a range of Hp dilutions (Figure 34).

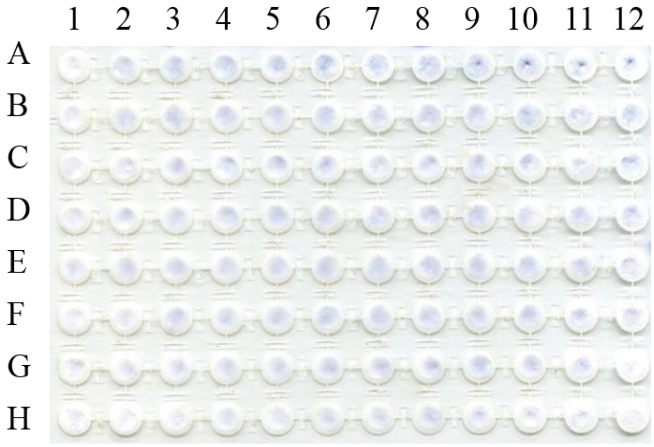

Figure 34 - Capture antibody dilution. Serial dilutions of capture antibody in coating buffer where dispensed onto the MP³. Rows A to H serial dilution of capture antibody: A=1:50 (24µg/ml) to H=1:100.000 (12ng/ml). Column 2 to 12 double dilution of Hp in WB (2=93µg/ml to 12=91ng/ml) and 1 negative control (WB). No colorimetric difference could be observed between the serial dilutions of capture antibody or the double dilutions of Hp.

Since conjugate and capture antibody are both purified rabbit anti-bovine haptoglobin, the same buffer (WB) used for dilution of the conjugate antibody was used to dilute the capture antibody. In this case, there was a visible difference in colorimetric reaction when different dilutions of Hp where evaluated. From these experiments, it was also possible to assess the optimal dilution of capture antibody, to achieved the best signal at the lowest possible antibody concentration. The optimal concentration chosen was 1:1000 (Figure 35).

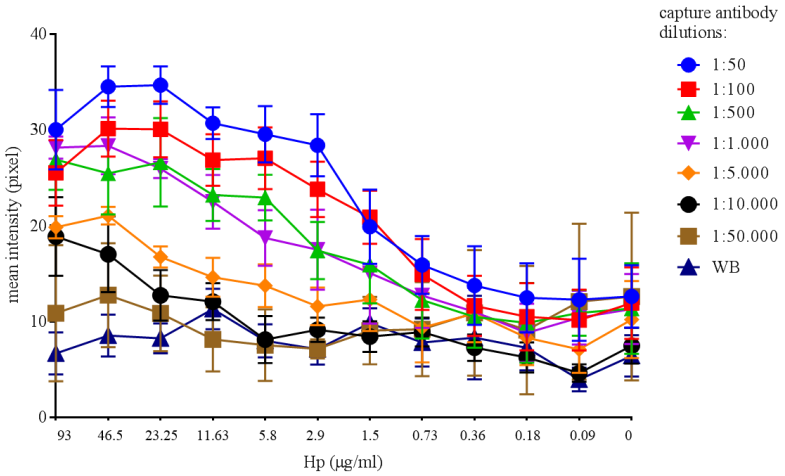

Figure 35 - Capture antibody titration. Capture antibody was diluted 1:50 then double diluted to 1:50.000. A volume of 2µl was applied to the paper pads sequentially in each row (A to G, row H was left as negative control=WB). After 10 min at RT, paper pads were blocked using 2µl of blocking buffer (10% milk protein) and allow to dry at RT for 10 min. Hp was diluted 1:10 (1=93µg/ml) in WB, then double diluted to 1:10240 (11=91ng/ml) and the last column was left as negative control (0=WB), 2µl of each dilution were applied to each column of the MP^3 and the last column was left as negative control (WB). After 10 min at RT, the MP^3 was washed as reported in Section 4.2.1. The conjugate antibody was diluted 1:750 in WB and 4µl were applied to each paper pad. Washing was applied after 90s incubation time and 4µl of substrate were added. After 10 min at RT, the MP^3 was scanned. The graph shows the mean pixel intensity (3 replicates) of each capture antibody dilutions against the Hp dilutions and error bars represent the SEM.

Finally, the coating timing was tested. As reported before, binding of reagents to the paper in P-ELISA is usually achieved by physical absorption and this was assumed by experiments done with the conjugate antibody, where despite vigorous washing, signal was still visible (Figure 36).

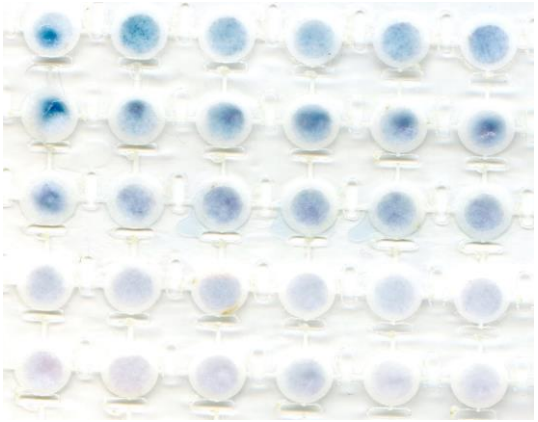

Figure 36 - Particular of an MP^3 showing conjugate antibody binding to the paper pads. A volume of 2µl of serial dilutions of conjugate antibody (1:50 to 1:5000) was applied sequentially to each row (6 replicates). After drying at RT for 10 min, the device was washed as reported in Section 4.2.1 and 4µl of substrate were added. After 10 min at RT, the MP^3 was scanned.

Therefore, the solution of capture antibody was deposited in the centre of the pad with a multichannel pipette. Since drying time for the MP^3 was visually assessed as complete by 10 minutes, a minimum time of 10 minutes at room temperature between deposition of the capture antibody and the following step in the assay was chosen.

4.2.4 Optimised sandwich Hp P-ELISA

Based on the results obtained, the optimised protocol for the sandwich Hp P-ELISA applied to the MP^3 was as follows: purified rabbit anti-bovine haptoglobin IgG was diluted to 1:1000 in WB. A volume of 2µL of the prepared solution was deposited onto each pad and the paper was allowed to dry at RT for 10 minutes. Non-specific binding was limited by the addition of 2µl of blocking buffer (10% milk protein) followed by drying at RT for 10 minutes. Standard bovine haptoglobin was diluted 1:5 in WB and then double diluted; 2µL of neat Hp solution and of each dilution were deposited onto the pads (sequentially in each column) and allowed to react for 10 minutes at RT. The device was washed with 100µl WB as described in Section 4.2.1. The purified rabbit anti-bovine haptoglobin IgG was conjugated with alkaline phosphatase (Chapter 8) then diluted 1:750 in WB. A volume of 4µl was then deposited onto each pad of the MP^3 and incubated at RT for 90 seconds. The device was washed again. A volume of 4µl of ready-to-use buffered alkaline phosphatase substrate solution was added to each pad. After 10 minutes at RT, the MP^3 was scanned using a desktop scanner.

4.3 Standard curve for the sandwich Hp P-ELISA

Using the MP^3 and the optimised sandwich Hp P-ELISA, it was possible to demonstrate that increasing concentrations of bovine standard Hp resulted in increasing intensity responses, based on a colorimetric reaction and visible with the naked eye (Figure 37).

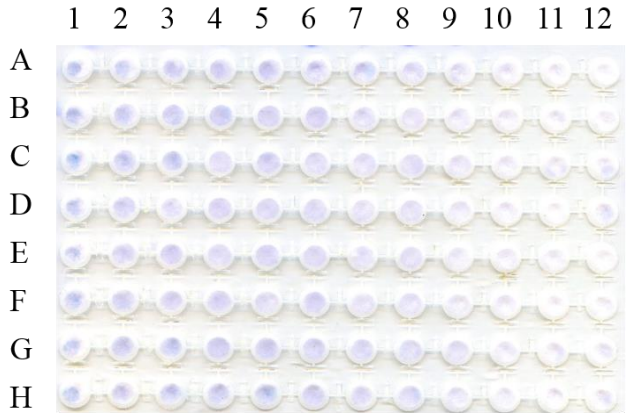

Figure 37 - Sandwich Hp P-ELISA on the MP^3. The protocol used is as reported in Section 4.2.4. Column 1 to 11 double dilution of Hp (1=0.93mg/ml to 11= 0.36µg/ml) and 12 negative control (WB). Rows A to H replicates (n=8).Some degree of unspecific binding can be seen in pads C, D, G and H 12.

Average pixel intensity values for each circular pad were analysed and correlated with the different concentrations of Hp. A standard curve was generated using non-linear regression and a sigmoid curve response (variable slope) was obtained (Figure 38), showing high correlation between pixel intensity and Hp concentration ($R^2 = 0.85$). The limit of detection (LOD) achieved was 1.7µg/ml, calculated as the mean of the negative control sample plus three times the standard deviation of the negative control sample and plateau of the signal intensity was found at an Hp concentration of 23.25µg/ml.

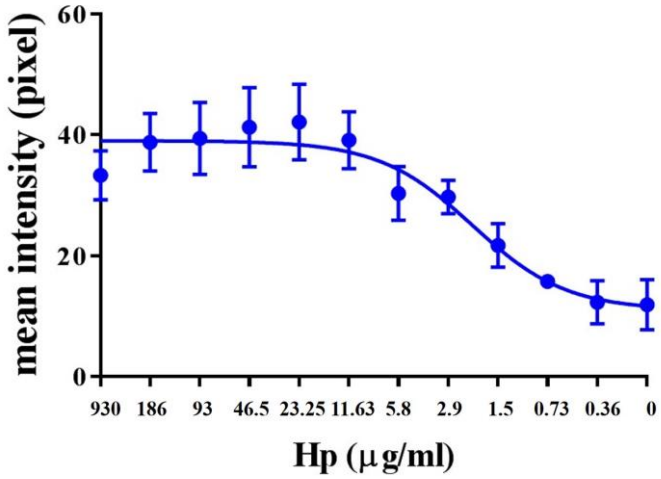

Figure 38 - Non-linear regression (variable slope) of mean pixel intensity in relation to Hp concentration (µg/ml). Each data point represents the mean of 8 replicates. Error bars represent standard deviations.

4.4 Cost-benefit analysis of lab-based vs MP^3 sandwich Hp P-ELISA

The total time required to perform a complete P-ELISA on the MP^3 was 40 minutes and multiple devices (up to 3) could be processed at the same time. The time and cost for performing the sandwich Hp P-ELISA assay on the MP^3 was considerably reduced when compared to the same assay performed in the conventional lab-based ELISA format, where reductions of 88% in cost and 93% in time were achieved (Table 1). A cost/sample of 0.13 pence (when samples are run in duplicates in each device) was calculated versus a £1/sample for the lab-based ELISA.

Table 1 - Cost-benefit analysis of performing the sandwich Hp ELISA on the MP³ or with the lab-based technique. # negligible cost.

	Hp P-ELISA on the MP³			**Lab-based Hp ELISA**		
	Volume (µL)	**Time (min)**	**Cost per plate**	**Volume (µL)**	**Time (min)**	**Cost per plate**
Capture antibody	2	10	£1	100	480	£5.5
Blocking buffer	2	10	#	200	60	#
Antigen (Hp)	2	10	£1.2	100	60	£15
Conjugate antibody	4	1.5	£3.4	100	60	£20
Substrate	4	10	£0.4	100	10	£10.5
Plate	-	-	£0.3	-	-	£1.5
Total	**14**	**41.5**	**£6.3**	**600**	**670**	**£52.5**

4.5 Discussion

This chapter describes the successful translation of a sandwich ELISA for the determination of Hp in serum from the lab-based format onto P-ELISA. The use of the previously developed MP³ was crucial for the optimisation of the assay conditions, allowing for the different variables to be tested with a systematic and standardized approach.

Within the optimisation process, an important contribution to the washing technique was made. To date, all P-ELISA applied to these type of devices (96-pad devices made of paper), are washed by depositing wash buffer and using a paper towel to absorb it through [3-5, 7-9, 11, 13]. Although all these studies report successful P-ELISAs, there is a lack of repeatability and also reduced control over the washing conditions. Using this technique in the initial experiments, it was noted how unpredictable was the timing for the washing buffer to completely adsorb through the device. This resulted in increased variability within the colorimetric reaction. An alternative approach was therefore explored to standardize the washing condition, which resulted in a constant

amount of washing buffer going through all the paper pads for the same amount of time. Furthermore, there could also be issues with health and safety associated with reagents and biological samples used within the assay and transferred onto the absorbing paper that would be manually handled by the operator. Potentially toxic reagents might be used or personnel could have specific allergies to certain products (i.e. milk proteins). In this case, spillage or handling of the impregnated absorbing towels could represent an additional constrain for the operator as well as for disposal. One reason why a vacuum manifold has not been used before could be related to the fabrication technique of these devices, which might not provide sufficient strength to withstand the vacuum pressure. On the contrary, the MP^3 has shown to be a robust device that can support strong pressure (up to -50Pa) without tearing of the paper pads. A similar approach has already been taken for a nitrocellulose based assay [14] which also employs a 96-well vacuum manifold. In this case, the whole nitrocellulose membrane is spotted with capture reagents, in a pattern to recreate a standard 96-well plate format. Using the MP^3, it was possible to apply controlled and vigorous washing on a low-cost substrate (£0.3/MP^3 vs approximately £2/nitrocellulose membrane), while maintaining the ease of fabrication (pipettes for physical absorption of capture reagents vs expensive reagent spotting systems). A possible criticism of this alternative washing technique, is the need for an increased amount of washing buffer. Generally, between 10 [3] to 20µl [11] of wash buffer are used, while an optimum amount of 100µl was estimated for the alternative washing technique. Although a significant increase in the amount of wash buffer is necessary, the cost of these buffers is usually negligible in comparison to the other reagents and would not considerably affect the overall cost when applied to P-ELISA.

Even though a different solid phase was used, most of the assay conditions were kept as per the conventional assay. The main differences were in the substrate, which was selected to be specific for membranes and also in the coating buffer used. Most of the P-ELISAs use phosphate-buffered saline (0.01M PBS, pH 7.4) [3, 11, 13, 15] or double distilled water [5, 8] as diluting buffers for the coating stage, while the one used in the conventional format (0.05M $NaHCO_3$ pH 9.6) is a commonly used coating buffer for lab-based ELISA[16]. The same WB was also used in the Hp P-ELISA for diluting all the reagents and for washing, which has simplified furthermore the P-ELISA compare to the lab-based format. In both cases, binding of proteins to the solid phase is achieved

by physical/passive absorption. In the case of the lab-based ELISA, this is due to hydrophobic interactions, which require higher pH than the isoelectric point of the protein to be attached, as well as long incubation times and specific temperature selection [17]. For the paper substrate, the interaction is based on dispersion and electrostatic forces, which makes the pH less important and therefore the type of buffer not so critical. Most P-ELISA rely on the simple method of binding, with a common incubation time of 10 minutes [3, 5, 9, 15], which is the average time for drying of these devices at room temperature. Although physical immobilisation on paper is not consider the most robust strategy [18], in this case it was still effective, despite application of vigorous washing (Figure 36). The possibility of using modified paper, by chitosan coating and glutaraldehyde cross-linking [11], to increase the binding capacity could be something worth exploring when translating the P-ELISA into a 3D µPAD format, where the presence of vertical and lateral flow might require a stronger immobilisation method or possibly a longer incubation period.

Although all conditions had been thoroughly investigated to optimise the assay, some degree of unspecific binding was still noted (Figure 37), which explains the LOD being higher than the one reported for the conventional lab-based ELISA. Through further optimisation or by considering alternative detection methods, the background noise could be reduced, with increase sensitivity of the assay. At this stage, however, this was not deemed necessary, given the clinically high concentration of circulating Hp and the rationale behind these experiments, which were aimed at translating the assay on the paper substrate.

Finally, although still requiring specific laboratory instruments (a vacuum manifold and pipettes) and non-portable equipment (a desktop scanner), this assay could potentially be carried out “in house” (i.e. within veterinary clinics) due to the considerably reduction in cost and time. Based on the standard curve generated, the recommended serum dilution could be 100-fold. Ovine serum presents a physiological range of 0.3-1.57 mg/ml for currently non-infested animals [2], which, at the proposed dilution, would be either below the LOD or within the detectable range of dilutions. The post-infestation rise to 3.53mg/ml [2], would be above the signal plateau and therefore would be considered a positive result. The total assay time was below 45 minutes for the P-

ELISA, compared to approximately 11 hours for the lab-based ELISA. The major factor in this considerable time reduction was the absence of the overnight coating incubation. Although this does not require much hands-on time, it requires planning of the diagnostic tests to be carried out. In the case of a disease outbreak, such as for sheep scab, it is not possible to forecast when the disease will occur and therefore it would be desirable to have a test that can be rapidly deployed on the same day and possibly within few hours.

4.6 Conclusions

The experiments carried out in this chapter demonstrated that the Hp assay for the diagnosis of sheep scab can be applied onto a new substrate (paper), showing direct correlation between the colorimetric signal and the concentration of Hp. The time and cost for performing this assay on paper are considerably reduced and, while the analytical performances are still below the conventional lab-based ELISA, the correlation of the signal with the diagnostic ranges of Hp concentration is sufficient for the tests to be used in clinically relevant situations. Furthermore, the use of the MP^3 provided a significant advantage in the translation and optimisation of the sandwich Hp P-ELISA and will form the basis for the final POC device. It also contributed to the available literature by providing improvements to the existing P-ELISA techniques, specifically by developing a more standardized and controlled washing technique for these devices.

4.7 References

[1] Eckersall, P.D. and Bell, R. Acute phase proteins: Biomarkers of infection and inflammation in veterinary medicine. *Veterinary Journal*, 2010. **185**(1): p. 23-27.

[2] Wells, B., Innocent, G.T., Eckersall, P.D., McCulloch, E., Nisbet, A.J., and Burgess, S.T.G. Two major ruminant acute phase proteins, haptoglobin and serum amyloid A, as serum biomarkers during active sheep scab infestation. *Veterinary Research*, 2013. **44**(103): p. 103-114.

[3] Cheng, C.M., Martinez, A.W., Gong, J., Mace, C.R., Phillips, S.T., Carrilho, E., Mirica, K.A., and Whitesides, G.M. Paper-based ELISA. *Angewandte Chemie (International ed. in English)*, 2010. **49**(28): p. 4771-4774.

[4] Badu-Tawiah, A.K., Lathwal, S., Kaastrup, K., Al-Sayah, M., Christodouleas, D.C., Smith, B.S., Whitesides, G.M., and Sikes, H.D. Polymerization-based signal amplification for paper-based immunoassays. *Lab on a Chip*, 2015. **15**(3): p. 655-659.

[5] Murdock, R.C., Shen, L., Griffin, D.K., Kelley-Loughnane, N., Papautsky, I., and Hagen, J.A. Optimization of a paper-based ELISA for a human performance biomarker. *Analytical Chemistry*, 2013. **85**(23): p. 11634-11642.

[6] Clark, C.R., Hines, K.K., and Mallia, A.K. 96-Well apparatus and method for use in enzyme-linked immunofiltration assay (ELIFA). *Biotechnology Techniques*, 1993. **7**(6): p. 461-466.

[7] Hsu, C.-K., Huang, H.-Y., Chen, W.-R., Nishie, W., Ujiie, H., Natsuga, K., Fan, S.-T., Wang, H.-K., Lee, J.Y.-Y., Tsai, W.-L., Shimizu, H., and Cheng, C.-M. Paper-based ELISA for the detection of autoimmune antibodies in body fluid—The case of bullous pemphigoid. *Analytical Chemistry*, 2014. **86**(9): p. 4605-4610.

[8] Costa, M.N., Veigas, B., Jacob, J.M., Santos, D.S., Gomes, J., Baptista, P.V., Martins, R., Inacio, J., and Fortunato, E. A low cost, safe, disposable, rapid and self-sustainable paper-based platform for diagnostic testing: lab-on-paper. *Nanotechnology*, 2014. **25**(9): p. 094006.

[9] Hsu, M.-Y., Yang, C.-Y., Hsu, W.-H., Lin, K.-H., Wang, C.-Y., Shen, Y.-C., Chen, Y.-C., Chau, S.-F., Tsai, H.-Y., and Cheng, C.-M. Monitoring the VEGF level in aqueous humor of patients with ophthalmologically relevant diseases via ultrahigh sensitive paper-based ELISA. *Biomaterials*, 2014. **35**(12): p. 3729-3735.

[10] Liu, X.Y., Cheng, C.M., Martinez, A.W., Mirica, K.A., Li, X.J., Phillips, S.T., Mascarenas, M., Whitesides, G.M., and Ieee. A portable microfluidic paper-based device for ELISA. *2011 Ieee 24th International Conference on Micro Electro Mechanical Systems*, 2011: p. 75-78.

[11] Wang, S., Ge, L., Song, X., Yu, J., Ge, S., Huang, J., and Zeng, F. Paper-based chemiluminescence ELISA: Lab-on-paper based on chitosan modified paper

device and wax-screen-printing. *Biosensors and Bioelectronics*, 2012. **31**(1): p. 212-218.

[12] Apilux, A., Ukita, Y., Chikae, M., Chailapakul, O., and Takamura, Y. Development of automated paper-based devices for sequential multistep sandwich enzyme-linked immunosorbent assays using inkjet printing. *Lab on a Chip*, 2013. **13**(1): p. 126-135.

[13] Tian, J., Li, X., and Shen, W. Printed two-dimensional micro-zone plates for chemical analysis and ELISA. *Lab on a Chip*, 2011. **11**(17): p. 2869-2875.

[14] Ramachandran, S., Singhal, M., McKenzie, K., Osborn, J., Arjyal, A., Dongol, S., Baker, S., Basnyat, B., Farrar, J., Dolecek, C., Domingo, G., Yager, P., and Lutz, B. A rapid, multiplexed, high-throughput flow-through membrane immunoassay: a convenient alternative to ELISA. *Diagnostics*, 2013. **3**(2): p. 244-260.

[15] Glavan, A.C., Christodouleas, D.C., Mosadegh, B., Yu, H.D., Smith, B.S., Lessing, J., Fernández-Abedul, M.T., and Whitesides, G.M. Folding analytical devices for electrochemical ELISA in hydrophobic R^H paper. *Analytical Chemistry*, 2014. **86**(24): p. 11999-12007.

[16] Crowther, J.R. Chapter 3. Stages in ELISA. Methods in molecular biology (Clifton, N.J.) ed. *The ELISA guidebook*, ed. Walker, J.M. Vol. 149. 2000: Humana Press. 43-78.

[17] He, J. Chapter 5.1 - Practical Guide to ELISA Development, in *The Immunoassay Handbook (Fourth Edition)*, Wild, D., Editor. 2013, Elsevier: Oxford. p. 381-393.

[18] Pelton, R. Bioactive paper provides a low-cost platform for diagnostics. *Trends in Analytical Chemistry*, 2009. **28**(8): p. 925-942.

Chapter 5 – Diagnosis of sheep scab by Pso o 2 indirect P-ELISA on the MP^3

5.1 Introduction

The recent development of a lab-based indirect ELISA for the detection of antibodies specific to a mite allergen (Pso o 2) has proven a highly sensitive diagnostic test for both clinical and sub-clinical sheep scab [1, 2]. The test can be very valuable during a sheep scab outbreak, where the main purpose is the exclusion of other common diseases causing similar clinical signs (e.g. pruritus and wool loss), like other ectoparasites [3], photosensitization [4] or scrapie [5]. In this case, all the animals showing clinical signs of the disease or a proportion of the affected ones can be sampled. Although skin scraping is still considered the routine technique for clinically evident sheep scab, it is relatively time consuming and requires a skilled operator for microscopic identification of ectoparasites [6]. A serological assay could be more appropriate when dealing with diseases at a flock rather than individual level [7].

The lab-based ELISA can also reliably diagnose sheep scab as early as 2 weeks post-infestation, where at least half (6/11) of the animals showed elevated serum IgG responses, while detection of mites using skin scraping would only achieve below 20% rate (2/11 animals) [8]. The test has also been shown to detect pre-clinical infestation during a natural outbreak of sheep scab [2]. The test could therefore represent a very valuable screening tool when animals are quarantined after being bought in, returning from away wintering or rented to other farms for mating.

The main problems, in both these situation, are the time from sample collection to result acquisition and the cost of the test. Although commercially available, this test is run by

a laboratory once a week for a cost of £9.50/sample[7] and a minimum of 12 animals should be sampled per flock.

In the case of an outbreak, the farmer would either have to wait potentially for a whole week (during which animals could infect neighbouring premises and the farm will be under movement restriction) or might decide to treat before having received the results. Furthermore, due to the antiparasitic drugs being relatively low-cost, the expenses of blank treatments would likely be cheaper than the overall cost of testing (including labour cost for gathering animals twice) [9]. It is obvious that having this assay as a low-cost POC test would further improve the diagnosis and appropriate usage of anti-parasitic drugs for sheep scab [10]. The same applies in case of quarantine treatments, where it might encourage farmers to screen all or a proportion of incoming animals, to prevent the disease from entering the flock.

The research question to address was the possibility of performing the other assay for the diagnosis of sheep scab on a paper substrate, specifically by looking at differentiation between infested and non-infested animals. The main foreseen challenges where related to the absence of standards for reference and the need to use serum samples. The aim of this chapter was therefore to translate the existing indirect Pso o 2 ELISA from its lab-based format onto P-ELISA, using the previously developed MP^3 and, once optimised, serum samples from naïve or scab infested sheep would be analysed and results compared with the lab-based ELISA.

5.2 Optimisation of the indirect Pso o 2 P-ELISA

A similar approach to the techniques explained in Chapter 4 was applied for the translation of this assay into a P-ELISA. The protocol of the indirect lab-based Pso o 2 ELISA can be found in Appendix B (Chapter 9) and a diagram of the assay is explained in Figure 39.

7 http://www.biobest.co.uk/assets/files/news/Sheep-scab-ELISA-Test-Press-Release.pdf

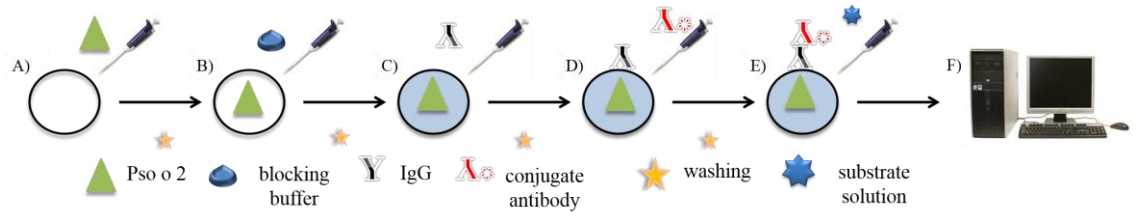

Figure 39- Diagram of the Pso o 2 ELISA. A) Deposition of capture antigen (Pso o 2). B) Blocking to prevent unspecific binding. C) Deposition of serum samples containing IgG. D) Deposition of conjugate antibody (conjugated rabbit anti-ovine IgG). E) Deposition of substrate. F) Recording of the assay results.

Specific parameters had to be optimised, as the working medium (serum) presents further challenges compared to buffer/standard solutions. The serum samples used for the optimisation were as reported in Section 2.2.2. All reagents mentioned in here, unless otherwise stated, were as reported in the protocol. Further reagents not reported in the protocol can be found in Section 2.3. Due to the nature of the P-ELISA assay, a different substrate solution (suitable for membranes) was sourced. In this case, a ready-to-use 3,3′,5,5′-Tetramethylbenzidine (TMB) Liquid Substrate System for Membranes was used (Sigma-Aldrich, UK. Catalogue No T0565).

Some of the conditions already optimised for the sandwich Hp P-ELISA (reagents volume, incubation timing at room temperature and washing of the MP^3) were tested again, confirming they were also suitable for this assay, while ad-hoc experiments were designed to evaluate conditions specific to this assay.

5.2.1 Titration and incubation of conjugate antibody

Initially, experiments were performed to assess the conjugate antibody titration and incubation time. Sequential dilutions of the conjugate antibody were deposited onto the MP^3 and washed after increasing incubation time. At 90s incubation time and with a 2000-fold dilution of the conjugate antibody, the signal was still visible but considerably reduced and these parameters were chosen for the assay. (Figure 40).

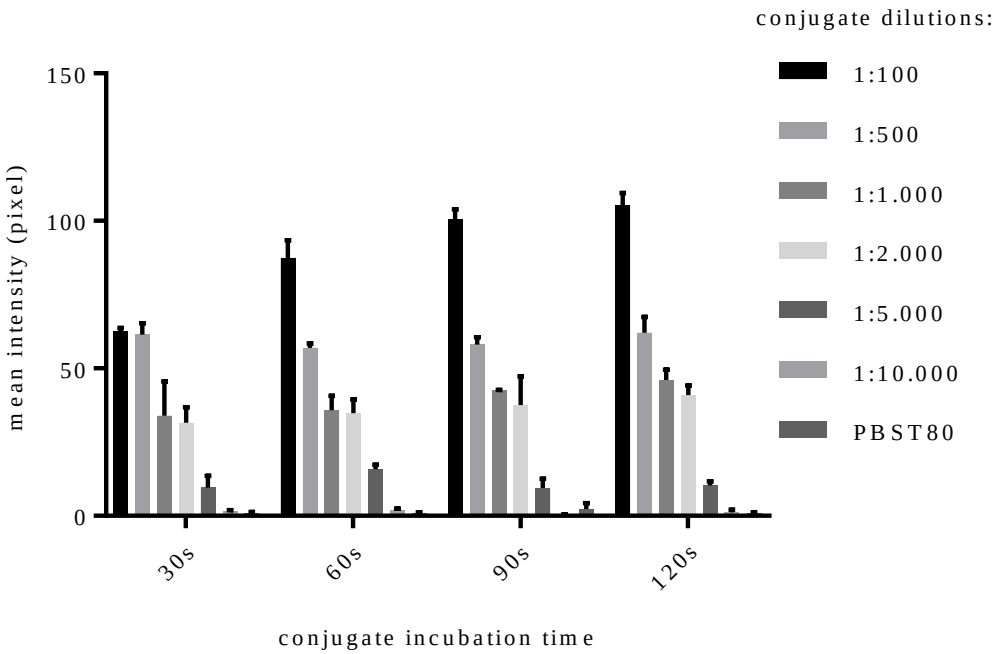

Figure 40 - Conjugate antibody titrations and incubation timing. The MP³ was placed in the vacuum manifold and 4µl conjugate antibody, diluted sequentially from 1:100 to 1:10000 with PBST80 used as negative control, were deposited. Washing was performed for 30s, 60s, 90s or 120s after conjugate deposition. A volume of 4µl substrate solution was added and the MP³ was scanned after 10 min. The graph shows the mean pixel intensity of 3 replicates and the bars show the SD.

5.2.2 Blocking buffer

Initial experiments showed that there was a high degree of non-specific binding (Figure 41).

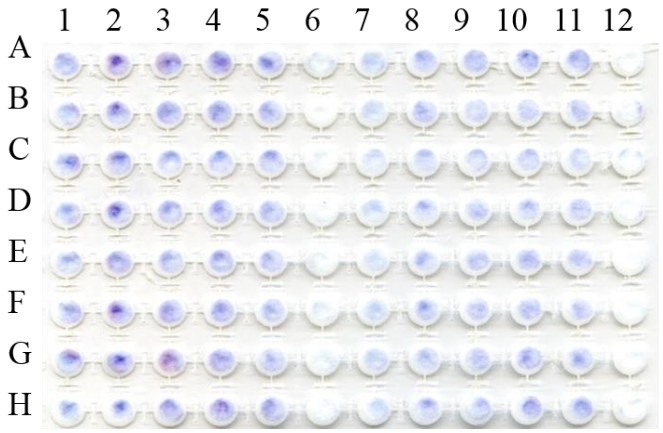

Figure 41 - High background noise due to non-specific binding. Coating antigen was diluted 1:10 and 2µl were deposited on the MP³. After drying at RT for 10 min, 2µl PBST80 were spotted on each pad. After 10 min at RT, 2µl of positive (column 1-5) and negative (column 7-12) control serum samples diluted 1:50 were spotted. Column 6 and 12 were kept as control (2µl PBST80). After 10 min, the MP³

was washed and 4µl conjugate antibody diluted 1:2000 were added and incubated for 90s. After washing, 4µl substrate were added and the MP³ was scanned after 10 min. There is a high degree of background noise in the negative serum samples.

Different blocking buffers were therefore assessed to reduce the degree of non-specific binding and background noise. Experiments showed that the optimum solution between the lowest background noise and a strong positive signal, was achieved using 5% (w/v) fish gelatine in PBSx10 (BB) (Figure 42).

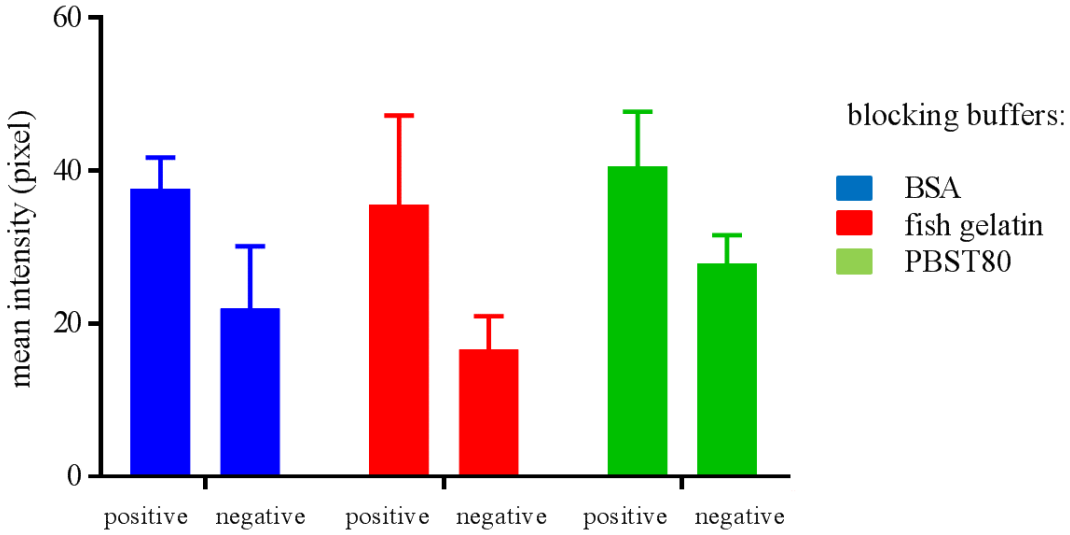

Figure 42 - Evaluation of blocking buffers. 2µl of coating antigen diluted 1:10 were deposited on the MP³. After drying at RT for 10 min, 2µl of the different blocking buffers under evaluation were spotted onto each pad in quadruplicate.: BSA (BSA 1%), fish gelatin (fish gelatin 5%) and PBST80. After 10 min at RT, 2µl of positive and negative control serum samples diluted 1:50 were spotted. After 10 min, the MP³ was washed and 4µl conjugate antibody diluted 1:2000 were added and incubated for 90s. After washing, 4µl substrate were added and the MP³ was scanned after 10 min. The graph shows the mean pixel intensity of 8 replicates for positive (first column) and negative (second column) serum samples and the error bars show the SD.

5.2.3 Checkerboard titrations

In order to achieve the best signal possible with the minimum concentration of reagents and samples, optimisation of the amount of coating antigen and serum dilution for the P-ELISA where investigated. To do so, a checkerboard titration, where serial dilutions of coating antigen are tested against serial dilutions of serum (used as positive and negative controls) was used.

The most suitable coating antigen dilution was 1:2 in double distilled water, with a concentration of rPso o 2 of 0.26mg/ml and for the serum dilutions, the optimum dilution was 1:50 in PBST80 (Figure 43). A two-way ANOVA showed there was no significant difference within the replicates values (column factor), but there was a significant difference ($p=0.017$) between the values obtained at different serum dilutions (row factor). Serum dilutions 1:50 and 1:100 where statistically significant different ($p<0.05$) when compared using Tukey's multiple comparison test to all the other serum dilutions for coating antigen either neat or diluted 1:2.

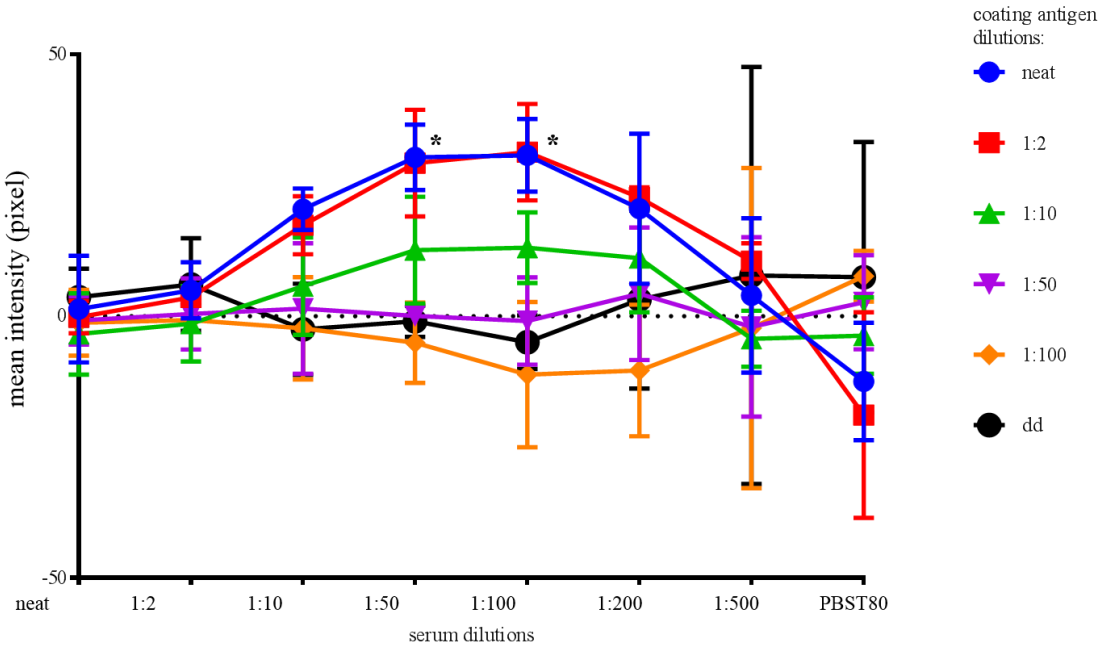

Figure 43 - Checkerboard titrations to evaluate coating antigen and serum dilutions. A volume of 2µl of coating antigen was deposited on the MP³ [neat to 1:100 and a control with double distilled water (dd)]. After drying at RT for 10 min, 2µl of BB were spotted onto each pad. After 10 min at RT, 2µl of positive (column 1-6) and negative (column 7-12) serum samples sequentially diluted (neat to 1:500 and the last row kept as negative control, PBST80) were spotted. After 10 min, the MP³ was washed and 4µl conjugate antibody diluted 1:2000 were added and incubated for 90s. After washing, 4µl substrate were added and the MP³ was scanned after 10 min. The graph shows the difference in mean pixel intensity between positive and negative serum (3 replicates) and the error bars the SD. *=p<0.05.

5.2.4 Serum incubation

To further improve the assay by increasing the colorimetric difference between positive and negative samples, an extended timing for serum incubation was evaluated. Ovine IgG has relatively low affinity for the Pso o 2 antigen (Dr. Francesca Nunn, Personal

Communication), which might require longer incubation time to improve the signal intensity. Based on this assumption, serum incubation time was extended to 15, 20 and 30 minutes. Results, however, showed a high degree of non-specific binding, as no difference was visible between positive and negative samples (Figure 44), therefore the serum incubation timing was kept at 10 minutes.

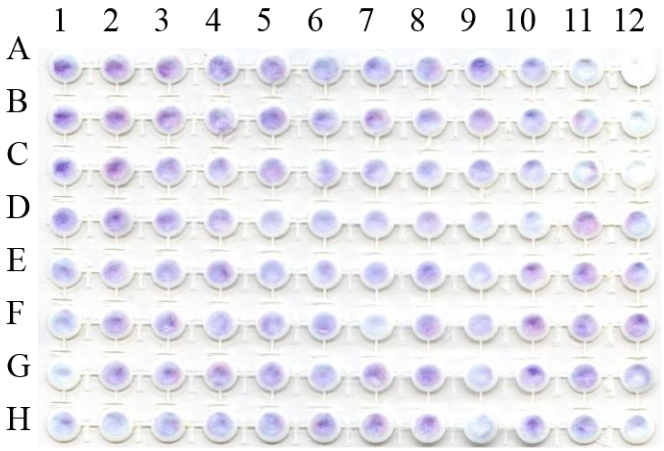

Figure 44 - Serum incubation timings. A volume of 2µl of coating antigen diluted 1:2 in double distilled water was deposited on the MP³. After drying at RT for 10 min, 2µl of BB were spotted onto each pad. After 10 min at RT, 2µl of positive (column 1-2, 5-6 and 9-10) and negative (column 3-4, 7-8 and 11-12) serum samples diluted 1:50 in PBST80 were spotted. After 30 min (column 1-4), 20 min (column 5-8) and 15 min (column 9-12), the MP³ was washed as reported in Section 4.2.1 and 4µl conjugate antibody diluted 1:2000 were added and incubated for 90s. After washing, 4µl substrate were added and the MP³ was scanned after 10 min. There is a high degree of background noise in the negative serum samples for all serum incubation timings tested.

5.2.5 Read-out timing

A reduction in the read-out timing from 10 to 5 minutes was possible with this P-ELISA as the development of a strong signal was readily detectable within 5 minutes of the addition of the substrate (Figure 45).

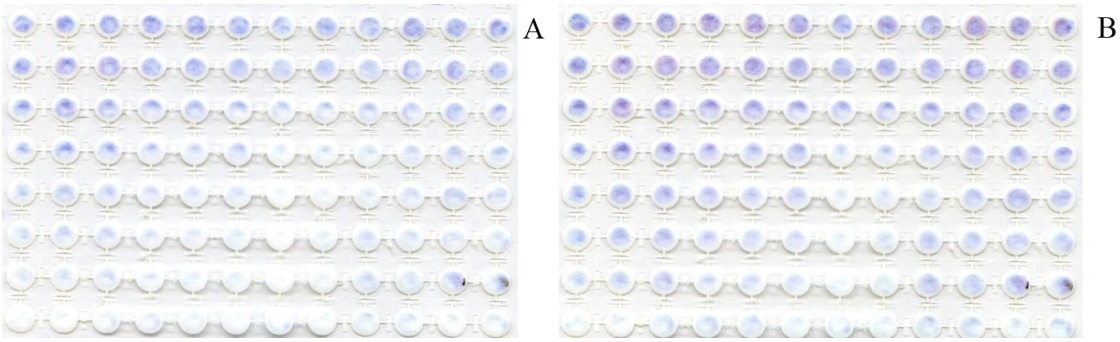

Figure 45 - Read-out timing. Indirect Pso o 2 P-ELISA carried out as per Section 5.2.6 A) The MP^3 is scanned 5 min after addition of substrate. B) The MP^3 is scanned 10 min after addition of substrate.

5.2.6 Optimised indirect Pso o 2 P-ELISA

Based on the results obtained, the optimised protocol for the indirect Pso o 2 P-ELISA applied to the MP^3 was as follows: rPso o 2 was diluted to 0.26mg/ml in double distilled water. A volume of 2µL of the prepared solution was deposited onto each pad and the paper was allowed to dry at RT for 10 minutes. Non-specific binding was limited by the addition of 2µl of BB (fish gelatin 5%) followed by drying at RT for 10 minutes. Serum samples were diluted 1:50 in PBST80 and 2µL were deposited onto the pads and allowed to react for 10 minutes at RT. The device was washed with 100µl WB as described in Section 4.2.1. The rabbit anti-ovine IgG HRP conjugate was diluted 1:2000 in PBST80 and 4µl were then deposited onto each pad of the MP^3 and incubated at RT for 90 seconds. The device was washed again. A volume of 4µl of ready-to-use substrate solution was added to each pad. After 5 minutes at RT, the MP^3 was scanned using a desktop scanner.

5.3 High-throughput analysis of data

During the larger scale experiments performed to optimise the two P-ELISAs, it was evident that the manual analysis of a considerable amount of data was extremely labour-intense and not suitable for a possible application as a POC device. To improve upon the previously used protocol (Section 2.5), using Image J after the image had been inverted and an oval selection of the area was manually drawn to each paper pad, a novel solution was explored, using a purpose-written MATLAB code to automate data analysis.

5.3.1 MATLAB code

Based on the protocol developed to analysed data on Image J, an algorithm was written in collaboration with Dr. Alan Faulkner-Jones and used to generate a code to be processed by MATLAB R2015b (The MatWorks®, Inc., US) (Chapter 10). To maintain the same output as the original data (analysis of mean grey pixel intensity) the algorithm automatically converts the image into grayscale and inverts it. The first problem encountered, however, was that the scanned MP^3 were in different positions (rows and columns will be at different angles, based on the position of the MP^3 within the scanner). To solve this problem, an algorithm was written to automatically rotate the picture so that rows and columns would be aligned, before the analysis took place. The operator manually locates a 6mm diameter circle on the first (A1) and last (H12) of the paper pads and double clicks each time. The algorithm automatically calculates the position of all the other pads within the picture and gives a mean pixel intensity value for all pads by generating an excel spreadsheet.

5.3.2 Image J vs MATLAB

A reduction from 210 to 4 (positioning of circle and double click x 2) manual steps was achieved using MATLAB. An average of 8.30 minutes was needed to fully analyse one MP^3 using Image J, while an average of 1 minute was necessary to analyse the same data using MATLAB. Data generated from Image J and MATLAB from the analysis of the same MP^3 were compared using Pearson correlation, showing agreement ($r=0.98$) between the two techniques (Figure 46). Data were analysed on two further MP^3, showing similar correlation ($r=0.97$ and $r=0.99$). Based on these results, the purpose-written MATLAB code was used for all future data analysis of this chapter.

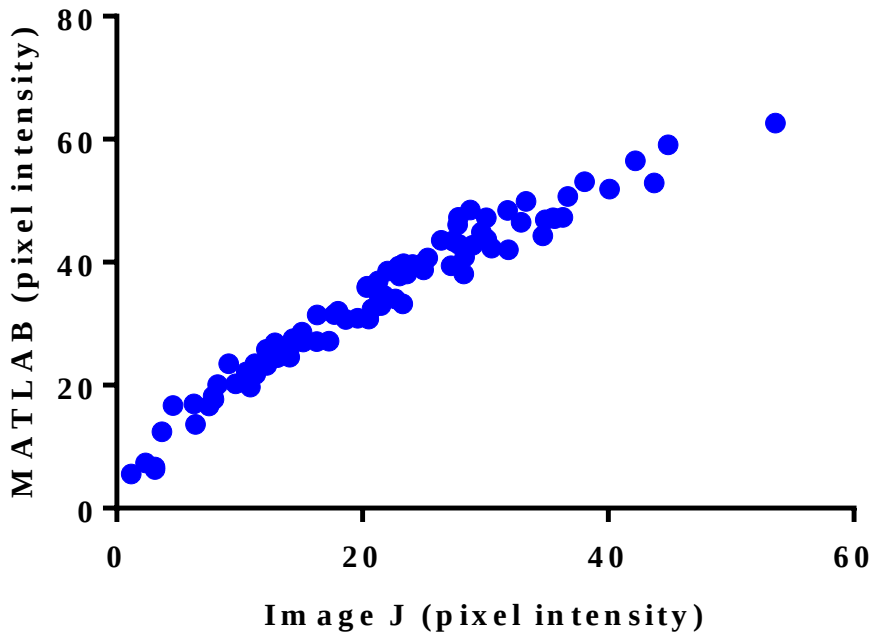

Figure 46 - Correlation between pixel intensity measurements obtained using Image J or the purpose-written MATLAB code. The graph shows the intensity of the pixel for each pad of the MP^3 (n=96) used for the evaluation of blocking buffers (Figure 42).

5.4 Performance of the Pso o 2 P-ELISA with ovine serum

In order to evaluate the application of the optimised Pso o 2 ELISA (protocol reported in Section 5.2.6) on the MP^3 in clinically relevant settings, analysis of ovine serum (Section 2.2) with known degree of infestation were performed.

5.4.1 Positive vs negative serum samples

To assess if the optimised Pso o 2 P-ELISA could differentiate between infested and naïve animals, a comparison of the mean pixel intensity between positive (n=6) and negative (n=6) control serum samples (Section 2.2.2) was performed using a Student's paired t-test. Two replicate MP^3 were used and samples were run as triplicates on each device (n=36). To analyse data from different MP^3 pixel intensity values were normalised. The average of 4 measurements from the control pads (paper pads where no serum was deposited) from the same MP^3 were subtracted from the pixel intensity values of each paper pad.

The mean pixel intensity for the positive samples was 37.91±1.8 (SEM) and 29.7±1.8 (SEM) for the negative samples, with a significant difference (p=0.001) between the two sets of data (Figure 47).

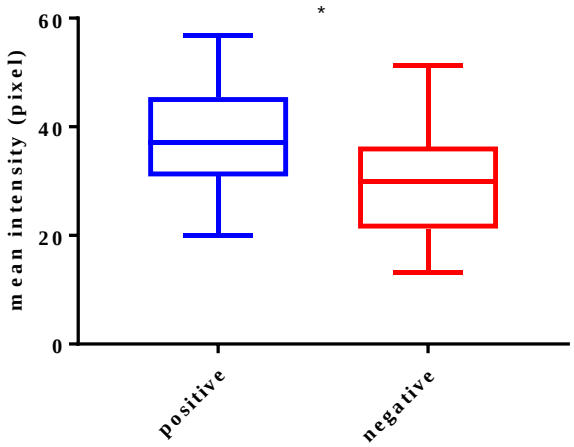

Figure 47 - Box-plot of positive and negative samples. Normalised pixel intensity obtained from serum of positive (n=36) and negative (n=36) control serum samples. *p=0.001.

5.4.2 Comparison of the results from the conventional lab-based ELISA and the P-ELISA

To assess whether the optimised Pso o 2 P-ELISA would provide comparable results to the conventional lab-based Pso o 2 ELISA (Chapter 9), samples were analysed with the two techniques and the results were compared. For the analysis, a total of 52 clinical samples (Section 2.2.1) were analysed using a total of 6 MP^3. Serum samples were run in duplicates and two platforms were run on the same day, while the other 4 were run sequentially on a different day. To analyse data from different MP^3 pixel intensity values were normalised. The average of 6 measurements from the control pads (paper pads where no serum was deposited) from the same MP^3 were subtracted from the pixel intensity values of each paper pad.

Samples analysed where classified as positive or negative based on the results from the conventional lab-based ELISA and agreement between the two tests was evaluated. Samples were considered positive by the MP^3 if they showed a positive result (pixel intensity equal or higher than the positive control) from at least 2 out of 3 replicates. If

the lab-based ELISA is considered as the "gold standard technique", then a sensitivity of 57.9% and a specificity of 87.8% were achieved by the test performed as P-ELISA on the MP^3 (Table 2). The measurement of agreement between test was k=0.56.

Table 2 - Comparison between samples testing positive or negative using the lab-based or the P-ELISA.

		Lab-based ELISA	
		Positive	**Negative**
P-ELISA	**Positive**	11	4
	Negative	8	29

Pearson correlation between the OD values from the lab-based ELISA and the mean pixel intensity of the P-ELISA was 0.54 (95% CI 0.32-0.7). When analysed at single time points, significant correlation where found at week 5, r=0.83 (95% CI 0.3-0.97) and week 6, r=0.89 (95% CI 0.5-0.98) (Figure 48).

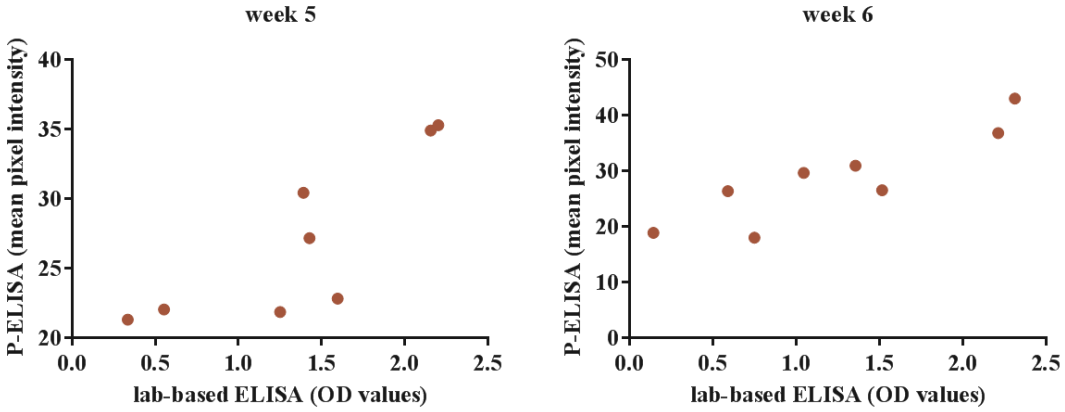

Figure 48 - Scatter plot of the correlation between lab-based ELISA and P-ELISA. The graphs show the correlation between OD values obtained with the lab-based ELISA and mean pixel intensity with the P-ELISA for blood samples taken at week 5 and at week 6 post-infestation.

5.5 Discussion

In this chapter, the translation and optimisation of a different lab-based ELISA into P-ELISA was demonstrated. Based on the knowledge acquired during the previous set of experiments, this process was significantly faster. The use of the MP^3 with a methodical approach could therefore potentially be implemented for translation of most, if not all, lab-based ELISA into P-ELISA. The biggest challenge, in this instance, was the absence of standards for optimisation of the technique and the need to use serum samples. The recent development of the lab-based ELISA and the availability of samples from experimentally infested animals were of paramount importance in this instance. Although, ideally, neat serum would be used at the POC, at this stage it was not suitable for the assay and an optimum dilution of 1:50 was chosen. Commonly, the lowest possible dilution would be chosen for lab-based immunological assay, in order to reduce sample usage to the minimum. In the case of POC tests, precise dilutions might not be achieved as the use of laboratory pipettes will not be available in the field. A more appropriate procedure could be the use of syringes or transfer pipettes where drops (rather than µl) of sample and buffer solution could be used for dilution. Furthermore, in the case of farm animals, blood samples are usually collected into 5 to 10 ml blood collection tubes, which means low sample volume is not usually an issue.

An interesting finding, during the optimisation process, was the reduction in the read-out timing compare to the previously optimised P-ELISA (5 minutes vs 10 minutes), with a further reduction in the overall assay timing from approximately 40 minutes to just over half an hour. Although at this stage, a 10 minutes serum incubation was deemed suitable for this assay, this might not be the case for other P-ELISA. Different P-ELISAs might require different timings at specific stages of the assay. If these assays were to be run in conjunction (e.g. multiplexing), there will be substantial advantages in using 3D µPADs, as the manipulation of fluid can be tailored to each assay [11].

A further contribution to the performance of P-ELISAs was made by the development of an automated procedure for image analysis, where a reduction from approximately 8 minutes to 1 minute for the analysis of one MP^3 was achieved. Most of the P-ELISA relying on colorimetric reactions are currently using Image J [12-14] or Photoshop® [15, 16] to analyse the scanned images of the devices. To date, only one study has

applied the use of a MATLAB code for automation of image analysis [17]. The main differences in the codes used are the creation of a mask to locate the paper pads within the image and the analysis in RGB instead of grayscale. A rapid and clear display of the test results for the end-user is still an area that needs further development [18]. As more research will hopefully be carried out on automatic image analysis, a standard code could be generated, which would then be tailored to suit the specific conditions.

Finally, the optimised protocol for indirect Pso o 2 P-ELISA was also applied for analysis of animal samples with known degrees of sheep scab infestation. Recently, an increasing number of studies have assessed the clinical performance of P-ELISA on disease diagnosis [13, 15, 16]. The possibility of applying research findings into practical applications is the mainstem of all interdisciplinary research and represent the final aim of this research project. The encouraging performances of the Pso o 2 P-ELISA in differentiating between positive (infested) and negative (naïve animals) could be used in clinical settings where an animal is showing clinical signs of the disease (i.e. pruritus and wool loss) as an alternative to the skin scraping method and as a rapid test compare to the conventional lab-based ELISA. In this case, all animals showing clinical signs would be sampled at the veterinary practice, as it is routinely done for skin scrapings, with results available within limited time (i.e. just over half an hour) and reliable results. This will allow for confirmation of the disease and targeted treatment to be applied for each animal. There was also a good correlation of the Pso o 2 P-ELISA with the conventional lab-based ELISA results, for samples at 6 weeks post-infestation. These results would allow for the P-ELISA to be used for field diagnosis of clinical sheep scab within the flock, as animals naturally infested will have been in contact with the parasite at different times, but they tend to show clinical signs from 8 weeks post-infestation [19] and are therefore likely to give a positive result at the test. In this case, as it is recommended for the conventional lab-based ELISA, a minimum of 12 animals per flock should be sampled to provide reliable results. When samples were compared at 2 weeks post-infestation, which is the earliest detection of sub-clinical infestation using the lab-based ELISA, correlation was low (results not shown). This was likely due to the lower sensitivity of the P-ELISA compared to the lab-based assay, and something that would need further consideration. A possible explanation for these results could be the level of background noise. Although there was a significant difference in signal

between positive and negative samples, mean intensity of the negative samples was around 29 pixels (Figure 47). Similar high background noise was also noticed for an indirect P-ELISA for the diagnosis of leishmaniosis in dogs [13], where they demonstrated a significant difference between positive and negative samples, but the mean intensity of the negative (non-infected animals) samples was high. The high degree of background noise was already noticed in the initial experiments, where a different blocking buffer was necessary to decrease the rate of non-specific binding. This problem was not encountered, for example, when the sandwich Hp P-ELISA was developed (mean intensity of the negative control of approximately 12 pixel). In the case of the Pso o 2 assay, however, a horseradish peroxidase (HRP) conjugate antibody was used, which has been reported to develop high colorimetric intensity in negative samples [20]. The lower analytical sensitivity is possibly one of the main criticisms toward paper-based immunoassay, especially where a colorimetric reaction is used [21]. Different solutions have been proposed to address this problem, like the use of polymerisation-based colorimetric methods [14] or the use of nanoparticle labels [22]. If a better sensitivity could be achieved, a useful application of this P-ELISA would be either the regular screening of flocks for early detection (e.g. sub-clinical) of diseases animals or sampling of incoming animals to prevent introduction of the disease into the flock.

5.6 Conclusions

In this chapter, the indirect Pso o 2 ELISA was successfully translated onto P-ELISA and used to analyse serum samples to detect specific antibodies against sheep scab. The differentiation between positive and negative samples would allow for the rapid test performed on the MP^3 to be used in clinical settings (i.e. a veterinary practice). The experiments performed have deepened the knowledge of some of the fundamental mechanisms involved in the interaction between biological substances and the paper substrate. In specific, the use of serum samples has highlighted the difficulties in preventing non-specific immunoglobulin (i.e. IgG) to bind to the paper, which has resulted in higher background noise than by using buffer solutions. It also allowed further improvement in the analysis of data, with a considerable reduction in time, a more user-friendly protocol and automated analysis of data.

5.7 References

[1] Nunn, F.G., Burgess, S.T., Innocent, G., Nisbet, A.J., Bates, P., and Huntley, J.F. Development of a serodiagnostic test for sheep scab using recombinant protein Pso o 2. *Molecular and Cellular Probes*, 2011. **25**(5-6): p. 212-8.

[2] Burgess, S.T., Innocent, G., Nunn, F., Frew, D., Kenyon, F., Nisbet, A.J., and Huntley, J.F. The use of a *Psoroptes ovis* serodiagnostic test for the analysis of a natural outbreak of sheep scab. *Parasite & Vectors*, 2012. **5**: p. 7-17.

[3] Cortinas, R. and Jones, C.J. Ectoparasites of cattle and small ruminants. *Veterinary Clinics of North America: Food Animal Practice*, 2006. **22**(3): p. 673-693.

[4] Sargison, N.D., Baird, G.J., Sotiraki, S., Gilleard, J.S., and Busin, V. Hepatogenous photosensitisation in Scottish sheep casued by *Dicrocoelium dendriticum. Veterinary Parasitology*, 2012. **189**(2-4): p. 233-237.

[5] Tyler, J.W. and Middleton, J.R. Transmissible spongiform encephalopathies in ruminants. *Veterinary Clinics of North America: Food Animal Practice*, 2004. **20**(2): p. 303-326.

[6] Ballweber, L.R. Diagnostic methods for parasitic infections in livestock. *Veterinary Clinics of North America: Food Animal Practice*, 2006. **22**(3): p. 695-705.

[7] Taylor, M.A. Parasitological examinations in sheep health management. *Small Ruminant Research*, 2010. **92**(1-3): p. 120-125.

[8] Ochs, H., Lonneux, J.F., Losson, B.J., and Deplazes, P. Diagnosis of psoroptic sheep scab with an improved enzyme-linked immunosorbent assay. *Veterinary Parasitology*, 2001. **96**(3): p. 233-242.

[9] Nieuwhof, G.J. and Bishop, S.C. Costs of the major endemic diseases of sheep in Great Britain and the potential benefits of reduction in disease impact. *Animal Science*, 2005. **81**: p. 23-29.

[10] Wells, B., Burgess, S.T.G., McNeilly, T.N., Huntley, J.F., and Nisbet, A.J. Recent developments in the diagnosis of ectoparasite infections and disease through a better understanding of parasite biology and host responses. *Molecular and Cellular Probes*, 2012. **26**(1): p. 47-53.

[11] Lisowski, P. and Zarzycki, P. Microfluidic paper-based analytical devices (μPADs) and micro total analysis systems (μTAS): development, applications and future trends. *Chromatographia*, 2013. **76**(19/20): p. 1201-1214.

[12] Cheng, C.M., Martinez, A.W., Gong, J., Mace, C.R., Phillips, S.T., Carrilho, E., Mirica, K.A., and Whitesides, G.M. Paper-based ELISA. *Angewandte Chemie (International ed. in English)*, 2010. **49**(28): p. 4771-4774.

[13] Costa, M.N., Veigas, B., Jacob, J.M., Santos, D.S., Gomes, J., Baptista, P.V., Martins, R., Inacio, J., and Fortunato, E. A low cost, safe, disposable, rapid and self-sustainable paper-based platform for diagnostic testing: lab-on-paper. *Nanotechnology*, 2014. **25**(9): p. 094006.

[14] Badu-Tawiah, A.K., Lathwal, S., Kaastrup, K., Al-Sayah, M., Christodouleas, D.C., Smith, B.S., Whitesides, G.M., and Sikes, H.D. Polymerization-based signal amplification for paper-based immunoassays. *Lab on a Chip*, 2015. **15**(3): p. 655-659.

[15] Hsu, M.-Y., Yang, C.-Y., Hsu, W.-H., Lin, K.-H., Wang, C.-Y., Shen, Y.-C., Chen, Y.-C., Chau, S.-F., Tsai, H.-Y., and Cheng, C.-M. Monitoring the VEGF level in aqueous humor of patients with ophthalmologically relevant diseases via ultrahigh sensitive paper-based ELISA. *Biomaterials*, 2014. **35**(12): p. 3729-3735.

[16] Hsu, C.-K., Huang, H.-Y., Chen, W.-R., Nishie, W., Ujiie, H., Natsuga, K., Fan, S.-T., Wang, H.-K., Lee, J.Y.-Y., Tsai, W.-L., Shimizu, H., and Cheng, C.-M. Paper-based ELISA for the detection of autoimmune antibodies in body fluid—The case of bullous pemphigoid. *Analytical Chemistry*, 2014. **86**(9): p. 4605-4610.

[17] Murdock, R.C., Shen, L., Griffin, D.K., Kelley-Loughnane, N., Papautsky, I., and Hagen, J.A. Optimization of a paper-based ELISA for a human performance biomarker. *Analytical Chemistry*, 2013. **85**(23): p. 11634-11642.

[18] Li, X., Ballerini, D.R., and Shen, W. A perspective on paper-based microfluidics: Current status and future trends. *Biomicrofluidics*, 2012. **6**(1): p. 011301 1-13.

[19] Bates, P. The pathogenesis and ageing of sheep scab lesions - part 1. *State Veterinary Journal*, 1997. **7**(3): p. 11-15.

[20] Lathwal, S. and Sikes, H.D. Assessment of colorimetric amplification methods in a paper-based immunoassay for diagnosis of malaria. *Lab on a Chip*, 2016: p. 1374-1382.

[21] Hu, J., Wang, S., Wang, L., Li, F., Pingguan-Murphy, B., Lu, T.J., and Xu, F. Advances in paper-based point-of-care diagnostics. *Biosensors and Bioelectronics*, 2014. **54**: p. 585-597.

[22] Pei, X., Zhang, B., Tang, J., Liu, B., Lai, W., and Tang, D. Sandwich-type immunosensors and immunoassays exploiting nanostructure labels: A review. *Analytica Chimica Acta*, 2013. **758**: p. 1-18.

Chapter 6 – Development of a microfluidic paper-based analytical device (µPAD) for point-of-care animal disease testing

6.1 Introduction

The opportunities offered by the application of microfluidic paper-based analytical devices (µPADs) for disease testing are incredible, meaning that testing can truly be done at the point-of-care (POC) and for a fraction of the cost of existing assay systems [1]. In the field of human medicine these devices are receiving increasing attention, the same, however, cannot be said for veterinary medicine. At present, studies on POC testing for animal diseases are still focused on the use of either dipstick [2-4] or lateral flow devices [5, 6], with very positive results, but also with the intrinsic drawbacks of these platforms.

Although in principle, fabrication techniques and detection methods would be the same, there is a clear need to show that these devices can also be applied for diagnosis of animal diseases. Making researchers and end-users aware of the advantages and of the possible applications offered by these new technologies is the first step in this direction [7]. At present, however, emphasis is often placed on achieving complicated 3D structures with impressive fluid flowing capabilities [8], while what is actually needed, especially in farm animal diagnostics, is a simple yet effective and low-cost solution to diagnose disease, which can be easily translated to the field.

The aim of this chapter was, therefore, the development of a µPAD suitable for point-of-care testing of animal diseases. Initially, a 2D device was developed in order to establish fluid flow dynamics and reaction timings. To evaluate the device an immunoassay, a direct Hp P-ELISA, was used as a model assay. Based on these results, a 3D µPAD was fabricated, which would allow for the manual steps done by the operator to be reduced (increase automation) and for multiplexing, with the final aim of having both diagnostic tests for sheep scab on a single device. The device was then tested with the same direct Hp ELISA, to show its functionality for application with biological assays. The main challenges foreseen where the suitable timings for

immunoreactions to occur in relation to the physics of the fluid flow, addressed with the 2D device, and the combination of vertical and horizontal fluid flow, as well as suitable packaging/assembly of the 3D device in order to obtain a constant fluid flow with no spillage in between layers and a working immunoassay.

6.2 Two-dimensional microfluidic paper-based analytical device (2D µPAD) design and fabrication

The designs for the 2D µPAD were based on the extensive literature available from the early paper-based devices [9-11]. In the development of a POC test, an ideal compromise between the fastest result possible and the timing of the immunological reactions is crucial. If the necessary time for reagents to react is not allowed, the analytical properties might be significantly affected [12]. This preliminary work was therefore fundamental to understand the physical properties (the length and the width of the channels and the effect of lamination), which can affect the flow rate and therefore the outcome of the immunological reactions.

6.2.1 Initial designs

A total of 13 paper prototypes and 15 lamination cut-out prototypes were designed, with a total of 27 different 2D µPADs produced. The prototypes can be summarised into two main types: the first group (design A) was structured as a central pad connected by channels to four side pads (Figure 49). This design was based on the extensive literature available from the early paper-based devices used for detection of glucose and protein [9-11], looking at having different analytes tested (up to 4) from one single sample. A slight modification to the designs reported in the literature was made to use a sample inlet with a wider diameter than the side pads, which allowed for a larger quantity of fluid to be deposited without spillage.

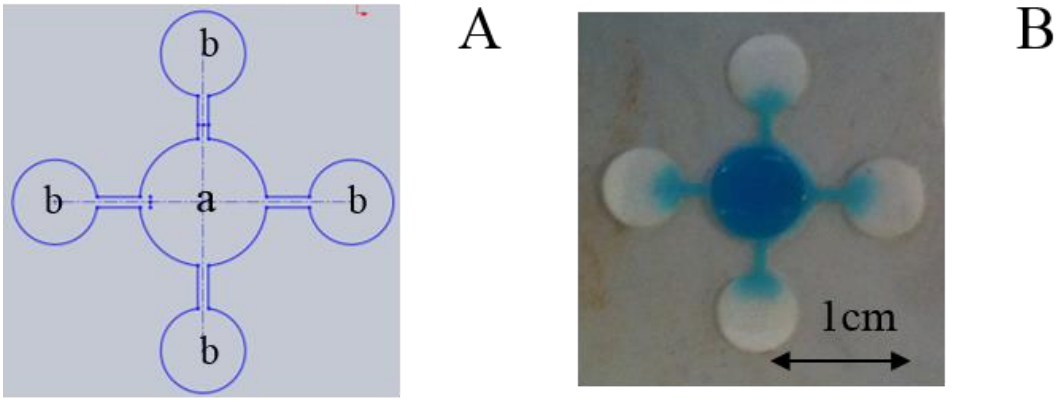

Figure 49 - Design A of the 2D devices. A) Schematic representation of the design A: central pad for sample inlet (r=3mm) (a) and 4 pads (r=2mm) for sample analysis (b) connected by microchannels (length=2mm, width=0.5mm). B) Picture taken 2 min after application of 20µl of food colouring in a.

A second group (design B) was also fabricated, with a central sample pad connected by microchannels to an absorbing pad and to a reagent-loading pad (Figure 50). The reasoning behind this design was taken from literature regarding lateral flow devices, where an absorbing pad is often used [13, 14] to improve the flow rate and to reduce the occurrence of non-specific binding between conjugate and substrate, eliminating the need for washing steps.

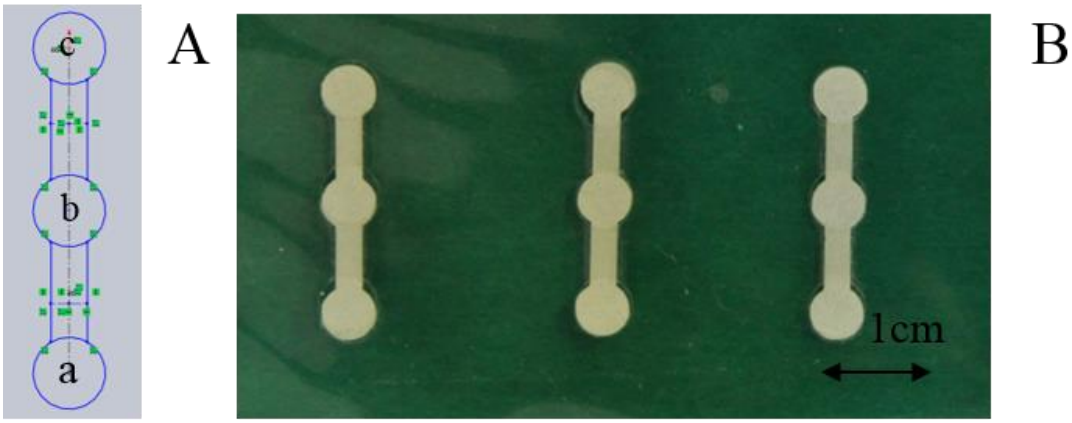

Figure 50 - Design B of the 2D devices. A) Schematic representation of the design B: pads (r=2mm) for reagents inlet (a), sample inlet (b) and absorbent pad (c), connected by microchannels (length=4.5mm, width=2mm). B) Picture showing the ready-to-use devices.

6.2.2 Lamination

The impact of the lamination on the flow rate can also be significant [15] and needs to be properly assessed. A set of experiments were performed to test different options for

lamination. Two different approaches were investigated: complete covering of the microfluidic channels with complete opening of the circular pads or partial covering of the whole device (lamination cut-out design smaller than the paper design). Testing of these two different methods showed that the first design resulted in a considerably slower flow rate (0.08mm/s vs 0.1mm/s) compared to the second design (Figure 51).

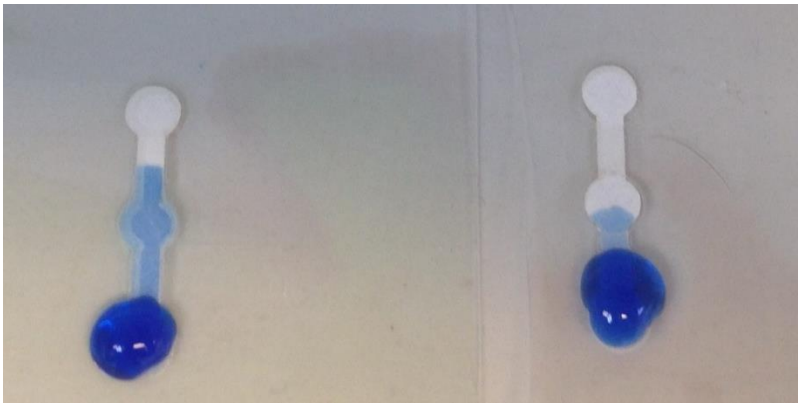

Figure 51 - Effect of lamination on the flow rate. On the left, the device has lamination that partially covers the paper cut-out. On the right, the device has lamination completely covering the microchannels and leaving the paper pads open. Picture taken 2 min after application of 50µl food colouring in the reagents inlet.

6.2.3 Final 2D µPAD

Based on the final aim of performing a complex biological assay on a µPAD, design B was deemed the most appropriate for applying the P-ELISA, mainly due to the need for an absorbent pad. Three different prototypes were produced for further testing, based on different lamination cut-out: devices 21, 22 and 24 (Figure 52).

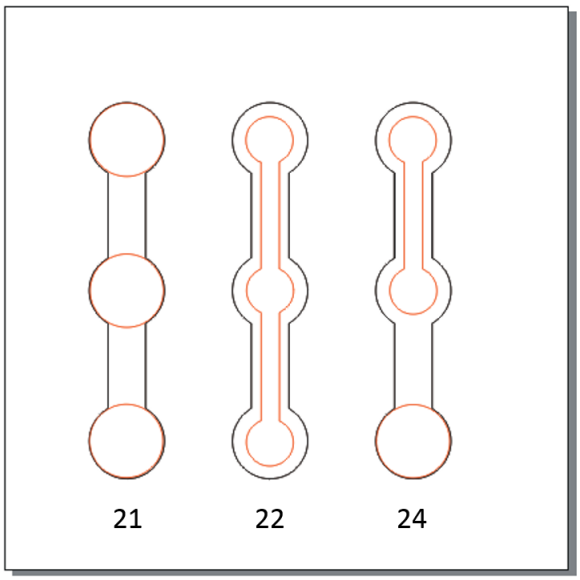

Figure 52 - The three final prototypes of the 2D µPAD. Black drawings represent the paper cut-out (design B) and red drawings the lamination cut-out. Device 21: the lamination is covering the two microchannels, leaving the paper pads completely opened (pads lamination r=2mm). Device 22: lamination cut-out is partially covering the whole device (pads: r=1.5mm, microchannels: length=5.5mm, width=1mm). Device 24: reagents inlet completely open and first microchannel completely covered; sample inlet, absorbent pad and second microchannel partially covered.

6.3 Direct Hp P-ELISA on the 2D µPAD

A direct Hp P-ELISA was applied to the final 2D µPADs to evaluate the performance of the device with an immunoassay. The protocol for the assay was based on the optimised haptoglobin (Hp) P-ELISA reported in Section 4.2.2, with specific modification to the reagent volumes to suit the 2D design. A total of 10 P-ELISAs were performed, showing colorimetric reaction where Hp was deposited on the 2D µPAD (Figure 53).

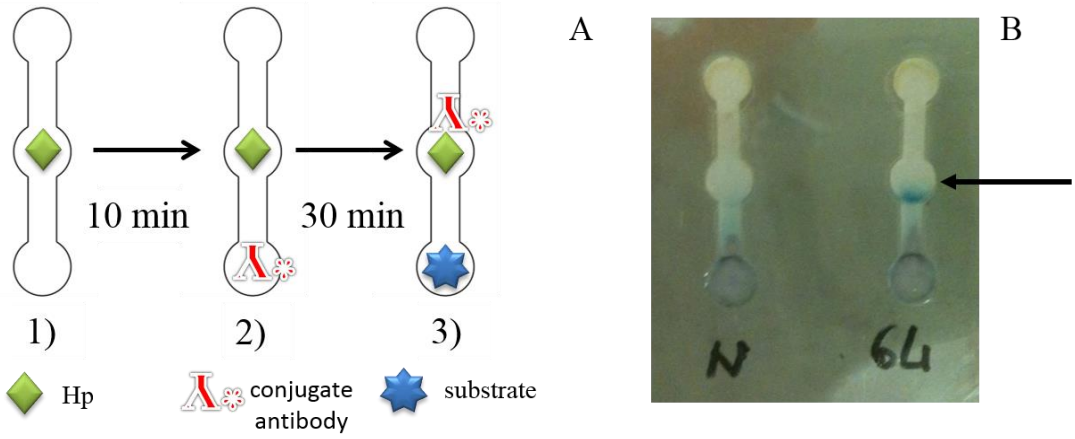

Figure 53 - Direct Hp P-ELISA on device 21. A) Schematic protocol for the P-ELISA on the 2D µPAD: 1) 0.7µl of sample (standard bovine Hp at concentration of 64 µg/ml or WB) were deposited in the sample inlet ; 2) after 10 min, 10µl of conjugate antibody diluted 1:750 were deposited in the reagents inlet; 3) after 30 min 10µl of substrate solution were deposited in the reagents inlet. B) Picture taken 10 min after application of substrate. N: WB, 64: 64µg/ml Hp. The black arrow indicates the colorimetric reaction following binding between Hp and conjugate.

The total time to perform the direct Hp P-ELISA using device 22 was shorter than using device 21 (device 21 total assay time: 50 minutes vs device 22 total assay time: 35 minutes). However, a longer incubation was necessary for the immunological reaction to proceed, as demonstrated by the absence of colorimetric reaction when device 22 was used (Figure 54).

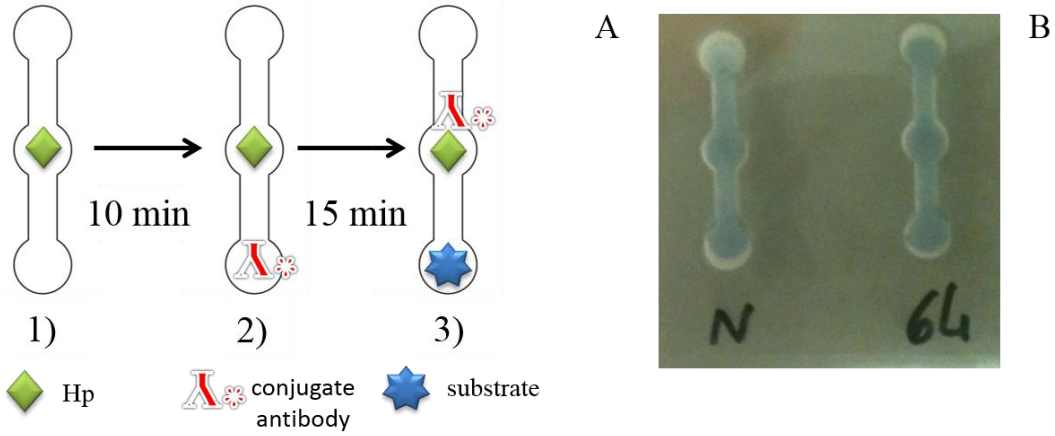

Figure 54 - Direct Hp P-ELISA on device 22. A) Schematic protocol for the P-ELISA on the 2D µPAD: 1) 0.7µl of sample (standard bovine Hp at concentration of 64 µg/ml or WB) were deposited in the sample inlet ; 2) after 10 min, 10µl of conjugate antibody diluted 1:750 were deposited in the reagents inlet; 3) after 15 min 10µl of substrate solution were deposited in the reagents inlet. B) Picture taken 10 min after application of substrate. N: WB, 64: 64µg/ml Hp. There is no colorimetric difference between the device containing Hp and the device with WB.

The deposition of reagents within the device could also affect the result of the assay as demonstrated by the lack of signal when conjugate and substrate were deposited directly onto the sample pad instead of the reagent loading inlet (Figure 55).

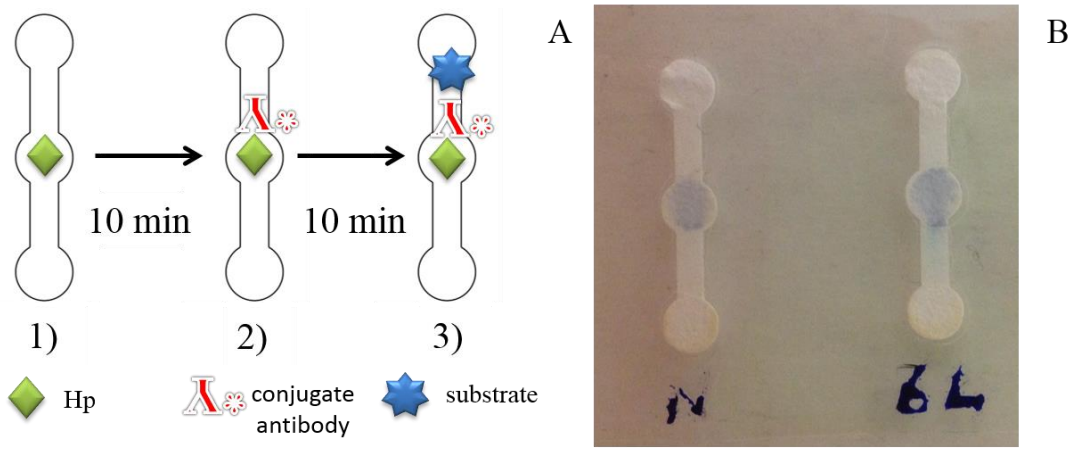

Figure 55 - Direct Hp P-ELISA on device 21 with different reagents depositions. A) Schematic protocol for the P-ELISA on the 2D µPAD: 1) 0.7µl of sample (standard bovine Hp at concentration of 64 µg/ml or WB) were deposited in the sample inlet ; 2) after 10 min, 5µl of conjugate antibody diluted 1:750 were deposited in the sample inlet; 3) after 10 min 5µl of substrate solution were deposited in the sample inlet. B) Picture taken 10 min after application of substrate. N: WB, 64: 64µg/ml Hp. There is no colorimetric difference between the device containing Hp (64) and the device with WB (N).

Furthermore, if the device was not allowed to dry after the conjugate had been deposited no colorimetric reaction was detectable in the sample pad (Figure 56).

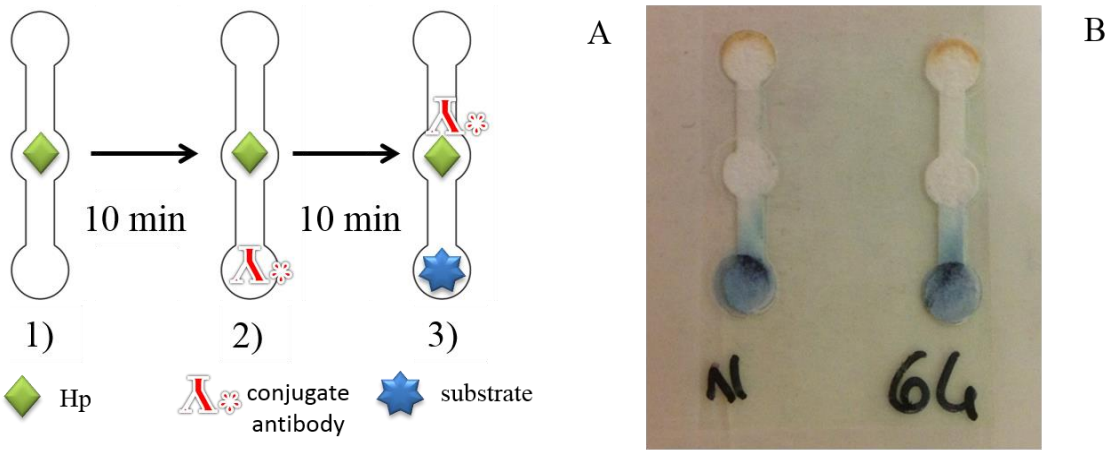

Figure 56 - Direct Hp P-ELISA on device 21 with different timing. A) Schematic protocol for the P-ELISA on the 2D µPAD: 1) 0.7µl of sample (standard bovine Hp at concentration of 64 µg/ml or WB) were deposited in the sample inlet ; 2) after 10 min, 10µl of conjugate antibody diluted 1:750 were deposited in the reagents inlet; 3) after 10 min 10µl of substrate solution were deposited in the reagents inlet. B) Picture taken 10 min after application of substrate. N: WB, 64: 64µg/ml Hp. There is no colorimetric difference between the device containing Hp (64) and the device with WB (N).

Finally, when device 24 was used, there was a detectable colorimetric reaction where Hp had been deposited and the total assay time was 35 minutes (Figure 57).

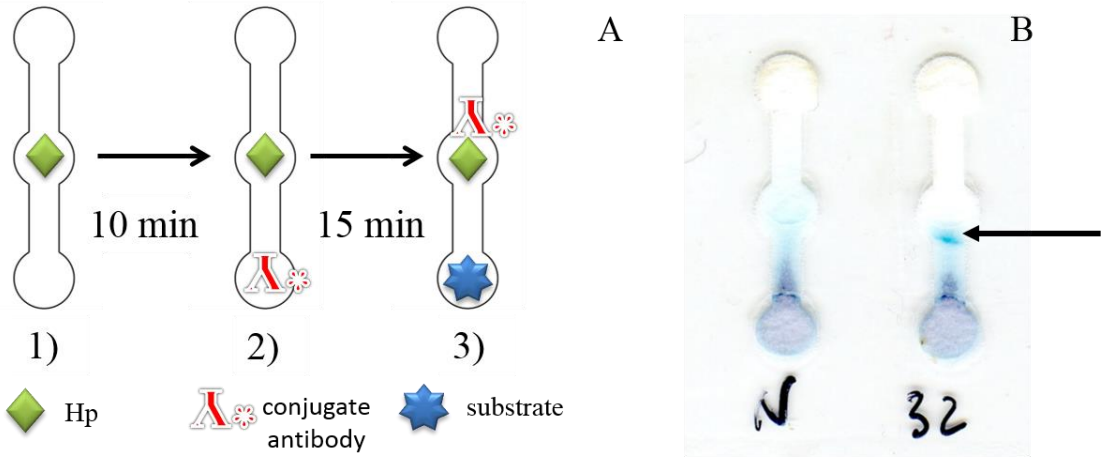

Figure 57 - Direct Hp P-ELISA on device 24. A) Schematic protocol for the P-ELISA on the 2D µPAD: 1) 0.7µl of sample (standard bovine Hp at concentration of 64 µg/ml or WB) were deposited in the sample inlet ; 2) after 10 min, 10µl of conjugate antibody diluted 1:750 were deposited in the reagents inlet; 3) after 30 min 10µl of substrate solution were deposited in the reagents inlet. B) Picture taken 10 min after application of substrate. N: WB, 32: 32µg/ml Hp. The black arrow indicates the colorimetric reaction following binding between Hp and conjugate.

6.4 Three-dimensional microfluidic paper-based analytical device (3D µPAD) design and fabrication

The rationale behind developing a 3D µPAD was to eliminate some of the steps required by the 2D format (e.g. conjugate addition), aiming at a final device that would only need addition of sample by the operator, as well as the possibility to perform multiple tests at one time.

6.4.1 Initial designs

A total of 20 prototypes of 3D µPADs were created. The main designs can be summarised into design C and design D, both designed to support multiple tests at once. The first one, made of two overlapping layers, was based on the concept of adding the sample and a wash buffer for rehydration of stored reagents (conjugate and substrate) at the same time, with geometries of the microfluidic allowing for difference in timing (sample reaching the test pad first, followed by the rehydrated conjugate and finally the rehydrated substrate) (Figure 58).

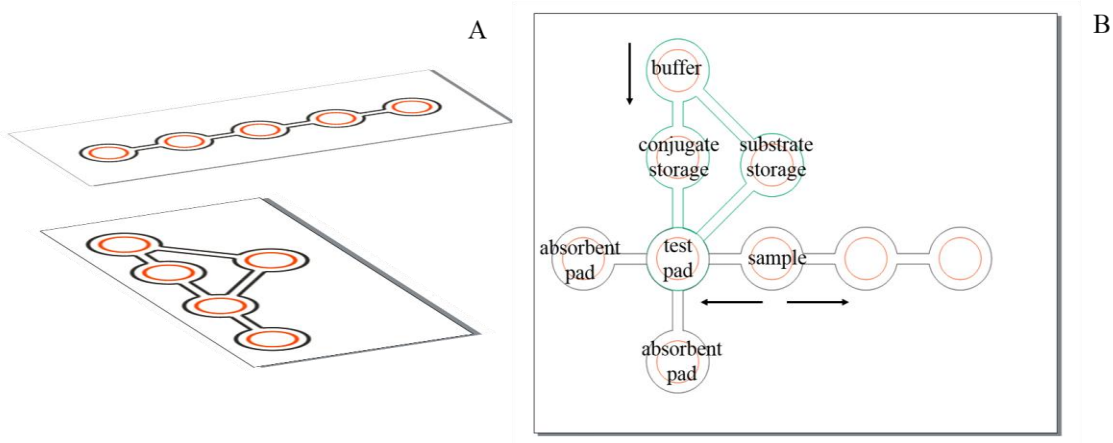

Figure 58 - Design C of the 3D µPAD. A) Exploded view showing the two overlapping layers of the device. The black drawing represents the paper cut-out and the red drawing represents the lamination cut-out. B) Schematic representation of the assay design: sample inlet, test pad, buffer inlet, conjugate storage pad, substrate storage pad and absorbent pads (x2). Paper pads r=3mm, microchannels width=1mm and length= 3mm. The black arrows show the fluid flow after the sample is introduced in the sample inlet and the buffer in the buffer inlet.

Design D (Figure 59) was composed of three layers, based on the concept of adding the sample and the substrate in sequential order. After the addition of the sample at the

device inlet, this would then move towards the stored conjugate and enable its rehydration. Incubation occurred while fluid was flowing to the test pad, where the immune-complex would be captured by a capture reagent on the test pad. After a period of incubation, the substrate would be added at the device inlet.

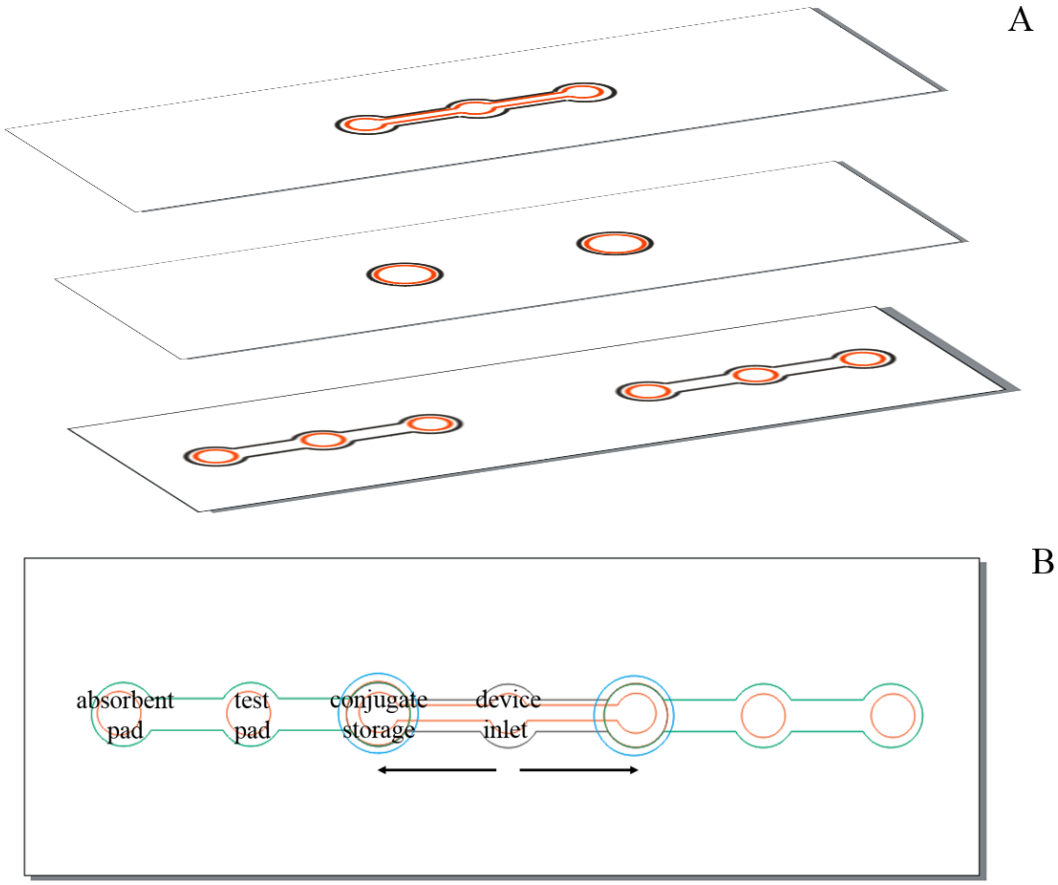

Figure 59 - Design D of the 3D µPAD. A) Exploded view showing the three overlapping layers of the device. The black drawing represents the paper cut-out and the red drawing represents the lamination cut-out. B) Schematic representation of the assay design: device inlet (for sequential addition of sample and substrate), conjugate storage pad, test pad and absorbent pads. Paper pads r=3mm, microchannels width=1mm and length= 3mm. The black arrows show the fluid flow from the device inlet to the other parts of the device.

6.4.2 Assembly of the 3D µPAD

One of the main challenges encountered when moving from the 2D to the 3D format, was the assembly of the device, with precise alignment and minimal space in between layers. The technique used for bonding adjacent layers together was based on the use of double-sided adhesive tape (3M™ Clear Double Sided Polyester Tape 9088-200

thickness, USA). Initially, small squares of tape were attached on the bottom side of the laminated layer then the device was assembled. This method, however, showed inconsistent results with some of the devices having a physical gap in between layers preventing vertical fluid flow (Figure 60).

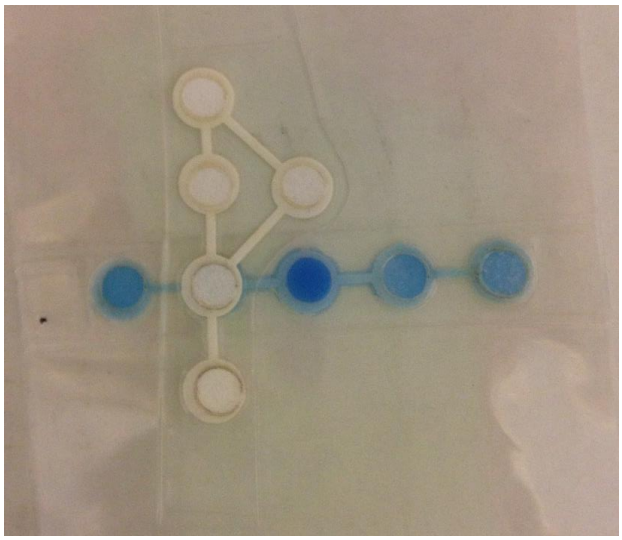

Figure 60 - Design C of the 3D µPAD with the original assembly technique. Assembly of the device is done by using four squares (roughly of 0.5mm^2) of double-sided tape at each corner of the laminated layer. Picture taken 10 min after application of 20µl food colouring in the sample inlet. The second layer of the device does not enter in direct contact with the first layer resulting in the absence of vertical fluid flow.

To solve this problem, different solutions were tested. Initially, an overall final lamination of the assembled device was considered. This approach had been previously reported in literature as a possible solution [16]. Although results were more consistent with this technique (Figure 61), thermal lamination could damage the pre-deposited reagents resulting in reduced assay performance and would also add a further fabrication step to the process.

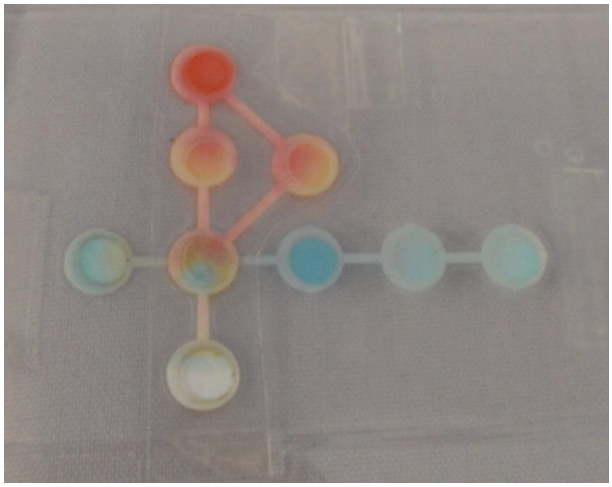

Figure 61 - Design C of the 3D µPAD with overall final lamination. Assembly of the device is done as per Figure 60, with an added lamination of the entire device. Picture taken 10 min after application of 10µl blue food colouring in the sample inlet and 10µl of red food colouring in the buffer inlet. Mixing of the two solutions can be seen in the test pad.

A different approach was therefore explored. The proposed solution, not reported before, was to preassemble a lamination and a double-sided adhesive sheet (3M™ 9471 Laminating Adhesive Rolls, 0.05mm thickness, USA) together (Figure 62A) and then apply the laser cutting to the assembly. This resulted in the laminated sheet and the double-sided adhesive sheet having the same surface and design (Figure 62B). Furthermore, based on the technique developed for the MP^3 fabrication, laser cutting of pre-designed alignment features allowed for an easier assembly of the final device. The new technique resulted in a consistent vertical flow rate within the device and a complete wet out of the device without spillage in between layers (Figure 62C).

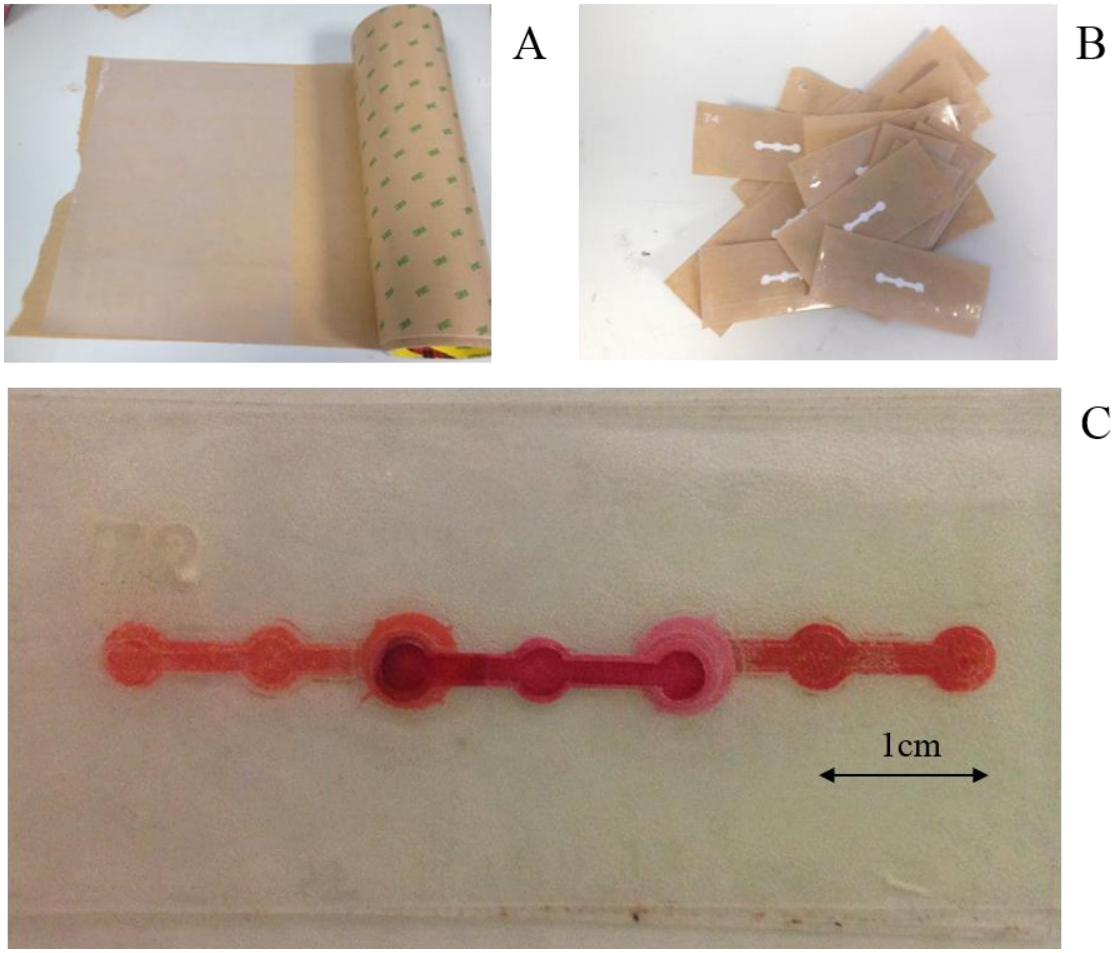

Figure 62 - Design D of the 3D µPAD with the new assembly technique. A) Lamination and double-sided adhesive sheets are assembled before laser cutting. B) Laminated layer of the device with the adhesive sheet matching the lamination design. Each layer of the device is ready for assembly, after removal of the adhesive sheet liner (brown coloured). C) Picture of the assembled device 10 min after application of 20 µl red food colour in the sample inlet, showing complete fluid flow through each layer of the device without spillage .

6.4.3 Final 3D µPAD

Based on the knowledge acquired from the experiments performed on the 2D µPAD and considering the required steps to perform multiple P-ELISA at the POC, design B was deemed as the most suitable solution and prototype 74 was chosen as the final 3D µPAD for further testing (Figure 63). The device comprised four layers, each with a specific function. Layer A (sample inlet layer) had a wider radius for addition and containment of the sample. Layer B (sample distribution layer) delivered the sample to two independent areas of the device. Layer C (conjugate storage layer) was for dry

reagent storage. Layer D (test layer) contained a single pad for reagents incubation and reaction, branching into two microchannels leading to a test pad (where the capture reagent is located and the result of the test is displayed) and from there into an absorbent pad. After cutting and lamination of each layer, the device was assembled by peeling off the liner of layer B, aligning layer C onto layer B and then layer D onto the two assembled layers. After removal of the liner from layer A, this was assembled onto the partial device to create the full device. The addition of laser cut numbers (74) directed the correct alignment of each layer. When 30µl of food colouring were applied, all devices tested (n=6) were completely wet out by 5 minutes, with no spillage and fluid was also observed to move through layers at the same speed (Figure 63B).

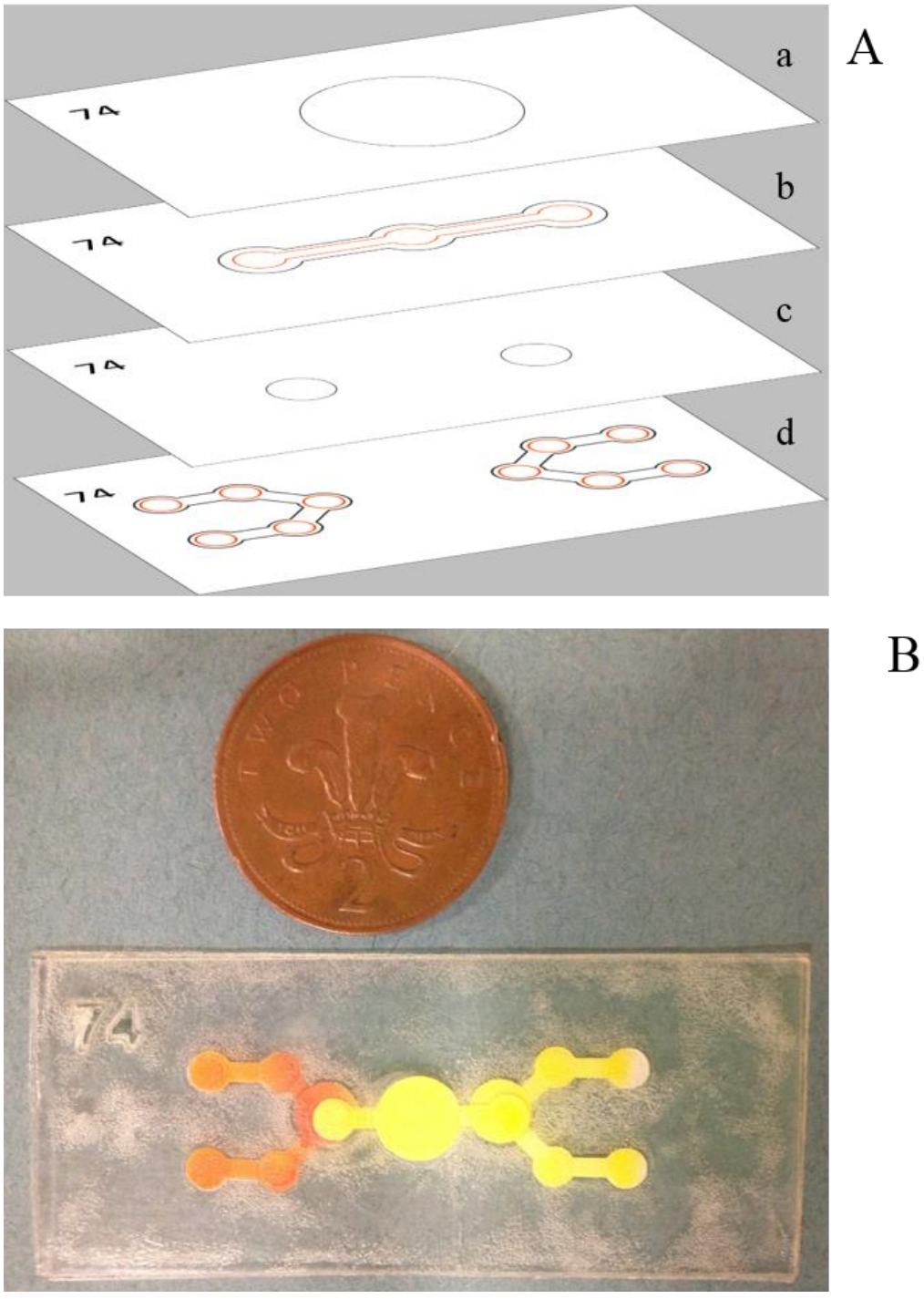

Figure 63 - Final 3D µPAD (prototype 74). A) Exploded view of the final 3D µPAD. The black drawings represent the paper cut-out and the red drawings the lamination cut-out. a) Layer A: sample inlet (paper pad r=8mm, lamination r=6mm). b) Layer B: sample distribution (paper pads r=2mm, microchannels length=4.5mm and width=2mm; lamination pads r=1.5mm, microchannels length=5.5mm and width=1mm). c) Layer C: conjugate storage (paper pad r=3mm, no lamination). d) Layer D: test (paper pads r=2mm, microchannels length=3mm width= 2mm, lamination pads r=1.5mm). B) Assembled 3D µPAD (70mm*30mm). To demonstrate mixing of a pre-deposited coloured sample, 2µl of red food colouring were deposited in layer C (left side only). After 10 min at RT, the device was assembled and 30µl yellow food colouring were added to layer A. Complete wet out was reached 5 min after addition of food colouring, and mixing of red and yellow food colouring can be seen on the left side of the device.

6.5 Direct Hp P-ELISA on the 3D µPAD

A direct Hp P-ELISA was also applied to the final 3D µPAD, based on the protocol used for the 2D device (Figure 53A). The aim was to assess the performance of the developed 3D µPAD as a diagnostic platform for immunoassay. The immunoreactions were evaluated in relation to the physics of the fluid flow (timing and volumes) as well as the location and binding of the reagents within the device. The initial experiments showed that complete wet out of the device was achieved, but the conjugate failed to reach the test pad, however it did react with the substrate within layer B (Figure 64).

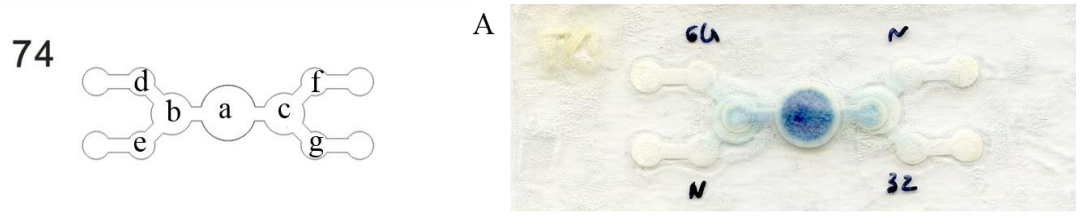

Figure 64 - Experiments on the 3D µPAD with a direct Hp P-ELISA to evaluate conjugate rehydration and flowing through the device. A) 2D schematic protocol for the P-ELISA on the 3D µPAD: 0.7µl of standard bovine Hp at concentration of 32 µg/ml (g) or 64µg/ml (d) and 0.7 µl WB (e and f) were deposited in the sample inlet; 2µl conjugate diluted 1:750 in WB were deposited in the conjugate storage pad (b and c); after 10 min at RT, 30µl of WB were added to the sample inlet (a); after 30 min at RT, 30µl substrate solution were deposited in the sample inlet (a). B) Picture taken 10 min after application of substrate. N: control (WB), 64: 64µg/ml Hp, 32: 32µg/ml Hp. There was no colorimetric reaction in any of test pads but there was evidence of reaction between the conjugate and substrate within layers A and B.

To prevent the conjugate from binding to the conjugate storage pad and diffusing into layer B, a blocking buffer was used to prevent absorption of reagents onto the device. Different blocking buffers were tested, with BSA 10% deemed as the most suitable (Figure 65). It was also noticed that a stronger signal could be achieved with a decrease in conjugate dilution, without causing an increase in the background signal (Figure 65C).

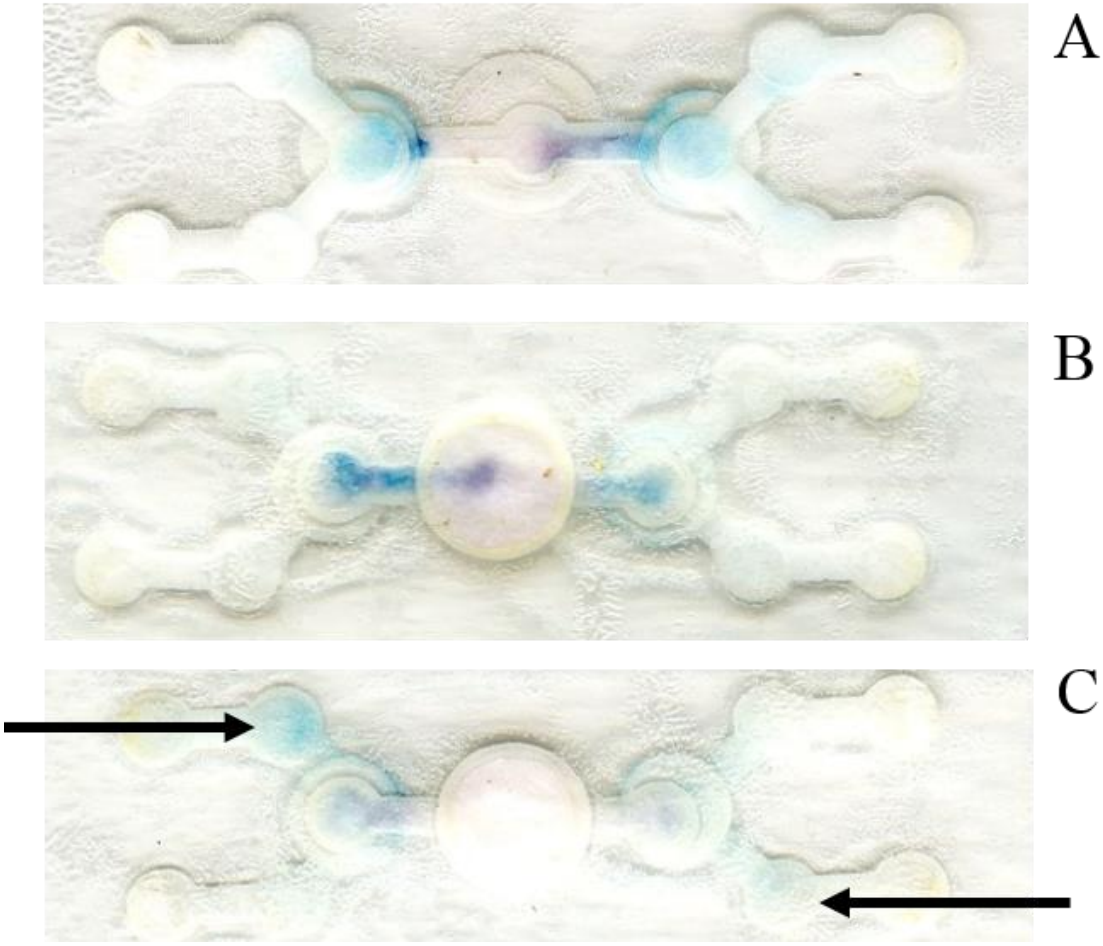

Figure 65 - Evaluation of conjugate blocking within the 3D µPAD. Layer B and layer C of the device were blocked with 2 µl of different solutions of blocking buffer, before a direct Hp P-ELISA was carried out as reported in Figure 64. Standard bovine Hp was at concentration of 64µg/ml in both pads (d and g), while conjugate was diluted 1:50 in WB for pad b and 1:200 in WB for pad c. A) The blocking buffer used is milk 10%. B) The blocking buffer used is fish gelatin 5%. C) The blocking buffer used is BSA 10%. The black arrows indicate the colorimetric reaction following binding between Hp and conjugate at the test pad. There was a noticeably stronger signal when a conjugate concentration of 1:50 was used (pad b).

Based on the results obtained, the optimised protocol for the direct Hp P-ELISA applied to the 3D µPAD was as follows: standard bovine haptoglobin was diluted to 64µg/ml in WB and 0.7µL were deposited onto the test pads d and g (Figure 64A) and 0.7µL of WB were deposited onto the test pads e and f (Figure 64A). The device was blocked with blocking buffer (BSA 10%) as follows: 0.7µL was applied to the first paper pad of layer D and 2µL was applied to layers C and B (Figure 63A). After 10 minutes at RT, 2µL of purified rabbit anti-bovine haptoglobin IgG diluted 1:50 in WB was deposited onto layer C and allowed to dry at RT for 10 minutes. The 3D µPAD was assembled and 30µl WB was deposited onto layer A. After 30 minutes at RT, 30µl of substrate

solution were added to layer A. After 10 minutes at RT, the 3D µPAD was scanned using a desktop scanner. A total of 3 replicates of the device were processed (n=6) and the image data was analysed as reported in Section 2.5. The mean pixel intensity of the positive pad (Hp) was 24.86±4.89 SEM (CI 12.3-37.4) and 6.61±0.67 SEM (CI 4.9-8.3) for the control pad (N), showing a significant difference (p=0.019) when a paired t-test was used to compare the measurements (Figure 66).

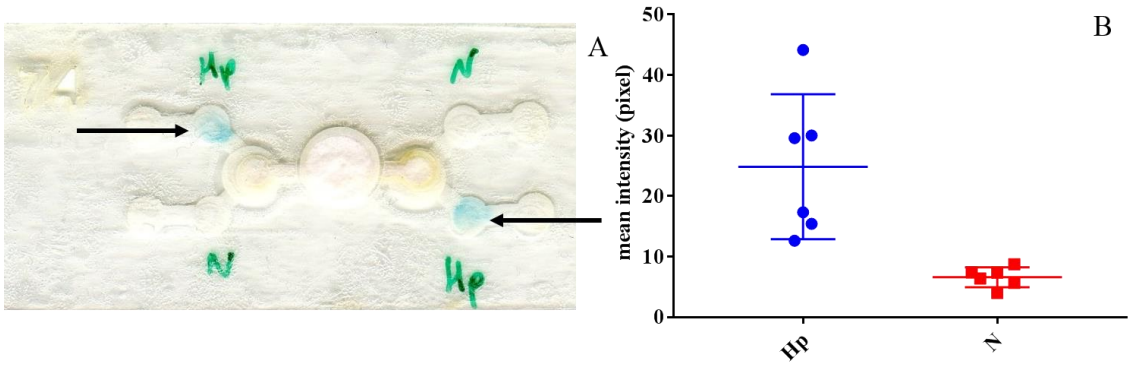

Figure 66 - Optimised direct Hp P-ELISA on the 3D µPAD. A) Picture taken 10 min after addition of the substrate. The black arrows indicate the colorimetric reaction following binding between Hp and conjugate at the test pad. B) Scatter plot of the mean pixel intensity obtained from 3 replicates (n=6) 3D µPAD. Hp: pad containing 64µg/ml Hp and N: control pad containing WB.

6.6 Discussion

In this final research chapter, the knowledge acquired to fabricate the MP^3 and to transfer lab-based ELISAs into P-ELISAs are combined with the final aim of fabricating a µPAD that could successfully perform an immunoassay at the POC. The fabrication method for the paper device, was already demonstrated as a valid alternative to the existing methods (Chapter 3) with additional advantages, such as, high resolution of fabrication, simplicity, versatility, robustness, low-cost and suitability for high environmental temperatures. In relation to fabrication, some fundamental knowledge was acquired during the transition from the MP^3 into the 2D and 3D format. Specifically, an alternative solution to simplify and effectively assemble the device was developed. The precise alignment and the removal of gaps between adjacent layers of 3D µPADs have been reported as some of the main hurdles of these type of platforms [17]. Solutions proposed include the use of cellulose powder [18], adhesive spray [19]

or lamination of the whole device [20]. The solution proposed herein exploits the same machinery (e.g. laser cutter) used for fabrication, by precisely cutting a thin double-sided adhesive sheet in the same shape as the lamination. This reduces the operator input and possibly human error by pre-assembling the adhesive sheet onto the device layers. Although the adhesive sheet is then laminated at high temperature (110°C), no evidence of leakage or loss of adhesiveness were observed once the device was assembled and tested. Furthermore, in the final device, one of the layers (the conjugate storage) is not laminated, which allows increased contact between layers and a complete usage of the surface available for reagent storage. An important contribution to the effect of lamination on timing, was also provided by the experiments performed on the 2D µPAD. In this case, a partially open device allowed for a faster flow rate, but was not compatible with the reaction time necessary for an immunoassay. Although one of the fundamental criteria for POC tests is rapidity [21] biological reactions also need a minimum time to proceed. Therefore, a combination of different lamination techniques has been used to tailor fluid flow according to the timing needed. A partially open layer was used to achieve fast sample distribution, while a complete covering of the microchannels within the test layer reduced the fluid flow allowing sufficient time for the biological reaction to occur.

In this respect, the µPADs, both the 2D and 3D versions, were also tested with an immunoassay, showing that the reaction occurs specifically where the conjugate binds to pre-deposited Hp, with minimal background noise (Figure 66). Compared to the P-ELISA applied on the MP^3, a two-step (instead of 5 step) process was required, with complete removal of the washing procedures. Experimental work was also initiated for the use of the sandwich Hp and the indirect Pso o 2 P-ELISA with serum (results not shown). In this case, the capture reagents were deposited in the test layer and serum from naïve and infested sheep were added to the sample inlet. This remained a two-step process, with further work planned to use a gold-labelled conjugate instead of either an ALP or HRP conjugate, with the final aim of reducing the whole assay to a one-step process (e.g. addition of sample). The developed 3D µPAD would also allow for the sample inlet (layer A) to provide a whole blood separation pad [22], which would remove the need for centrifuging whole blood, making the device truly suitable for

"pen-side" use. A stage that needs further investigation is the long-term storage of the device, with specific reference to the performance of the immunoassay. Experiments were carried out on the same day of the conjugate antibody deposition. Further experiments would be required to evaluate if similar results can be obtained within days or weeks after deposition of the reagents, taking also into account different methods for storage of the 3D µPAD (e.g., refrigeration or vacuum packed).

At this stage, the total time from sample addition to results was 40 minutes. However, a waiting time of 30 minutes between the two steps of the assay was based on the 2D µPAD experimental work and additional testing on the 3D format could possibly reduce it further. Total timing for immunoassays carried out on 3D µPAD vary from 15-30 minutes [23] to 45 minutes [22], which is generally considered satisfactory. Likewise, the total volume of sample used is comparable to other studies using similar devices, where between 20µl [24] and 80µl [25] are usually required.

Finally, the 3D µPAD developed here allows for two immunoassays to be run in parallel. However, two further microchannels could be added to the design in layer B, leading to the corresponding test layers which could perform a total of four independent tests on the same sample. Furthermore, by scaling down the device, a single chip could easily support up to four 3D µPADs, allowing for multiple samples to be tested at the same time.

6.7 Conclusions

To conclude the research, a functional 3D µPAD was developed and fabricated, based on the technique of laser cutting and lamination for fabrication and the use of a laser cut double-sided adhesive sheet for precise and close-fitting assembly. An immunoassay for the detection of Hp was also successfully applied on the device. This demonstrated the proof-of-concept that the developed 3D µPAD is suitable as a diagnostic platform for immunoassay. To use the device in clinical settings, more complex assays (e.g. sandwich ELISA with pre-deposition of a capture antibody) would be required. The

device has great potential for application as a "pen-side" test for sheep scab and, to widen its application, as a platform for animal disease testing.

6.8 References

[1] Tomazelli Coltro, W.K., Cheng, C.-M., Carrilho, E., and de Jesus, D.P. Recent advances in low-cost microfluidic platforms for diagnostic applications. *Electrophoresis*, 2014. **35**(16): p. 2309-2324.

[2] Yang, Y., Li, Q., Wang, S., Chen, X., and Du, A. Rapid and sensitive detection of Babesia bovis and Babesia bigemina by loop-mediated isothermal amplification combined with a lateral flow dipstick. *Veterinary Parasitology*, 2016. **219**: p. 71-76.

[3] Khunthong, S., Jaroenram, W., Arunrut, N., Suebsing, R., Mungsantisuk, I., and Kiatpathomchai, W. Rapid and sensitive detection of shrimp yellow head virus by loop-mediated isothermal amplification combined with a lateral flow dipstick. *Journal of Virological Methods*, 2013. **188**(1–2): p. 51-56.

[4] Pazzola, M., Piras, G., Noce, A., Dettori, M.L., and Vacca, G.M. Evaluation of the rapid assay Betastar Combo 3.0 for the detection of Penicillin, Amoxicillin, Cefazolin and Oxytetracycline in individual sheep milk. *Small Ruminant Research*, 2015. **124**: p. 127-131.

[5] Boulangé, A., Pillay, D., Chevtzoff, C., Biteau, N., Comé de Graça, V., Rempeters, L., Theodoridis, D., and Baltz, T. Development of a rapid antibody test for point-of-care diagnosis of animal African trypanosomosis. *Veterinary Parasitology*, 2017. **233**: p. 32-38.

[6] Nguyen, T.-T., Motsiri, M.S., Taioe, M.O., Mtshali, M.S., Goto, Y., Kawazu, S.-I., Thekisoe, O.M.M., and Inoue, N. Application of crude and recombinant ELISAs and immunochromatographic test for serodiagnosis of animal trypanosomosis in the Umkhanyakude district of KwaZulu-Natal province, South Africa. *The Journal of Veterinary Medical Science*, 2015. **77**(2): p. 217-220.

[7] Kumar, A.A., Hennek, J.W., Smith, B.S., Kumar, S., Beattie, P., Jain, S., Rolland, J.P., Stossel, T.P., Chunda-Liyoka, C., and Whitesides, G.M. From the

Bench to the Field in Low-Cost Diagnostics: Two Case Studies. *Angewandte Chemie (International ed. in English)*, 2015. **54**(20): p. 5836-5853.

[8] Sechi, D., Greer, B., Johnson, J., and Hashemi, N. Three-dimensional paper-based microfluidic device for assays of protein and glucose in urine. *Analytical Chemistry*, 2013. **85**(22): p. 10733-10737.

[9] Martinez, A.W., Phillips, S.T., Butte, M.J., and Whitesides, G.M. Patterned paper as a platform for inexpensive, low-volume, portable bioassays. *Angewandte Chemie (International ed. in English)*, 2007. **46**(8): p. 1318-1320.

[10] Fenton, E.M., Mascarenas, M.R., Lopez, G.P., and Sibbett, S.S. Multiplex lateral-flow test strips fabricated by two-dimensional shaping. *Acs Applied Materials & Interfaces*, 2009. **1**(1): p. 124-129.

[11] Lu, Y., Shi, W.W., Jiang, L., Qin, J.H., and Lin, B.C. Rapid prototyping of paper-based microfluidics with wax for low-cost, portable bioassay. *Electrophoresis*, 2009. **30**(9): p. 1497-1500.

[12] Apilux, A., Ukita, Y., Chikae, M., Chailapakul, O., and Takamura, Y. Development of automated paper-based devices for sequential multistep sandwich enzyme-linked immunosorbent assays using inkjet printing. *Lab on a Chip*, 2013. **13**(1): p. 126-135.

[13] Abe, K., Kotera, K., Suzuki, K., and Citterio, D. Inkjet-printed paperfluidic immuno-chemical sensing device. *Analytical and Bioanalytical Chemistry*, 2010. **398**(2): p. 885-893.

[14] Kim, Y.K. and Kim, H. Immuno-strip biosensor system to detect enrofloxacin residues. *Journal of Industrial and Engineering Chemistry*, 2009. **15**(2): p. 229-232.

[15] Cassano, C.L. and Fan, Z.H. Laminated paper-based analytical devices (LPAD): fabrication, characterization, and assays. *Microfluidics and Nanofluidics*, 2013. **15**(2): p. 173-181.

[16] Schilling, K.M., Jauregui, D., and Martinez, A.W. Paper and toner three-dimensional fluidic devices: programming fluid flow to improve point-of-care diagnostics. *Lab on a Chip*, 2013. **13**(4): p. 628-631.

[17] Yetisen, A.K., Akram, M.S., and Lowe, C.R. Paper-based microfluidic point-of-care diagnostic devices. *Lab on a Chip*, 2013. **13**(12): p. 2210-2251.

[18] Martinez, A.W., Phillips, S.T., and Whitesides, G.M. Three-dimensional microfluidic devices fabricated in layered paper and tape. *Proceedings of the National Academy of Sciences of the United States of America*, 2008. **105**(50): p. 19606-19611.

[19] Lewis, G.G., DiTucci, M.J., Baker, M.S., and Phillips, S.T. High throughput method for prototyping three-dimensional, paper-based microfluidic devices. *Lab on a Chip*, 2012. **12**(15): p. 2630-2633.

[20] Schonhorn, J.E., Fernandes, S.C., Rajaratnam, A., Deraney, R.N., Rolland, J.P., and Mace, C.R. A device architecture for three-dimensional, patterned paper immunoassays. *Lab on a Chip*, 2014. **14**(24): p. 4653-4658.

[21] Peeling, R.W., Holmes, K.K., Mabey, D., and Ronald, A. Rapid tests for sexually transmitted infections (STIs): the way forward. *Sexually Transmitted Infections*, 2006. **82**: p. V1-V6.

[22] Xu, G.L., Nolder, D., Reboud, J., Oguike, M.C., van Schalkwyk, D.A., Sutherland, C.J., and Cooper, J.M. Paper-origami-based multiplexed malaria diagnostics from whole blood. *Angewandte Chemie (International ed. in English)*, 2016. **55**(49): p. 15250-15253.

[23] Lewis, G.G., Robbins, J.S., and Phillips, S.T. Point-of-care assay platform for quantifying active enzymes to femtomolar levels using measurements of time as the readout. *Analytical Chemistry*, 2013. **85**(21): p. 10432-10439.

[24] Ge, L., Wang, S., Song, X., Ge, S., and Yu, J. 3D Origami-based multifunction-integrated immunodevice: low-cost and multiplexed sandwich chemiluminescence immunoassay on microfluidic paper-based analytical device. *Lab on a Chip*, 2012. **12**(17): p. 3150-3158.

[25] Gerbers, R., Foellscher, W., Chen, H., Anagnostopoulos, C., and Faghri, M. A new paper-based platform technology for point-of-care diagnostics. *Lab on a Chip*, 2014. **14**(20): p. 4042-4049.

Chapter 7 – Summary of the research and recommendations for further work

7.1 Summary of the research

In this thesis, the development of microfluidic paper-based analytical devices (µPADs), based on a new fabrication technique and specifically designed to suit point-of-care animal disease testing, has been described. Different devices have been developed within the research program and their analytical performances have been tested using sheep scab as the model disease, in light of future practical applications of these devices for point-of-care screening of infested animals (Figure 67).

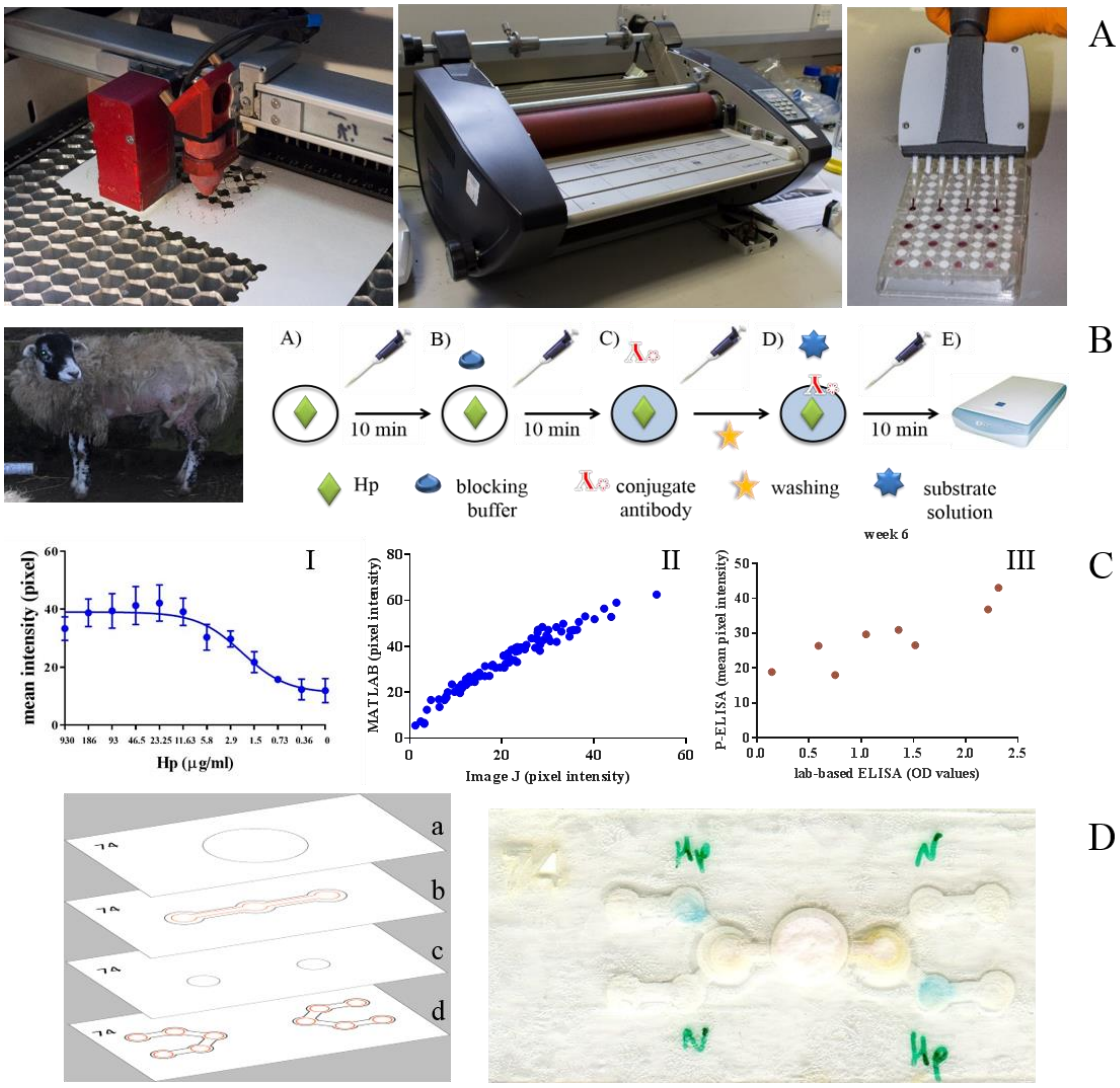

Figure 67 - Summary of the research. A) The novel fabrication technique for production of µPADs. B) Schematic of the P-ELISA developed on the MP^3 for sheep scab diagnosis. C) Performance of the µPADs for POC test of sheep scab: standard curve for Hp measurement (I); correlation between image analysis using Image J and the purpose-written MATLAB code (II); correlation between results from the lab-based ELISA and the P-ELISA for Pso o 2 measurement at week 6 post-infestation (III). D) Final 3D µPAD with the optimised direct Hp P-ELISA.

The new fabrication technique is based on a combination of paper cutting and lamination (Figure 67A). This method is simple, rapid and of high-resolution and can produce robust, versatile and low-cost devices. Using this technique, a replicate of a 96-well microplate for P-ELISA, named MP^3, a 2D and a 3D µPAD were fabricated. During the development of these devices, alternative assembly methods for both the MP^3 and the 3D µPAD were engineered, which allowed for easy and precise assemble of the devices. Novel fabrication methods, like "draw your assay", which uses a ball-point pen to create microfluidic channels [1] or printing of cellulose powder onto a polymer film [2], show the need for practical and simple ideas to reduce the costs and

simplify the fabrication process. Very recently a new concept of low-cost devices has also been introduced, called paper hybrid microfluidic platforms. A combination of paper and other materials, like PMMA [3], PDMS [4], cotton [5] or glass [6] are combined to fully exploit the properties of each material [7]. The novel fabrication technique developed here can be considered an example of this recently characterised class of microfluidic platform.

Another interesting application of microfluidic paper-based devices has been proposed to streamline the process of optimising assay conditions [8]. Within the time frame of this research project, it was possible to translate two lab-based ELISAs (Hp and Pso o 2) into P-ELISAs using the MP^3 (Figure 67B). The length of time to analyse the data was also decreased considerably by developing an alternative solution for automatic data analysis (Figure 67C). This is of great relevance for data interpretation at the POC, where a rapid answer is an essential characteristic of these type of tests. Furthermore, due to the reduced volumes of reagents and the low-cost of consumables, the development of the μPADs prototypes and the optimisation of the assays conditions were relatively low-cost.

Important advances in the point-of-care diagnosis of sheep scab have also been achieved. P-ELISAs for Hp and Pso o 2 (Figure 67C) were developed and, although each step of these assays needs to be manually performed by the operator, overall timing and cost were significantly reduced. While it cannot be strictly considered a POC test, a P-ELISA on the MP^3 can still offer the possibility to carry "in-house" (e.g. within veterinary clinics) testing as other ELISA test kits have been commercialised [9] or possibly even "on-farm" testing, as is the case for common parasitology techniques for faecal egg counts that can currently be performed on farm [10]. Furthermore, the application of the 3D μPAD for Hp detection means that the possibility of a "pen-side" test for sheep scab is now a real possibility (Figure 67D).

Finally, but possibly most importantly, the overall success of this PhD project was possible due to the strong collaboration between the two institutes and the people

involved, engineers and biologists, working closely together in a truly interdisciplinary space.

7.2 Future work

In view of the results obtained and aiming at a continuation of this research, the following areas will need to be addressed in the future:

- To validate the 3D µPAD with serum from animals with known and varying degrees of pathology, in a multiplex format for parallel detection of Hp and Pso o 2. Samples are already available and, after optimisation of conditions like sample and reagent dilutions, results obtained from the two lab-based ELISAs could be compared with results from the multiplexed 3D µPAD.

- To make the 3D µPAD a true "pen-side" test, by using whole blood instead of serum samples. In this case, the sample inlet could act as a blood separation membrane, removing the need for a centrifuge. This method has been successfully employed before [11, 12], although it has never been applied to animal blood, which would provide the first proof-of-concept of this method. Implementing it even further, would be the use of a pin-prick derived blood sample [13, 14] removing the hurdle of blood collection by jugular veni-puncture.

- To further improve the analytical performance of the µPADs. Improvement of limit of detection, sensitivity and specificity are still perceived as one of the main challenges in microfluidics [15]. The use of an alternative method to colorimetric detection, like electrochemical [16, 17] or potentiometric sensors [18], could be applied both to the MP^3 and the 3D µPAD to enhance detection of circulating Hp and Pso o 2 antibodies.

- To widen the utility of the MP^3, by translating other immunoassays into P-ELISA. Lab-based ELISAs already exist for other important diseases of sheep, for example Enzootic Abortion of Ewes (a zoonotic agent causing serious

abortion storms) [19] and Maedi-Visna/Caprine Arthritis Encephalitis (an important wasting disease of small ruminants) [20]. For both conditions, official schemes are in place in the UK for accreditation of flocks as free from the disease, which requires annual testing[8]. These diseases would therefore be well suited for a "pen-side" test for regular screening of animals.

- To obtain POC interpretation of the test results. During this project, a high-throughput image analysis procedure was developed. The use of desktop scanners, however, is only suited for research and laboratory settings. A recurrent theme in literature is the use of smart phone cameras for image capture [21], which could be used as part of telemedicine approach [22]. Results generated by the µPADs could be compared using a desktop scanner and a smart phone camera, possibly looking at developing a smart phone app to include the algorithm already developed here for image analysis.

- To look at commercialisation of the µPADs. Last, but not least, the applications related to this project should be taken from the laboratory to the end-users. Field trials could be designed, looking at involving farmers, vets and diagnostic laboratories into trialling the new sheep scab tests, with the possible final aim of patenting the µPADs developed [23].

7.3 Conclusions

Research projects on µPADs have seen an exponential increase since the concept was first introduced. They represent an excellent solution for low-cost and rapid diagnosis in low-resource settings and, as demonstrated through this research, they can also be applied to animal disease diagnostics. The application of these new technologies could make a real change toward an improved and more sustainable human and animal health. However, only true collaboration between engineers, scientists, vets, medics and industry partners will enable this to happen.

[8] https://www.sruc.ac.uk/info/120113/premium_sheep_and_goat_health_schemes

7.4 References

[1] Oyola-Reynoso, S., Heim, A.P., Halbertsma-Black, J., Zhao, C., Tevis, I.D., Çınar, S., Cademartiri, R., Liu, X., Bloch, J.-F., and Thuo, M.M. Draw your assay: Fabrication of low-cost paper-based diagnostic and multi-well test zones by drawing on a paper. *Talanta*, 2015. **144**: p. 289-293.

[2] Tian, J., Li, X., and Shen, W. Printed two-dimensional micro-zone plates for chemical analysis and ELISA. *Lab on a Chip*, 2011. **11**(17): p. 2869-2875.

[3] Sanjay, S.T., Dou, M., Sun, J., and Li, X. A paper/polymer hybrid microfluidic microplate for rapid quantitative detection of multiple disease biomarkers. *Scientific reports*, 2016. **6**: p. 30474.

[4] Dou, M., Dominguez, D.C., Li, X., Sanchez, J., and Scott, G. A versatile PDMS/paper hybrid microfluidic platform for sensitive infectious disease diagnosis. *Analytical Chemistry*, 2014. **86**(15): p. 7978-7986.

[5] Lin, S.C., Hsu, M.Y., Kuan, C.M., Wang, H.K., Chang, C.L., Tseng, F.G., and Cheng, C.M. Cotton-based diagnostic devices. *Scientific Reports*, 2014. **4**: p. 6976-6988.

[6] Zuo, P., Li, X., Dominguez, D.C., and Ye, B.-C. A PDMS/paper/glass hybrid microfluidic biochip integrated with aptamer-functionalized graphene oxide nano-biosensors for one-step multiplexed pathogen detection. *Lab on a Chip*, 2013. **13**(19): p. 3921-3928.

[7] Dou, M., Sanjay, S.T., Benhabib, M., Xu, F., and Li, X. Low-cost bioanalysis on paper-based and its hybrid microfluidic platforms. *Talanta*, 2015. **145**: p. 43-54.

[8] Meredith, N.A., Volckens, J., and Henry, C.S. Paper-based microfluidics for experimental design: screening masking agents for simultaneous determination of Mn(ii) and Co(ii). *Analytical Methods*, 2017. **9**(3): p. 534-540.

[9] Litster, A.L., Pressler, B., Volpe, A., and Dubovic, E. Accuracy of a point-of-care ELISA test kit for predicting the presence of protective canine parvovirus and canine distemper virus antibody concentrations in dogs. *Veterinary Journal*, 2012. **193**(2): p. 363-366.

[10] Godber, O.F., Phythian, C.J., Bosco, A., Ianniello, D., Coles, G., Rinaldi, L., and Cringoli, G. A comparison of the FECPAK and Mini-FLOTAC faecal egg counting techniques. *Veterinary Parasitology*, 2015. **207**(3–4): p. 342-345.

[11] Yang, X., Forouzan, O., Brown, T.P., and Shevkoplyas, S.S. Integrated separation of blood plasma from whole blood for microfluidic paper-based analytical devices. *Lab on a Chip*, 2012. **12**(2): p. 274-280.

[12] Ge, L., Wang, S., Song, X., Ge, S., and Yu, J. 3D Origami-based multifunction-integrated immunodevice: low-cost and multiplexed sandwich chemiluminescence immunoassay on microfluidic paper-based analytical device. *Lab on a Chip*, 2012. **12**(17): p. 3150-3158.

[13] Xu, G.L., Nolder, D., Reboud, J., Oguike, M.C., van Schalkwyk, D.A., Sutherland, C.J., and Cooper, J.M. Paper-origami-based multiplexed malaria diagnostics from whole blood. *Angewandte Chemie (International ed. in English)*, 2016. **55**(49): p. 15250-15253.

[14] Pollock, N.R., Rolland, J.P., Kumar, S., Beattie, P.D., Jain, S., Noubary, F., Wong, V.L., Pohlmann, R.A., Ryan, U.S., and Whitesides, G.M. A paper-based multiplexed transaminase test for low-cost, point-of-care liver function testing. *Science Translational Medicine*, 2012. **4**(152): p. 129-139.

[15] Hu, J., Wang, S., Wang, L., Li, F., Pingguan-Murphy, B., Lu, T.J., and Xu, F. Advances in paper-based point-of-care diagnostics. *Biosensors and Bioelectronics*, 2014. **54**: p. 585-597.

[16] Zhao, C. and Liu, X. A portable paper-based microfluidic platform for multiplexed electrochemical detection of human immunodeficiency virus and hepatitis C virus antibodies in serum. *Biomicrofluidics*, 2016. **10**(2): p. 024119 1-10.

[17] Narang, J., Malhotra, N., Singhal, C., Mathur, A., Chakraborty, D., Anil, A., Ingle, A., and Pundir, C.S. Point of care with micro fluidic paper based device integrated with nano zeolite-graphene oxide nanoflakes for electrochemical sensing of ketamine. *Biosensors & Bioelectronics*, 2017. **88**: p. 249-257.

[18] Tarasov, A., Gray, D.W., Tsai, M.-Y., Shields, N., Montrose, A., Creedon, N., Lovera, P., O'Riordan, A., Mooney, M.H., and Vogel, E.M. A potentiometric biosensor for rapid on-site disease diagnostics. *Biosensors and Bioelectronics*, 2016. **79**: p. 669-678.

[19] Wilson, K., Livingstone, M., and Longbottom, D. Comparative evaluation of eight serological assays for diagnosing *Chlamydophila abortus* infection in sheep. *Veterinary Microbiology*, 2009. **135**(1–2): p. 38-45.

[20] Polledo, L., Gonzalez, J., Fernandez, C., Miguelez, J., Martinez-Fernandez, B., Morales, S., Ferreras, M.C., and Garcia Marin, J.F. Simple control strategy to reduce the level of Maedi-Visna infection in sheep flocks with high prevalence values (> 90%). *Small Ruminant Research*, 2013. **112**(1-3): p. 224-229.

[21] Capitán-Vallvey, L.F., López-Ruiz, N., Martínez-Olmos, A., Erenas, M.M., and Palma, A.J. Recent developments in computer vision-based analytical chemistry: A tutorial review. *Analytica Chimica Acta*, 2015. **899**: p. 23-56.

[22] Vella, S.J., Beattie, P., Cademartiri, R., Laromaine, A., Martinez, A.W., Phillips, S.T., Mirica, K.A., and Whitesides, G.M. Measuring markers of liver function using a micropatterned paper device designed for blood from a fingerstick. *Analytical Chemistry*, 2012. **84**(6): p. 2883-2891.

[23] Yetisen, A.K. and Volpatti, L.R. Patent protection and licensing in microfluidics. *Lab on a Chip*, 2014. **14**(13): p. 2217-2225.

Chapter 8 – Appendix A

8.1 Lab-based sandwich ELISA for the determination of Haptoglobin concentration

8.1.1 Standard bovine haptoglobin (Hp)

Standard bovine haptoglobin (0.93mg/ml, Life Diagnostics Inc., USA) was kept at -80°C and thawed at room temperature before use.

8.1.2 Antibody conjugation

Purified rabbit anti-bovine haptoglobin IgG (Life Diagnostics, USA; Catalogue No. 18120) was conjugated with alkaline phosphatase (Innova biosciences, Cambridge, UK; Catalogue No. 702-0010) according to manufacturer's instruction as described below; 3.7µl of LL-Modifier was added to lyophilized product in the vial and gently mixed by pipetting up and down. 37µl (0.1mg rabbit anti bovine Hp) was then added into the vial, mixed and left at room temperature overnight. 3.7µl of LL-Quencher was added the next day. The conjugate was ready for use after 30 minutes. 200µl of phosphate buffered saline (PBS) was added to the conjugate to give a final volume about 244.4µl, and an antibody concentration of 0.4mg/ml. This was stored at 4^{o}C until used.

8.1.3 Coating

Unconjugated purified rabbit anti-bovine haptoglobin IgG (Life Diagnostics, USA; Catalogue No. 18120) was diluted to a final concentration of 0.125µg/ml in coating buffer (0.05M $NaHCO_3$ pH 9.6). 100µl was dispensed into individual wells of Nunc-Maxisorp 96 MicroWell™ plate (Nunc International, Rochester, NY) and incubated at 4^{o}C overnight.

8.1.4 Washing

After discarding the antibody solution, each well was washed with 250µl of wash buffer [(WB) 0.02M Tris-HCl with 0.05% Tween-20 (pH 7.4)], four times.

8.1.5 Blocking

Unoccupied binding sites were blocked by adding 200µl of blocking buffer, 10% (w/v) Marvel milk protein in WB, and incubated at 37ºC for 60 minutes.

8.1.6 Addition of standards and samples

After washing, standard bovine haptoglobin (Hp) was diluted to 1025ng/ml in WB and then double diluted until it reached 8ng/ml. Milk samples were also diluted at 1:800 or 1:1000 in WB. Serum samples were diluted 1:40 in WB. 100µl of each Hp, milk and serum samples were added into duplicate wells and incubated at 37 °C for 60 minutes.

8.1.7 Addition of conjugate antibody

Wells were washed, and 100µl of the alkaline phosphatase-conjugated antibody diluted at 1:10,000 in WB were dispensed into each well of the ELISA plate and incubated at room temperature (RT) for 60 minutes.

8.1.8 Addition of substrate

After washing, substrate solution, BluePhos® Microwell phosphatase substrate system by KPL (Catalogue No 50-88-00) was made up according to manufacturer's instruction and 100µl was added into each well for colour development taking approximately 10 minutes. APstop^{TM} solution (KPL Catalogue No 50-89-00) was used by adding 100µl per well, to stop further colour development after the optimum was reached.

8.1.9 Absorbance reading

The absorbance was read at 595nm using Fluostar OPTIMA plate reader (BMG Labtech Ltd.) and the results analysed and calculated using the associated FLUOstar OPTIMA Software V1.32 R2 using a 4 parameter-fit standard curve plotted on a Log-linear scale.

8.1.10 Assay validation

Precision of the assay was determined by calculating the means of inter- and intra-assay coefficients of variation (CV) of 11 inter-assay repeats of two controls and 23 samples in one run assay, respectively. Limit of detection (sensitivity) of the assay was determined from 4 blanks samples plus 3 standard deviations. The specificity of the assay was assessed by western immunoblots, nitrocellulose membrane incubation in conjugate Ab, followed by detection using enzyme substrate, of Hp containing milk and serum samples and samples spiked with known concentrations of standard bovine Hp. Recovery was assessed by determining Hp concentration of the spiked samples using the ELISA assay.

Chapter 9 – Appendix B

9.1 Lab-based indirect ELISA for the detection of ovine IgG binding to recombinant Pso o 2

9.1.1 Recombinant Psorptes ovis Pso o2 (rPso o 2)

The rPso o 2 (0.51mg/ml, Dundee Cell, UK) was kept at 4°C. It was brought to room temperature (RT) and thoroughly mixed by vortexing before use.

9.1.2 Coating

The rPso o 2 was diluted in double distilled water to a concentration of 2.5µg/ml. 50µl were dispensed into individual wells of flat bottomed, medium binding 96-well plates (Greiner code 655001) and incubated at RT overnight.

9.1.3 Washing

After discarding the antigen solution, each well was washed with 300µl of wash buffer [(WB) phosphate buffered saline (PBS) with 0.05% Tween-20], six times.

9.1.4 Blocking

Unoccupied binding sites were blocked by adding 100µl of blocking buffer [(PBST80) 0.5M NaCl PBS with 0.05% Tween 80] and incubated at 37ºC for 60 minutes.

9.1.5 Addition of animal samples

After washing, 50µl of ovine serum samples diluted 1:400 in PBST80 were added into duplicate wells and incubated at 37 °C for 60 minutes.

9.1.6 Addition of conjugate antibody

Wells were washed, and 50µl of rabbit anti-ovine IgG horse radish peroxidase conjugate (DAKO P0163) diluted at 1: 2,000 in PBST80 were dispensed into each well and incubated at 37 °C for 60 minutes.

9.1.7 Addition of substrate

After washing, 50 µl of substrate solution [3,3',5,5'-Tetramethylbenzidine TMB (KPL Catalogue No 52-00-00)] was added into each well for colour development taking approximately 10 minutes. TMB stopping solution [(100% diethylene glycol (KPL Catalogue No 50-85-06)] was used by adding 50µl per well, to stop further colour development after the optimum was reached.

9.1.8 Absorbance reading

The absorbance was read at 450nm using the Sunrise™ TECAN plate reader (Tecan Trading AG, Switzerland) and the results analysed using the associated Magellan™ software V6.

Chapter 10 – Appendix C

10.1 MATLAB code for high-throughput analysis of data on the MP^3

```
function [Wt] = Valentina2(RGB_I, c_dia, mode)
% function [Wt] = Valentina(RGB_I, mode)
% Image analysis algorithm to automatically analyse the mean intensity
of
% each well in the microfluidic device
%
%   Inputs:  RGB_I    = input image
%            c_dia    = circle diameter for well region-of-interest
%            mode     = intensity mode
%                         - 'blue'  = Extract blue channel as
grayscale
%                         - 'red'   = Extract red channel as grayscale
%                         - 'green' = Extract green channel as
grayscale
%                         - 'gray'  = Standard grayscale conversion
%   Outputs: Wt       = Coordinates and mean intensity of each well
%
% Version 2.21
% Algorithm created by Alan Faulkner-Jones  January 2016

close all
% ---------------------- User Defined Variables --------------------
----
if(~exist('RGB_I','var'))
%     RGB_I = imread('005.jpg');
    [filename,pathname] = uigetfile('*.*','Select the image file');
    imagefile = fullfile(pathname,filename);
    if isequal(imagefile,0) % Catch "Cancel"
        return
    else
        RGB_I = imread(imagefile);
    end
end
if(~exist('c_dia','var'))
    c_dia = 15;
end
if(~exist('mode','var'))
%     mode = 'gray';
    mode = 'blue';
end

% --------------------------- Transform image ----------------------
----
% Reduce the size of the image to speed up execution
I = imresize(RGB_I,0.15);

% Using user-specified mode transform to grayscale
switch mode
    case 'blue'
        I2 = I(:,:,1);
    case 'red'
        I2 = I(:,:,2);
```

```
    case 'green'
        I2 = I(:,:,3);
    otherwise
        I2 = rgb2gray(I);
end

% Invert the image
I2 = imcomplement(I2);

% Calculate deviation from orthogonal and straighten the image
angle = horizon(I2, 0.1, 'hough');
I2 = imrotate(I2,-angle,'bilinear','crop');

% Ask the user to position two ellipses on the opposing corner wells
to
% calculate the coordinates of the entire array
figure(1), imshow(I2);
title('Move the circles to A1, H12 and double-click each one');
set(gcf, 'Position', get(0,'Screensize')); % Maximize figure.
hold on
h1 = imellipse(gca, [20 20 30 30]);
h2 = imellipse(gca, [size(I2,2)-30 size(I2,1)-30 30 30]);
position1 = wait(h1);
position2 = wait(h2);
hold off


scsz = get(0,'Screensize');
% h=msgbox('Please Wait','Computing');
h = dialog('Position',[(scsz(3)/2)-125 (scsz(4)/2)-50 250 100],...
    'Name', 'Message');
txt = uicontrol('Parent',h,...
    'Style','text',...
    'Position',[20 20 210 40],...
    'String','Computing, please wait.');

% ----------- Calculate array coordinates and measure intensity ------
----
% Calculate well spacings
x_spc = (mean(position2(:,1)) - mean(position1(:,1))) / 11;
y_spc = (mean(position2(:,2)) - mean(position1(:,2))) / 7;

Wt = zeros(96,3);           % Create empty array to store data

figure(1), imshow(I2);
title('Calculated mean intensity in each well');
hold on
n = 1;
for i = mean(position1(:,1)):x_spc:mean(position2(:,1))
    for j = mean(position1(:,2)):y_spc:mean(position2(:,2))
        plot(i,j, 'r+')                     % Plot well centres
        [a,b] = circle(i,j,c_dia);
        plot(a,b, '-b')                     % Plot circles
        avg_i = mean(I2(roipoly(I2,a,b)));  % Calculate mean intensity
        text(i+c_dia,j+c_dia,int2str(avg_i),'Color','r')% Display
intensity valve
        Wt(n,:) = [i,j,avg_i];              % Save to array
        n = n+1;
```

```
    end
end

delete(h)

% Reshape the array to 12x8 for ease of cell identification
WtR = reshape(Wt(:,3),[8,12]);

% ------------------------ Output File Setup ------------------------
----
% Create excel spreadsheet with same names as input file
token = strcat(strtok(filename, '.'),'.xlsx');
% [filename2, pathname2] = uiputfile;
[filename2, pathname2] = uiputfile( ...
    {'*.xlsx', 'Excel Workbook'}, ...
    'Save Excel Data File As', ...
    token);
if isequal([filename2,pathname2],[0,0]) % Catch "Cancel"
    return
else
    % If we have reached this point, then we need to create the file
    File2 = fullfile(pathname2,filename2); % Create new file
    xlswrite(File2,{filename},1,'A1')
    % Create and insert row and column headers
    Col_h = {'1','2','3','4','5','6','7','8','9','10','11','12'};
    Row_h = {'A';'B';'C';'D';'E';'F';'G';'H'};
    xlswrite(File2,Col_h,1,'B3')
    xlswrite(File2,Row_h,1,'A4')
    % Write intensity data
    xlswrite(File2,WtR,1,'B4')
end
h = msgbox('Operation Completed','Done');
end

function [a,b] = circle(x,y,r)
%x and y are the coordinates of the center of the circle
%r is the radius of the circle
%0.01 is the angle step, bigger values will draw the circle faster but
%you might notice imperfections (not very smooth)
ang=0:0.01:2*pi;
xp=r*cos(ang);
yp=r*sin(ang);
a = x+xp;
b = y+yp;
end
```